

Fast Accurate Beam and Channel Tracking for Two-dimensional Phased Antenna Arrays

Yu Liu^{*§}, Jiahui Li^{*§}, Xiujun Zhang[§], Shidong Zhou^{*§}

^{*}Dept. of EE, Tsinghua University, Beijing, 100084, China

[§]National Laboratory for Information Science and Technology, Tsinghua University, Beijing, 100084, China

Abstract

The sparsity and the severe attenuation of millimeter-wave (mmWave) channel imply that highly directional communication is needed. The narrow beam produced by large array requires accurate alignment, which can be achieved by beam training with large exploration overhead in static scenarios. However, this training expense is prohibitive when serving fast-moving users. In this paper, we focus on accurate two-dimensional (2D) beam and channel tracking problem in mmWave mobile communication. The minimum exploration overhead of 2D tracking is given in theory first. Then the time-varying channels are divided into three cases: Quasi-static Case, Dynamic Case I and Dynamic Case II. We further develop three tracking algorithms corresponding to these three cases. The proposed algorithms have several salient features: (1) fading channel supportive: they can simultaneously track the channel gain and 2D beam direction in fading channel environments; (2) low exploration overhead: they achieve the minimum exploration requirement for 2D tracking; (3) fast tracking speed and high tracking accuracy: in Quasi-static Case and Dynamic Case I, the tracking error is proved to converge to the minimum Cramér-Rao lower bound (CRLB). In Dynamic Case II, our tracking algorithm outperforms existing algorithms with lower tracking error and faster tracking speed in simulation.

I. INTRODUCTION

Millimeter-wave (mmWave) mobile communication is currently a hot topic due to its much wider bandwidth compared with sub-6GHz spectrum. In mmWave channels, the much shorter wavelength leads to much higher propagation attenuation. Fortunately, with the shorter wavelength, the narrower beam and larger array gain can be formed with a given array aperture providing compensation for the propagation loss [1]–[5]. However, the narrower beam also

implies the requirement of more accurate beam alignment, which can be achieved by beam training at the expense of significant exploration overhead in static or quasi-static scenarios [6]–[11]. While in mobile communication, the fast change of wireless channel either in the direction or the channel gain makes beam training inefficient and inaccurate. Therefore, accurate beam tracking with low exploration overhead is crucial for serving fast-moving users in mmWave communication system.

Moreover, the large array gain requirement of mmWave mobile communication implies a large number of antenna elements in the array. However, due to the high cost of AD/DA devices and the high energy consumption of mmWave RF chains, the number of RF chains should be kept much smaller than that of antenna elements, leading to hybrid beamforming or even analog beamforming for cost-effective and energy-efficient systems [3]–[5], [12], [13]. In analog beamforming, since only one RF chain is available with a certain set of programmable phase shifters at a certain time (forming a so-called **exploring beamforming vector (EBV)** in this paper), only one direction (or dimension) of the channel can be observed. A randomly selected EBV may most probably lead to missing the real propagation ray and result in an observation of very low signal-to-noise ratio (SNR). What is interesting is that an EBV resulting highest SNR is also inappropriate, since the observation could not provide any information of direction variation. Hence it is crucial to select informative EBVs dynamically to achieve as accurate direction information as possible. Since the EBVs should be designed according to historical observations with noise, this process is really tracking rather than estimation.

Some beam tracking methods have been proposed in [9], [14]–[16], which utilize historical exploring directions and observations to obtain current estimates. However, the EBVs are not optimized in those tracking algorithms, which may lead to poor observations. A beam tracking algorithm is proposed in [17], trying to optimize the EBVs, assuming that the channel gain is known. In [18], the authors start to jointly track the channel gain and the beam direction with optimal EBVs. Despite the progress, the proposed algorithm is based on uniform linear array (ULA) antennas, which can only support one-dimensional (1D) beam tracking. While in several mobile scenarios, e.g., dense urban area [19] or unmanned aerial vehicle (UAV) scenarios [20], both horizontal and vertical directions are variable and need to be tracked. The algorithm designed for 1D beam tracking in [18] could not be efficiently applied to the two-dimensional (2D) problems directly.

In this paper, we focus on accurate 2D beam and channel tracking problem. The mmWave

wireless system in this paper periodically works in exploration and communication mode. In the exploration stage of one **exploration and communication cycle (ECC)**, the transmitter sends q pre-defined pilot sequences. Then the receiver points in one exploring direction in the duration of each pilot sequence and makes an estimate of the channel gain and the direction of the incoming beam at the end of the q -th exploration. In the communication stage of one ECC, the beam is aligned in the estimated direction. Based on this structure, we care about the following questions:

- 1) What is the minimum exploration overhead q in each ECC?
- 2) How to determine the q exploring directions?
- 3) How to track the beam direction and the channel gain for different time-varying channels, e.g., slowly changing channels and fast fading channels?
- 4) How is the accuracy, convergence and stability of the tracking algorithm?

To answer these questions, we perform theoretical analysis on 2D beam tracking and propose corresponding algorithms to efficiently track different time-varying channels. The main contributions of this paper are summarized as follows:

1) It is proved that for the unique estimate of the channel gain and the 2D beam direction within one ECC, the minimum exploring overhead in each ECC is $q = 3$.

2) Dynamic beam and channel tracking strategies for three different time-varying channels are proposed and optimized. The salient advantages of these tracking algorithms are given below:

i) For channels changing slowly, i.e., with quasi-static channel gain and beam direction (called **Quasi-static Case** in this paper), optimal exploring directions are derived which are proved to be determined only by the array size, and approach constants as the array size goes large enough. The tracking error of our proposed algorithm is proved to converge to the minimum Cramér-Rao lower bound (CRLB).

ii) For channels with quasi-static beam direction and fast-changing channel gain (called **Dynamic Case I** in this paper), the scenario where the channel gain satisfies Rayleigh distribution is studied as a special case in this paper. An algorithm for beam only tracking is proposed, and it is proved to converge and achieve the minimum CRLB on beam direction.

iii) For channels with fast-changing beam direction and channel gain (called **Dynamic Case II** in this paper), simulation result shows that our algorithm can achieve faster and more accurate tracking performance compared with existing methods.

The rest of this paper is organized as follows: The system model is described in Section II. In Section III, the tracking problem with some constraints is formulated. Then the minimum exploration overhead of joint 2D beam and channel tracking is given in theory in Section IV. In Section V and Section VI, tracking problem for Quasi-static Case (Section V) and Dynamic Case I (Section VI) are studied separately. The tracking performance bounds are derived and corresponding tracking algorithms are developed with convergence and optimality analysis. In Section VII, a tracking algorithm is developed for Dynamic Case II. Numerical results are obtained to verify the performance of our proposed tracking algorithms In Section VIII.

Notations: We use lower case letters such as a and \mathbf{a} to denote scalars and column vectors. Respectively, $|\mathbf{a}|$ and $\|\mathbf{a}\|_2$ represent the module and 2-norm of the vector \mathbf{a} . Upper case boldface letters, e.g., \mathbf{A} , are used to denote matrices. The superscript $(\bar{\cdot})$, $(\cdot)^T$, $(\cdot)^H$ are utilized to denote conjugate, transpose and conjugate-transpose. For a matrix \mathbf{A} , its inverse and pseudo-inverse are written as \mathbf{A}^{-1} and \mathbf{A}^+ . The identity matrix of order q is denoted by \mathbf{J}_q . Let $\mathcal{CN}(\mu, \sigma^2)$ represent the symmetric complex Gaussian distribution with mean μ and variance σ^2 , and $\mathcal{N}(\mu, \sigma^2)$ stand for the real Gaussian distribution with mean μ and variance σ^2 . Statistical expectation is denoted by $\mathbb{E}[\cdot]$. The real (imaginary) part is represented as $\text{Re}\{\cdot\}$ ($\text{Im}\{\cdot\}$). The natural logarithm of a scalar y is obtained by $\log(\cdot)$ and the phase angle of a complex number z is written as $\angle z$.

II. SYSTEM MODEL

We consider a mmWave receiver equipped with a planar phased antenna array¹, as shown in Fig. 1. The planar array consists of $M \times N$ antenna elements that are placed in a rectangular area, where $M(N)$ antenna elements are equally distributed along x -axis (y -axis) with a distance d_1 (d_2) between neighboring antenna elements². These antenna elements are connected to the same RF chain via different phase shifters. The system periodically works in exploration and communication mode. The angle of arrival (AoA) and channel gain in each ECC are assumed to be constant and can be different in different ECCs. In the exploration stage of one ECC, the transmitter sends q same pre-defined pilot sequence \mathbf{s} , where \mathbf{s} contains L_s symbols, i.e.,

¹Note that tracking is needed at both the transmitter and receiver. However, considering the transmitter-receiver reciprocity, the beam and channel tracking of both sides have similar designs. Hence, we focus on beam and channel tracking on the receiver side.

²To obtain different resolutions in the horizontal direction and vertical direction, the antenna numbers along different directions may not be the same, i.e., $M \neq N$ [21]. To suppress sidelobe, the antennas may be unequally spaced, i.e., $d_1 \neq d_2$ [22].

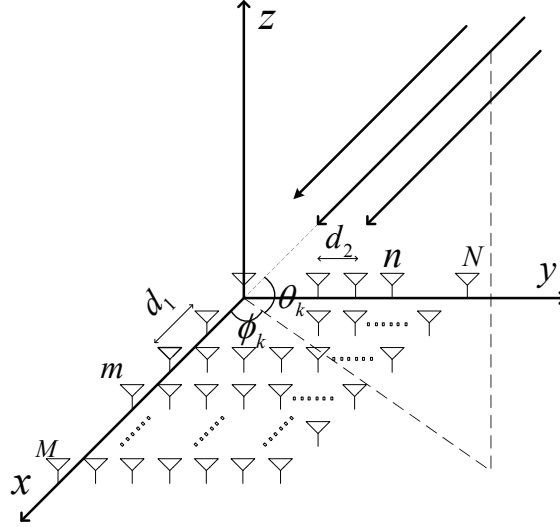


Fig. 1: 2D phased antenna array.

$\mathbf{s} \in \mathbb{C}^{1 \times L_s}$, and $|\mathbf{s}|^2 = E_p$ is the transmit energy of each pilot sequence. Then the receiver points in one exploring direction in the duration of each pilot sequence and makes an estimate of the channel gain and the direction of the incoming beam at the end of the q -th exploration. In the communication stage of one ECC, the beam is aligned in the estimated direction.

A. Channel Model

In mmWave channels, only a few paths exist due to the weak scattering effect [4]. Because the beam formed by a large array in the mmWave system is quite narrow, the interaction between multi-paths is relatively weak. In other words, the incoming beam paths are usually sparse in space, making it possible to track each path independently [23]. Hence, we focus on the method for tracking one path. Different paths can be tracked separately by using the same method. In k -th ECC, the direction of the incoming beam path is denoted by (θ_k, ϕ_k) , where $\theta_k \in [0, \pi/2]$ is the elevation AoA and $\phi_k \in [-\pi, \pi)$ is the azimuth AoA. Then the channel vector of this path during k -th ECC is

$$\mathbf{h}_k = \beta_k \mathbf{a}(\mathbf{x}_k), \quad (1)$$

where $\beta_k = \beta_k^{\text{re}} + j\beta_k^{\text{im}}$ is the complex channel gain, $\mathbf{x}_k = [x_{k,1}, x_{k,2}]^T = \left[\frac{Md_1 \cos(\theta_k) \cos(\phi_k)}{\lambda}, \frac{Nd_2 \cos(\theta_k) \sin(\phi_k)}{\lambda} \right]^T$ is the **direction parameter vector (DPV)** determined by (θ_k, ϕ_k) ,

$$\mathbf{a}(\mathbf{x}_k) = [a_{11}(\mathbf{x}_k) \cdots a_{1N}(\mathbf{x}_k) \ a_{21}(\mathbf{x}_k) \cdots a_{MN}(\mathbf{x}_k)]^T \quad (2)$$

is the steering vector with $a_{mn}(\mathbf{x}_k) = e^{j2\pi(\frac{m-1}{M}x_{k,1} + \frac{n-1}{N}x_{k,2})}$ ($m = 1, \dots, M; n = 1, \dots, N$), and λ is the wavelength.

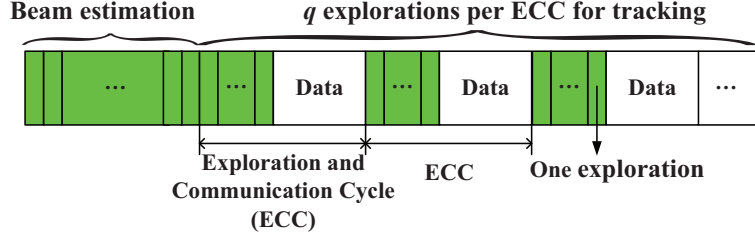


Fig. 2: The frame structure for tracking.

B. RF and Base Band Preprocessing

Let $\mathbf{w}_{k,i} \in \mathbb{C}^{MN \times 1}$ be the EBV for receiving the i -th ($i = 1, \dots, q$) pilot sequence in k -th ECC. The entries of $\mathbf{w}_{k,i}$ are of the same amplitude with $|\mathbf{w}_{k,i}|_l = \frac{1}{\sqrt{MN}}$, where $[\mathbf{w}_{k,i}]_l$ denotes the l -th element of $\mathbf{w}_{k,i}$. After phase shifting and combining, the i -th received sequence in k -th ECC at the baseband output of the RF chain is given by

$$\boldsymbol{\nu}_k = \mathbf{w}_{k,i}^H \mathbf{h}(\mathbf{x}_k) \mathbf{s} + \boldsymbol{\zeta}_{k,i} = \beta_k \mathbf{w}_{k,i}^H \mathbf{a}(\mathbf{x}_k) \mathbf{s} + \boldsymbol{\zeta}_{k,i}, \quad (3)$$

where $\boldsymbol{\zeta}_{k,i}^T \sim \mathcal{CN}(\mathbf{0}, \sigma_z^2 \mathbf{J}_{L_s})$ is a circularly symmetric complex Gaussian random vector with \mathbf{J}_{L_s} denoting the identity matrix of L_s order. By match filtering on the received sequence $\boldsymbol{\nu}_k$, the i -th observation in k -th ECC is given below:

$$y_{k,i} = \boldsymbol{\nu}_k \frac{\mathbf{s}^H}{|\mathbf{s}|} = \beta_k \mathbf{w}_{k,i}^H \mathbf{a}(\mathbf{x}_k) \mathbf{s} \frac{\mathbf{s}^H}{|\mathbf{s}|} + \boldsymbol{\zeta}_{k,i} \frac{\mathbf{s}^H}{|\mathbf{s}|} \stackrel{(a)}{=} |\mathbf{s}| \beta_k \mathbf{w}_{k,i}^H \mathbf{a}(\mathbf{x}_k) + z_{k,i}, \quad (4)$$

where Step (a) is due to the definition $z_{k,i} \triangleq \boldsymbol{\zeta}_{k,i} \frac{\mathbf{s}^H}{|\mathbf{s}|}$. It is clear that $z_{k,i}$ is a complex Gaussian random variable with $z_{k,i} \sim \mathcal{CN}(0, \sigma_z^2)$. Let $\mathbf{W}_k \triangleq [\mathbf{w}_{k,1}, \dots, \mathbf{w}_{k,q}]$, $\mathbf{z}_k \triangleq [z_{k,1}, \dots, z_{k,q}]^T$ and $\mathbf{y}_k \triangleq [y_{k,1}, \dots, y_{k,q}]^T$ denote the **exploring beamforming matrix (EBM)**, the noise vector and the observation vector respectively. Then we can rewrite (4) as follows:

$$\mathbf{y}_k = |\mathbf{s}| \beta_k \mathbf{W}_k^H \mathbf{a}(\mathbf{x}_k) + \mathbf{z}_k. \quad (5)$$

C. Tracking Loop

The frame structure of our system is given in Fig. 2. It is assumed that the beam estimator can output an initial estimate that falls in the main lobe of the DPV:

$$\mathcal{B}(\mathbf{x}_k) \triangleq (x_{k,1} - 1, x_{k,1} + 1) \times (x_{k,2} - 1, x_{k,2} + 1). \quad (6)$$

Then our tracking starts from this initial estimate of the channel gain and the DPV.

In the exploration stage of k -th ECC, the receiver needs to choose an EBM \mathbf{W}_k based on previously used EBMs $\mathbf{W}_1, \dots, \mathbf{W}_{k-1}$ and historical observation vectors $\mathbf{y}_1, \dots, \mathbf{y}_{k-1}$. By

applying \mathbf{W}_k , we can get the observation vector \mathbf{y}_k . Then the estimate $\hat{\boldsymbol{\psi}}_k \triangleq [\hat{\beta}_k^{\text{re}}, \hat{\beta}_k^{\text{im}}, \hat{x}_{k,1}, \hat{x}_{k,2}]^T$ of the channel parameter vector $\boldsymbol{\psi}_k \triangleq [\beta_k^{\text{re}}, \beta_k^{\text{im}}, x_{k,1}, x_{k,2}]^T$ is obtained by using all EBMs and observation vectors available. From a control system perspective, $\boldsymbol{\psi}_k$ is the system state, $\hat{\boldsymbol{\psi}}_k$ is the estimate of the system state, the EBM \mathbf{W}_k is the control action and \mathbf{y}_k is a non-linear noisy observation determined by the system state and control action. Hence, the task of a tracking design is to find the following strategy:

$$\mathbf{W}_k = \mathbf{F}_k^c(\mathbf{W}_1, \dots, \mathbf{W}_{k-1}, \mathbf{y}_1, \dots, \mathbf{y}_{k-1}) \quad (7)$$

$$\hat{\boldsymbol{\psi}}_k = \mathbf{F}_k^e(\mathbf{W}_1, \dots, \mathbf{W}_k, \mathbf{y}_1, \dots, \mathbf{y}_k), \quad (8)$$

where \mathbf{F}_k^c denotes the control function in k -th ECC while \mathbf{F}_k^e denotes the estimation function in k -th ECC.

III. PROBLEM FORMULATION

Let $\Xi_k = (\mathbf{F}_k^c, \mathbf{F}_k^e)$ denote a *causal* beam and channel tracking scheme in k -th ECC. Then the beam and channel tracking problem is formulated as:

$$\min_{\Xi_k} \frac{1}{MN} \mathbb{E} \left[\left\| \hat{\mathbf{h}}_k - \mathbf{h}_k \right\|_2^2 \right] \quad (9)$$

$$\text{s.t. } \mathbb{E} \left[\hat{\mathbf{h}}_k \right] = \mathbf{h}_k, \quad (10)$$

$$(1), (2), (5), (7), (8)$$

where the constraint (10) ensures that $\hat{\mathbf{h}}_k \triangleq \hat{\beta}_k \mathbf{a}(\hat{\mathbf{x}}_k)$ is an unbiased estimate of the channel vector $\mathbf{h}_k = \beta_k \mathbf{a}(\mathbf{x}_k)$.

Problem (9) is challenging due to the following reasons:

1) It is a constrained partially observed Markov decision process (C-POMDP) that is quite difficult to solve optimally [24] [25].

2) There are $M \times N$ phase shifts to adjust in each EBV $\mathbf{w}_{k,i}$. This makes the optimization of EBV too complicated due to the high degree of design freedom.

3) To obtain $\hat{\boldsymbol{\psi}}_k$ in k -th ECC, k EBMs, i.e., $\mathbf{W}_1, \dots, \mathbf{W}_k$, need to be designed, making it difficult to optimize so many beamforming matrices simultaneously when k is not quite small.

4) The time-varying features of the channel in (1) restrict the tracking algorithm and system performance. Hence, it is hard to design a tracking method for a general channel model in (1).

These challenges above make it extremely difficult to solve this problem optimally. Hence, we add some reasonable constraints in this paper to take the first step of optimal tracking policy:

1) EBV constraint. Instead of general phase shifts, we use steering vectors to design the EBVs,

$$\mathbf{w}_{k,i} = \frac{1}{\sqrt{MN}} \mathbf{a}(\boldsymbol{\omega}_{k,i}), \quad (11)$$

where $\boldsymbol{\omega}_{k,i} \triangleq [\omega_{k,i1}, \omega_{k,i2}]^T$ denotes the i -th exploring DPV in k -th ECC. This ensures that only two variables need to be designed for each EBV.

2) Exploring direction constraint. Although the exploring DPV in (11) can be any form, however, considering the tracking accuracy, it is better to make sure that $\boldsymbol{\omega}_{k,i}$ falls within the main lobe of the DPV in (6). Thus, it is a reasonable choice to use the currently estimated direction to perform a certain offset for exploring. For this purpose, we use such an architecture in this paper. That is, the i -th exploring DPV in k -th ECC, i.e., $\boldsymbol{\omega}_{k,i}$ in (11), is determined by the previous estimated DPV plus an exploring offset $\boldsymbol{\Delta}_{k,i}$. Considering the design of the offsets that change in different ECCs is also very complicated, we adopt fixed exploring offsets $\boldsymbol{\Delta}_i (i = 1, 2, 3)$ in this paper:

$$\boldsymbol{\omega}_{k,i} = \hat{\mathbf{x}}_{k-1} + \boldsymbol{\Delta}_i, i = 1, 2, 3. \quad (12)$$

Therefore, the EBV in (11) can be rewritten as

$$\mathbf{w}_{k,i} = \frac{1}{\sqrt{MN}} \mathbf{a}(\hat{\mathbf{x}}_{k-1} + \boldsymbol{\Delta}_i), i = 1, 2, 3. \quad (13)$$

3) Time-varying channel constraint. The channel vector in (1) is determined by two parts: the channel gain β_k and the DPV \mathbf{x}_k , both of which may change slowly or fast. Therefore, four possible cases exist:

- (i) Both the channel gain and the DPV change slowly;
- (ii) The channel gain changes fast while the DPV changes slowly;
- (iii) The channel gain changes slowly while the DPV changes fast;
- (iv) Both the channel gain and the DPV change fast.

These four cases correspond to different practical scenarios, which can be modeled as follows:

A. Quasi-static Case: $\beta_k \approx \beta_{k-1}, \mathbf{x}_k \approx \mathbf{x}_{k-1}$

When both β_k and \mathbf{x}_k change slowly, e.g., the user keeps static or quasi-static, the channel can be seen as approximately fixed. For the sake of convenience, we assume that $\beta_k = \beta = \beta^{\text{re}} + j\beta^{\text{im}}$, $\mathbf{x}_k = \mathbf{x} = [x_1, x_2]^T$ in this case.

B. Dynamic Case: $\beta_{k+1} \neq \beta_k, \mathbf{x}_k \approx \mathbf{x}_{k-1}$

For channels that β_k changes fast while \mathbf{x}_k changes slowly, e.g., the user moves fast without rotating, the beam direction can be seen as approximately fixed, i.e., $\mathbf{x}_k = \mathbf{x}$, when the distance between transmitter and receiver is very large compared with the wavelength. In order to distinguish with other dynamic scenarios, this case is called Dynamic Case I.

C. Dynamic Case: $\beta_k \approx \beta, \mathbf{x}_{k+1} \neq \mathbf{x}_k$

This case requires that the channel gain keeps static or quasi-static while the beam direction changes fast. However, in mmWave channels, the fast change of beam direction usually leads to the fast change of channel gain since the propagation paths change. This case exists only when the antenna array rotates around the first antenna element which keeps static. This is not the usual case and is not studied in this paper.

D. Dynamic Case: $\beta_{k+1} \neq \beta_k, \mathbf{x}_{k+1} \neq \mathbf{x}_k$

This case happens in most fast moving scenarios except Dynamic Case I, e.g., the user moves while the receiver array rotates. In order to distinguish with Dynamic Case I, we call it Dynamic Case II.

With the EBV constraint, the exploring direction constraint and the time-varying channel constraint, the beam and channel tracking problem in k -th ECC can be reformulated as:

$$\begin{aligned} \min_{\Xi} \quad & \frac{1}{MN} \mathbb{E} \left[\left\| \hat{\mathbf{h}}_k - \mathbf{h}_k \right\|_2^2 \right] \\ \text{s.t.} \quad & (1), (2), (5), (7), (8), (10), (13). \end{aligned} \quad (14)$$

IV. HOW MANY EXPLORATIONS ARE NEEDED IN EACH ECC?

Before further studying the tracking problem in (14), we will first study the number of explorations needed in this section.

Under the constraint in (11), two explorations in each ECC are sufficient to jointly track the channel gain and 1D beam direction according to [18]. When tracking the horizontal and vertical beam direction simultaneously, it is straight forward that four explorations are feasible by separately using two explorations to track each dimension of the 2D beam direction. However, with four explorations, the channel gain is updated twice in each ECC, possibly leading to redundancy. Since it will cost time resource for each exploration, we may try to answer the

question that can we reduce the times of exploration, or what is the minimum number of the explorations required?

Then the following lemma is proposed to help determine the minimum exploration overhead q in each ECC:

Lemma 1. *If the EBVs are of steering vector forms, i.e., $\mathbf{w}_{k,i} = \frac{1}{\sqrt{MN}}\mathbf{a}(\boldsymbol{\omega}_{k,i})$, and the observation vector in (5) is noiseless, then*

1) *to obtain a unique estimate of the channel parameter vector $\boldsymbol{\psi}_k$ within one ECC, at least 3 explorations are needed in each ECC;*

2) *to obtain a unique estimate of the DPV \mathbf{x}_k within one ECC, at least 3 explorations are needed in each ECC.*

Proof. proof See Appendix A. ■

Lemma 1 tells us that at least three explorations are required in each ECC no matter we want to jointly estimate β_k and \mathbf{x}_k or just estimate \mathbf{x}_k . Hence, the minimum exploration overhead in each ECC is $q = 3$, i.e., the EBM $\mathbf{W}_k = [\mathbf{w}_{k,1}, \mathbf{w}_{k,2}, \mathbf{w}_{k,3}]$.

In the next three sections, we will separately study the tracking problem for Quasi-static Case, Dynamic Case I and Dynamic Case II. In these three cases, a set of same symbols are used for the sake of writing convenience: the EBM \mathbf{W}_k , the observation vector \mathbf{y}_k and the estimate of channel parameter vector $\hat{\boldsymbol{\psi}}_k$. The values of these symbols may vary for different cases. However, it will cause little confusion as long as noticing the case where these symbols appear.

V. QUASI-STATIC TRACKING: PERFORMANCE BOUND, CONVERGENCE AND OPTIMALITY

The beam and channel tracking problem for Quasi-static Case is studied here. In Quasi-static Case where $\boldsymbol{\psi}_k = \boldsymbol{\psi} \triangleq [\beta^{\text{re}}, \beta^{\text{im}}, x_1, x_2]^T$ and $\mathbf{h}_k = \mathbf{h} \triangleq \beta\mathbf{a}(\mathbf{x})$, the conditional probability density function of the observation vector \mathbf{y}_k is given by

$$p_S(\mathbf{y}_k | \boldsymbol{\psi}, \mathbf{W}_k) = \frac{1}{\pi^3 \sigma_z^6} e^{-\frac{\|\mathbf{y}_k - |s|\beta \mathbf{W}_k^H \mathbf{a}(\mathbf{x})\|_2^2}{\sigma_z^2}}. \quad (15)$$

In this section, we will first provide the lower bound of tracking error in Quasi-static Case. Then we develop a tracking algorithm and prove this algorithm can converge to the minimum CRLB asymptotically.

A. Cramér-Rao Lower Bound of Tracking Error

The Cramér-Rao lower bound theory gives the lower bound of the unbiased estimation error [26]. Based on this, we introduce the following lemma to obtain the lower bound of tracking error in Quasi-static Case:

Lemma 2. *In Quasi-static Case, given $\mathbf{W}_1, \dots, \mathbf{W}_k$, the MSE of the channel vector in (14) is lower bounded as follows:*

$$\frac{1}{MN} \mathbb{E} \left[\left\| \hat{\mathbf{h}}_k - \mathbf{h} \right\|_2^2 \right] \geq \frac{1}{MN} \text{Tr} \left\{ \left(\sum_{l=1}^k \mathbf{I}_S(\boldsymbol{\psi}, \mathbf{W}_l) \right)^{-1} (\mathbf{V}^H \mathbf{V}) \right\}, \quad (16)$$

where \mathbf{V} is the Jacobian matrix given by

$$\mathbf{V} \triangleq \frac{\partial \mathbf{h}}{\partial \boldsymbol{\psi}^T} = \left[\frac{\partial \mathbf{h}}{\partial \beta^{\text{re}}}, \frac{\partial \mathbf{h}}{\partial \beta^{\text{im}}}, \frac{\partial \mathbf{h}}{\partial x_1}, \frac{\partial \mathbf{h}}{\partial x_2} \right] = \left[\mathbf{a}(\mathbf{x}), j\mathbf{a}(\mathbf{x}), \beta \frac{\partial \mathbf{a}(\mathbf{x})}{\partial x_1}, \beta \frac{\partial \mathbf{a}(\mathbf{x})}{\partial x_2} \right] \quad (17)$$

and the Fisher information matrix $\mathbf{I}_S(\boldsymbol{\psi}, \mathbf{W}_l)$ is given by

$$\mathbf{I}_S(\boldsymbol{\psi}, \mathbf{W}_l) \triangleq \mathbb{E} \left[\frac{\partial \log p_S(\mathbf{y}_l | \boldsymbol{\psi}, \mathbf{W}_l)}{\partial \boldsymbol{\psi}} \cdot \frac{\partial \log p_S(\mathbf{y}_l | \boldsymbol{\psi}, \mathbf{W}_l)}{\partial \boldsymbol{\psi}^T} \right] = \frac{2|\mathbf{s}|^2}{\sigma_z^2} \text{Re} \{ \mathbf{V}^H \mathbf{W}_l \mathbf{W}_l^H \mathbf{V} \}. \quad (18)$$

Proof. See Appendix B. ■

The CRLB in (16) is a function of the EBMs $\mathbf{W}_1, \dots, \mathbf{W}_k$. It is hard to optimize so many EBMs simultaneously. Consider any tracking algorithm that can converge to the DPV \mathbf{x} . Then given any error $e_x > 0$, there exists some k_0 so that when $k > k_0$, $\|\hat{\mathbf{x}}_k - \mathbf{x}\| < e_x$. In other words, when $k > k_0$, $\mathbf{W}_k \approx \mathbf{W} = [\mathbf{w}_1, \mathbf{w}_2, \mathbf{w}_3]^T$, where \mathbf{w}_i is defined below:

$$\mathbf{w}_i = \frac{1}{\sqrt{MN}} \mathbf{a}(\mathbf{x} + \boldsymbol{\Delta}_{S,i}), i = 1, 2, 3 \quad (19)$$

with $\boldsymbol{\Delta}_{S,1}, \boldsymbol{\Delta}_{S,2}, \boldsymbol{\Delta}_{S,3}$ denoting the fixed exploring offsets in Quasi-static Case. Hence, as $k \rightarrow +\infty$, the asymptotic CRLB in (16) is given by

$$\begin{aligned} & \lim_{k \rightarrow +\infty} \frac{k}{MN} \text{Tr} \left\{ \left(\sum_{l=1}^k \mathbf{I}_S(\boldsymbol{\psi}, \mathbf{W}_l) \right)^{-1} (\mathbf{V}^H \mathbf{V}) \right\} \\ &= \frac{1}{MN} \text{Tr} \{ \mathbf{I}_S(\boldsymbol{\psi}, \mathbf{W})^{-1} (\mathbf{V}^H \mathbf{V}) \} \triangleq C_S(\boldsymbol{\psi}, \mathbf{W}), \end{aligned} \quad (20)$$

where $C_S(\boldsymbol{\psi}, \mathbf{W})$ is the normalized CRLB since the CRLB in (16) decreases with k .

According to (20), by optimizing only one EBM \mathbf{W} , we can further get the *minimum normalized CRLB*:

$$C_S^{\min}(\boldsymbol{\psi}) = \min_{\mathbf{W}} C_S(\boldsymbol{\psi}, \mathbf{W}) = C_S(\boldsymbol{\psi}, \mathbf{W}_S^*). \quad (21)$$

Solving problem (21) yields the optimal EBM $\mathbf{W}_S^* = [\mathbf{w}_{S,1}^*, \mathbf{w}_{S,2}^*, \mathbf{w}_{S,3}^*]$:

$$\mathbf{w}_{S,i}^* = \frac{1}{\sqrt{MN}} \mathbf{a}(\mathbf{x} + \Delta_{S,i}^*), i = 1, 2, 3, \quad (22)$$

where $\Delta_{S,1}^*, \Delta_{S,2}^*, \Delta_{S,3}^*$ denote the optimal exploring offsets.

B. Asymptotically Optimal EBM

Let us consider the optimal EBM \mathbf{W}_S^* . In (21), three EBVs need to be optimized, i.e., three 2D exploring offsets need to be determined. It is hard to get analytical results for such a six-dimensional non-convex problem. Numerical search is a feasible way to obtain the three optimal exploring offsets. However, these optimal exploring offsets may be related to some system parameters, e.g., the channel gain β , the DPV \mathbf{x} and the antenna array size M, N . Once these system parameters change, numerical search has to be re-conducted, resulting in high complexity. This leads to the question: how do these parameters affect optimal offsets and cause the difference of CRLB. Then the following lemma is provided to answer this question:

Lemma 3. *In Quasi-static Case, the optimal exploring offsets $\Delta_{S,1}^*, \Delta_{S,2}^*, \Delta_{S,3}^*$ have the following three properties:*

- 1) $\Delta_{S,1}^*, \Delta_{S,2}^*, \Delta_{S,3}^*$ are invariant to the channel gain β ;
- 2) $\Delta_{S,1}^*, \Delta_{S,2}^*, \Delta_{S,3}^*$ are invariant to the DPV \mathbf{x} ;
- 3) $\Delta_{S,1}^*, \Delta_{S,2}^*, \Delta_{S,3}^*$ converge to constant values as $M, N \rightarrow +\infty$:

$$\tilde{\Delta}_{S,i}^* \triangleq \lim_{M, N \rightarrow +\infty} \Delta_{S,i}^*, i = 1, 2, 3.$$

Proof. See Appendix C. ■

Lemma 3 reveals that $\Delta_{S,1}^*, \Delta_{S,2}^*, \Delta_{S,3}^*$ are only related to array size M, N . Hence, the numerical search times can be reduced to one for a particular array size M, N . Numerically, we find later that even if $\Delta_{S,1}^*, \Delta_{S,2}^*, \Delta_{S,3}^*$ may change for different array sizes, $\tilde{\Delta}_{S,1}^*, \tilde{\Delta}_{S,2}^*, \tilde{\Delta}_{S,3}^*$ can be used to take the place of $\Delta_{S,1}^*, \Delta_{S,2}^*, \Delta_{S,3}^*$ as long as M and N are sufficiently large. Therefore, the numerical search times is reduced to one in the end.

By numerical search in the main lobe of the DPV in (6), we can obtain the asymptotically optimal exploring offsets $\tilde{\Delta}_{S,1}^*, \tilde{\Delta}_{S,2}^*, \tilde{\Delta}_{S,3}^*$ in TABLE I and Fig. 3. With these offsets, a general way to generate the asymptotically optimal EBM $\tilde{\mathbf{W}}_S^* = [\tilde{\mathbf{w}}_{S,1}^*, \tilde{\mathbf{w}}_{S,2}^*, \tilde{\mathbf{w}}_{S,3}^*]$ is obtained to achieve the minimum CRLB as below:

TABLE I: Asymptotically optimal exploring offsets in Quasi-static Case.

$\tilde{\Delta}_{S,1}^*$	$\tilde{\Delta}_{S,2}^*$	$\tilde{\Delta}_{S,3}^*$
$[-0.0963, 0.5098]^T$	$[-0.2906, -0.2906]^T$	$[0.5098, -0.0963]^T$

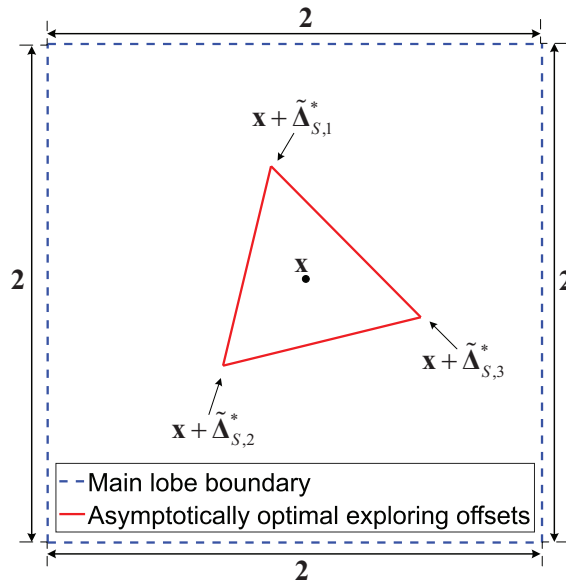


Fig. 3: Asymptotically optimal exploring offsets in Quasi-static Case.

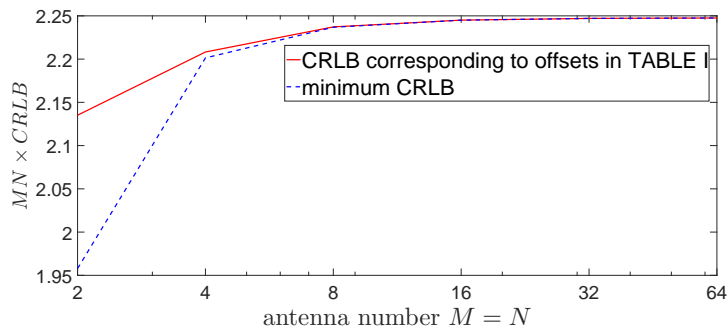


Fig. 4: Performance of offsets in TABLE I

$$\tilde{\mathbf{w}}_{S,i}^* = \frac{1}{\sqrt{MN}} \mathbf{a}(\mathbf{x} + \tilde{\Delta}_{S,i}^*), i = 1, 2, 3. \quad (23)$$

By adopting $\tilde{\Delta}_{S,1}^*$, $\tilde{\Delta}_{S,2}^*$, $\tilde{\Delta}_{S,3}^*$ to smaller size antenna arrays, we compare the minimum CRLB and the CRLB achieved by $\tilde{\Delta}_{S,1}^*$, $\tilde{\Delta}_{S,2}^*$, $\tilde{\Delta}_{S,3}^*$ in TABLE I. As illustrated in Fig. 4, when the antenna number $M = N \geq 8$, we can approach the minimum CRLB with a relative error less than 0.1% by using $\tilde{\Delta}_{S,1}^*$, $\tilde{\Delta}_{S,2}^*$, $\tilde{\Delta}_{S,3}^*$. Therefore, with $\tilde{\Delta}_{S,1}^*$, $\tilde{\Delta}_{S,2}^*$, $\tilde{\Delta}_{S,3}^*$, the minimum CRLB is obtained for different beam directions, different channel gains and different antenna numbers

when $M = N \geq 8$.

C. Joint Beam and Channel Tracking

Before we have provided a low-complexity numerical method to design the optimal EBM and obtain the minimum CRLB, given that the DPV \mathbf{x} is known. However, in a real tracking problem, the DPV \mathbf{x} is unknown and the EBMs need to be adjusted dynamically. In addition, a sequence of optimal beamforming matrices can only tell us what the minimum CRLB is, but it can not tell us which tracking algorithm can achieve the minimum CRLB. In this subsection, we propose a specific tracking algorithm to approach the minimum CRLB.

The proposed tracker is motivated by the following minimization problem:

$$\min_{\mathbf{W}_k} \left\{ \min_{\hat{\boldsymbol{\psi}}} \mathbb{E} \left[\sum_{l=1}^k \left\| \mathbf{s}_l \mathbf{W}_l^H \hat{\mathbf{h}} - \mathbf{y}_l \right\|_2^2 \right] \right\} \quad (24)$$

$$\text{s.t. } \hat{\boldsymbol{\psi}} \triangleq \left[\hat{\beta}^{\text{re}}, \hat{\beta}^{\text{im}}, \hat{x}_1, \hat{x}_2 \right]^T \quad (25)$$

$$\hat{\beta} \triangleq \hat{\beta}^{\text{re}} + j\hat{\beta}^{\text{im}}, \hat{\mathbf{x}} \triangleq [\hat{x}_1, \hat{x}_2]^T \quad (26)$$

$$\hat{\mathbf{h}} \triangleq \hat{\beta} \mathbf{a}(\hat{\mathbf{x}}), \quad (27)$$

where the exact value and the gradient of the objective function are not available and can only be observed via the noisy vectors $\mathbf{y}_1, \dots, \mathbf{y}_k$. Hence, (24) is a stochastic optimization problem [28].

A two-layer nested optimization algorithm is proposed to find the solution of (24). In the *inner layer* of (24), we use stochastic Newton's method [29] to update the estimate, given by

$$\begin{aligned} \hat{\boldsymbol{\psi}}_k &= \hat{\boldsymbol{\psi}}_{k-1} - b_k \mathbf{H}_S \left(\hat{\boldsymbol{\psi}}_{k-1}, \mathbf{W}_k \right)^{-1} \frac{\partial \left\| \mathbf{s}_k \mathbf{W}_k^H \hat{\mathbf{h}} - \mathbf{y}_k \right\|_2^2}{\partial \hat{\boldsymbol{\psi}}} \Bigg|_{\hat{\boldsymbol{\psi}} = \hat{\boldsymbol{\psi}}_{k-1}} \\ &\stackrel{(a)}{=} \hat{\boldsymbol{\psi}}_{k-1} - b_k \sigma_z^2 \mathbf{H}_S \left(\hat{\boldsymbol{\psi}}_{k-1}, \mathbf{W}_k \right)^{-1} \frac{\partial \log p_S(\mathbf{y}_k | \boldsymbol{\psi}, \mathbf{W}_k)}{\partial \boldsymbol{\psi}} \Bigg|_{\boldsymbol{\psi} = \hat{\boldsymbol{\psi}}_{k-1}}, \end{aligned} \quad (28)$$

where b_k is the step-size for Stochastic Newton's method, Step (a) is obtained by substituting

(15) into (28) and $\mathbf{H}_S(\hat{\boldsymbol{\psi}}_{k-1}, \mathbf{W}_k)$ is the Hessian matrix defined below:

$$\begin{aligned} \mathbf{H}_S(\hat{\boldsymbol{\psi}}_{k-1}, \mathbf{W}_k) &\triangleq \frac{\partial^2 \mathbb{E} \left[\left\| \mathbf{s} | \mathbf{W}_k^H \hat{\mathbf{h}} - \mathbf{y}_k \right\|_2^2 \right]}{\partial \hat{\boldsymbol{\psi}} \partial \hat{\boldsymbol{\psi}}^T} \Big|_{\hat{\boldsymbol{\psi}} = \hat{\boldsymbol{\psi}}_{k-1}} \\ &= -\mathbb{E} \left[\sigma_z^4 \frac{\partial \log p_S(\mathbf{y}_k | \boldsymbol{\psi}, \mathbf{W}_k)}{\partial \boldsymbol{\psi}} \frac{\partial \log p_S(\mathbf{y}_k | \boldsymbol{\psi}, \mathbf{W}_k)}{\partial \boldsymbol{\psi}^T} \right] \Big|_{\boldsymbol{\psi} = \hat{\boldsymbol{\psi}}_{k-1}} \\ &= -\sigma_z^4 \mathbf{I}_S(\hat{\boldsymbol{\psi}}_{k-1}, \mathbf{W}_k). \end{aligned} \quad (29)$$

In the end, the estimate is updated as follow:

$$\begin{aligned} \hat{\boldsymbol{\psi}}_k &= \hat{\boldsymbol{\psi}}_{k-1} - b_k \sigma_z^2 \mathbf{H}_S(\hat{\boldsymbol{\psi}}_{k-1}, \mathbf{W}_k)^{-1} \frac{\partial \log p_S(\mathbf{y}_k | \boldsymbol{\psi}, \mathbf{W}_k)}{\partial \boldsymbol{\psi}} \Big|_{\boldsymbol{\psi} = \hat{\boldsymbol{\psi}}_{k-1}} \\ &\stackrel{(b)}{=} \hat{\boldsymbol{\psi}}_{k-1} + b_{S,k} \mathbf{I}_S(\hat{\boldsymbol{\psi}}_{k-1}, \mathbf{W}_k)^{-1} \frac{\partial \log p_S(\mathbf{y}_k | \boldsymbol{\psi}, \mathbf{W}_k)}{\partial \boldsymbol{\psi}} \Big|_{\boldsymbol{\psi} = \hat{\boldsymbol{\psi}}_{k-1}}, \end{aligned} \quad (30)$$

where Step (b) results from (29) and the definition that $b_{S,k} \triangleq \frac{b_k}{\sigma_z^2}$. Here, $b_{S,k}$ is the tracking step-size that will be specified after.

In the outer layer of (24), as to be shown in Section V-D, it is equivalent to minimize the CRLB, i.e., $C_S(\hat{\boldsymbol{\psi}}_{k-1}, \mathbf{W}_k)$, which leads to that the exploring offsets equal to $\tilde{\Delta}_{S,1}^*$, $\tilde{\Delta}_{S,2}^*$, $\tilde{\Delta}_{S,3}^*$.

Finally, the proposed tracking algorithm is summarized in Algorithm 1.

D. Asymptotic Optimality Analysis

We care about the following three questions of the proposed algorithm:

- 1) *Is the tracking algorithm convergent?*
- 2) *If the tracking algorithm is convergent, can it converge to the channel parameter vector $\boldsymbol{\psi}$?*
- 3) *If the tracking algorithm converges to the channel parameter vector $\boldsymbol{\psi}$, what is the gap between the tracking error and the minimum CRLB in (21)?*

Theorem 10.2.2 in [30, Section 10.2] proves that the tracking procedure in the form of (30) can converge to $\boldsymbol{\psi}$ and achieve the minimum CRLB under some constraints. Unfortunately, our tracking algorithm cannot satisfy the necessary requirements for this theorem. Since it is hard to answer the three questions at once, we try to deal with them one by one.

To answer the first question, i.e., the convergence of the proposed algorithm, we can apply Theorem 5.2.1 in [31, Section 5.2.1] to the tracking problem, which gives the conditions that

Algorithm 1 Joint Beam and Channel Tracking for Quasi-static Case

1) **Exploration and Receive:** Transmit 3 pilot sequences in each ECC. The corresponding EPV for receiving the i -th pilot sequence in k -th ECC is given below:

$$\mathbf{w}_{k,i} = \frac{1}{\sqrt{MN}} \mathbf{a} \left(\hat{\mathbf{x}}_{k-1} + \tilde{\Delta}_{S,i}^* \right), i = 1, 2, 3, \quad (31)$$

where $\hat{\mathbf{x}}_k \triangleq [\hat{x}_{k,1}, \hat{x}_{k,2}]^T$ and $\tilde{\Delta}_{S,i}^*$ ($i = 1, 2, 3$) are given by TABLE I. After match filtering, the observation vector \mathbf{y}_k is obtained in (3).

2) **Estimate Update:** The estimate $\hat{\boldsymbol{\psi}}_k = [\hat{\beta}_k^{\text{re}}, \hat{\beta}_k^{\text{im}}, \hat{x}_{k,1}, \hat{x}_{k,2}]^T$ is updated by

$$\hat{\boldsymbol{\psi}}_k = \hat{\boldsymbol{\psi}}_{k-1} + \frac{2|\mathbf{s}|}{\sigma_z^2} b_{S,k} \mathbf{I}_S \left(\hat{\boldsymbol{\psi}}_{k-1}, \mathbf{W}_k \right)^{-1} \begin{bmatrix} \text{Re} \left\{ \mathbf{e}_k^H (\mathbf{y}_k - \hat{\mathbf{y}}_k) \right\} \\ \text{Im} \left\{ \mathbf{e}_k^H (\mathbf{y}_k - \hat{\mathbf{y}}_k) \right\} \\ \text{Re} \left\{ \tilde{\mathbf{e}}_{k1}^H (\mathbf{y}_k - \hat{\mathbf{y}}_k) \right\} \\ \text{Re} \left\{ \tilde{\mathbf{e}}_{k2}^H (\mathbf{y}_k - \hat{\mathbf{y}}_k) \right\} \end{bmatrix}, \quad (32)$$

where $\mathbf{e}_k = \mathbf{W}_k^H \mathbf{a}(\hat{\mathbf{x}}_{k-1})$, $\hat{\mathbf{y}}_k = |\hat{\beta}_{k-1}| \mathbf{W}_k^H \mathbf{a}(\hat{\mathbf{x}}_{k-1})$, $\tilde{\mathbf{e}}_{k1} = \hat{\beta}_{k-1} \mathbf{W}_k^H \frac{\partial \mathbf{a}(\hat{\mathbf{x}}_{k-1})}{\partial x_1}$, $\tilde{\mathbf{e}}_{k2} = \hat{\beta}_{k-1} \mathbf{W}_k^H \frac{\partial \mathbf{a}(\hat{\mathbf{x}}_{k-1})}{\partial x_2}$ and the Fisher information matrix $\mathbf{I}_S \left(\hat{\boldsymbol{\psi}}_{k-1}, \mathbf{W}_k \right)$ is defined in (18). Here, $b_{S,k}$ is the step-size that will be specified after.

ensure $\hat{\boldsymbol{\psi}}_k$ converges. In Theorem 5.2.1 of [31], the stable point is a crucial concept. To study the stable points of our problem, we first rewrite (30) as (33):

$$\hat{\boldsymbol{\psi}}_k = \hat{\boldsymbol{\psi}}_{k-1} + b_{S,k} \boldsymbol{\varsigma}_k, \quad (33)$$

where $\boldsymbol{\varsigma}_k$ is the updating direction defined as:

$$\boldsymbol{\varsigma}_k \triangleq \mathbf{I}_S \left(\hat{\boldsymbol{\psi}}_{k-1}, \mathbf{W}_k \right)^{-1} \left. \frac{\partial \log p_S(\mathbf{y}_k | \boldsymbol{\psi}, \mathbf{W}_k)}{\partial \boldsymbol{\psi}} \right|_{\boldsymbol{\psi} = \hat{\boldsymbol{\psi}}_{k-1}}. \quad (34)$$

This updating direction $\boldsymbol{\varsigma}_k$ is a random vector, which can be divided into a deterministic part $\mathbf{f} \left(\hat{\boldsymbol{\psi}}_{k-1}, \boldsymbol{\psi} \right)$ and a zero mean stochastic part $\hat{\mathbf{z}}_k$, i.e.,

$$\boldsymbol{\varsigma}_k \triangleq \mathbf{f} \left(\hat{\boldsymbol{\psi}}_{k-1}, \boldsymbol{\psi} \right) + \hat{\mathbf{z}}_k, \quad (35)$$

where $\mathbf{f}(\hat{\boldsymbol{\psi}}_{k-1}, \boldsymbol{\psi})$ is defined as follows:

$$\begin{aligned} \mathbf{f}(\hat{\boldsymbol{\psi}}_{k-1}, \boldsymbol{\psi}) &\triangleq \mathbb{E} \left[\mathbf{I}_S(\hat{\boldsymbol{\psi}}_{k-1}, \mathbf{W}_k)^{-1} \frac{\partial \log p_S(\mathbf{y}_k | \boldsymbol{\psi}, \mathbf{W}_k)}{\partial \boldsymbol{\psi}} \Big|_{\boldsymbol{\psi}=\hat{\boldsymbol{\psi}}_{k-1}} \right] \\ &= \frac{2|\mathbf{s}|^2}{\sigma_z^2} \mathbf{I}_S(\hat{\boldsymbol{\psi}}_{k-1}, \mathbf{W}_k)^{-1} \begin{bmatrix} \text{Re} \left\{ \mathbf{e}_k^H (\beta \mathbf{W}_k^H \mathbf{a}(\mathbf{x}) - \hat{\beta}_{k-1} \mathbf{e}_k) \right\} \\ \text{Im} \left\{ \mathbf{e}_k^H (\beta \mathbf{W}_k^H \mathbf{a}(\mathbf{x}) - \hat{\beta}_{k-1} \mathbf{e}_k) \right\} \\ \text{Re} \left\{ \tilde{\mathbf{e}}_{k1}^H (\beta \mathbf{W}_k^H \mathbf{a}(\mathbf{x}) - \hat{\beta}_{k-1} \mathbf{e}_k) \right\} \\ \text{Re} \left\{ \tilde{\mathbf{e}}_{k2}^H (\beta \mathbf{W}_k^H \mathbf{a}(\mathbf{x}) - \hat{\beta}_{k-1} \mathbf{e}_k) \right\} \end{bmatrix}, \end{aligned} \quad (36)$$

and $\hat{\mathbf{z}}_k$ is given by

$$\begin{aligned} \hat{\mathbf{z}}_k &\triangleq \mathbf{I}_S(\hat{\boldsymbol{\psi}}_{k-1}, \mathbf{W}_k)^{-1} \frac{\partial \log p_S(\mathbf{y}_k | \boldsymbol{\psi}, \mathbf{W}_k)}{\partial \boldsymbol{\psi}} \Big|_{\boldsymbol{\psi}=\hat{\boldsymbol{\psi}}_{k-1}} - \mathbf{f}(\hat{\boldsymbol{\psi}}_{k-1}, \boldsymbol{\psi}) \\ &= \frac{2|\mathbf{s}|}{\sigma_z^2} \mathbf{I}_S(\hat{\boldsymbol{\psi}}_{k-1}, \mathbf{W}_k)^{-1} \begin{bmatrix} \text{Re} \{ \mathbf{e}_k^H \mathbf{z}_k \} \\ \text{Im} \{ \mathbf{e}_k^H \mathbf{z}_k \} \\ \text{Re} \{ \tilde{\mathbf{e}}_{k1}^H \mathbf{z}_k \} \\ \text{Re} \{ \tilde{\mathbf{e}}_{k2}^H \mathbf{z}_k \} \end{bmatrix}. \end{aligned} \quad (37)$$

Thus, the tracking procedure in (30) can be rewritten as

$$\hat{\boldsymbol{\psi}}_k = \hat{\boldsymbol{\psi}}_{k-1} + b_{S,k} \left(\mathbf{f}(\hat{\boldsymbol{\psi}}_{k-1}, \boldsymbol{\psi}) + \hat{\mathbf{z}}_k \right) \quad (38)$$

According to [31, Section 4.3], a stable point $\hat{\boldsymbol{\psi}}_{k-1}$ of $\mathbf{f}(\hat{\boldsymbol{\psi}}_{k-1}, \boldsymbol{\psi})$ satisfies two conditions:

1) $\mathbf{f}(\hat{\boldsymbol{\psi}}_{k-1}, \boldsymbol{\psi}) = \mathbf{0}$; 2) $\frac{\partial \mathbf{f}(\hat{\boldsymbol{\psi}}_{k-1}, \boldsymbol{\psi})}{\partial \hat{\boldsymbol{\psi}}_{k-1}^T}$ is negative definite. Hence, we define the stable points set as below:

$$\mathcal{S} \triangleq \left\{ \hat{\boldsymbol{\psi}}_{k-1} : \mathbf{f}(\hat{\boldsymbol{\psi}}_{k-1}, \boldsymbol{\psi}) = \mathbf{0}, \frac{\partial \mathbf{f}(\hat{\boldsymbol{\psi}}_{k-1}, \boldsymbol{\psi})}{\partial \hat{\boldsymbol{\psi}}_{k-1}^T} \prec \mathbf{0} \right\}. \quad (39)$$

The channel parameter vector $\boldsymbol{\psi}$ is a stable point: when $\hat{\boldsymbol{\psi}}_{k-1} = \boldsymbol{\psi}$,

1) $\beta \mathbf{W}_k^H \mathbf{a}(\mathbf{x}) = \hat{\beta}_{k-1} \mathbf{e}_k$ in (36). Hence, $\mathbf{f}(\boldsymbol{\psi}, \boldsymbol{\psi}) = \mathbf{0}$;

2) $\frac{\partial \mathbf{f}(\hat{\boldsymbol{\psi}}_{k-1}, \boldsymbol{\psi})}{\partial \hat{\boldsymbol{\psi}}_{k-1}^T} \Big|_{\hat{\boldsymbol{\psi}}_{k-1}=\boldsymbol{\psi}} = -\mathbf{J}_4$ by derivation, where \mathbf{J}_4 is a 4-order identity matrix. Thus, $\frac{\partial \mathbf{f}(\hat{\boldsymbol{\psi}}_{k-1}, \boldsymbol{\psi})}{\partial \hat{\boldsymbol{\psi}}_{k-1}^T} \Big|_{\hat{\boldsymbol{\psi}}_{k-1}=\boldsymbol{\psi}}$ is negative definite.

Therefore, $\boldsymbol{\psi}$ is a stable point, i.e., $\boldsymbol{\psi} \in \mathcal{S}$. Other stable points in \mathcal{S} correspond to the local optimal points of the beam and channel tracking problem, which are without the main lobe $\mathcal{B}(\mathbf{x})$.

We adopt the diminishing step-size in (40), given by [30]–[32]

$$b_{S,k} = \frac{\epsilon_S}{k + K_{S,0}}, k = 1, 2, \dots \quad (40)$$

where $K_{S,0} \geq 0$ and $\epsilon_S > 0$. Then the following theorem is developed to study the convergence of the proposed algorithm:

Theorem 1 (Convergence to a Unique Stable Point). *If $b_{S,k}$ is given by (40) with $\epsilon_S > 0$ and $K_{S,0} \geq 0$, then $\hat{\boldsymbol{\psi}}_k$ converges to a unique stable point in \mathcal{S} with probability one.*

Proof. See Appendix D. ■

Therefore, for the general step-size in (40), $\hat{\boldsymbol{\psi}}_k$ converges to a unique stable point. Except for the channel parameter vector $\boldsymbol{\psi}$, the antenna array gain of other stable points in \mathcal{S} is quite low, resulting in low tracking accuracy. Unfortunately, the estimated DPV may jump out of the main lobe in the tracking process and converge to other local optimal points due to the existence of observation noise. Hence, one key challenge is to ensure that the tracking algorithm converges to $\boldsymbol{\psi}$ rather than other stable points. Then we develop the following theorem to answer the second question:

Theorem 2 (Convergence to the DPV \mathbf{x}). *If (i) the initial estimate of \mathbf{x} is within the main lobe, i.e., $\hat{\mathbf{x}}_0 \in \mathcal{B}(\mathbf{x})$, and (ii) $b_{S,k}$ is given by (40) with $\epsilon_S > 0$, then there exist some $K_{S,0} \geq 0$ and $R > 0$ such that*

$$P(\hat{\mathbf{x}}_k \rightarrow \mathbf{x} \mid \hat{\mathbf{x}}_0 \in \mathcal{B}(\mathbf{x})) \geq 1 - 8e^{-\frac{R|\mathbf{s}|^2}{\epsilon_S^2 \sigma_z^2}}. \quad (41)$$

Proof. See Appendix E. ■

It is assumed that the beam estimator in Fig. 2 can output an initial estimate $\hat{\mathbf{x}}_0$ within the main lobe $\mathcal{B}(\mathbf{x})$. Under the condition $\hat{\mathbf{x}}_0 \in \mathcal{B}(\mathbf{x})$, Theorem 2 tells us the probability of $\hat{\mathbf{x}}_k \rightarrow \mathbf{x}$ is related to $\frac{|\mathbf{s}|^2}{\epsilon_S^2 \sigma_z^2}$. Hence, we can reduce the step-size and increase the transmit SNR $\frac{|\mathbf{s}|^2}{\sigma_z^2}$ to make sure that $\hat{\mathbf{x}}_k \rightarrow \mathbf{x}$ with probability one. Since $\hat{\boldsymbol{\psi}}_k$ converge to a unique stable point corresponding to the local optimal point, $\hat{\boldsymbol{\psi}}_k \rightarrow \boldsymbol{\psi}$ is also achieved when $\hat{\mathbf{x}}_k \rightarrow \mathbf{x}$.

The third question is answered by the following theorem:

Theorem 3 (Convergence to \mathbf{x} with minimum CRLB). *If (i) $\hat{\boldsymbol{\psi}}_k \rightarrow \boldsymbol{\psi}$ and (ii) $b_{S,k}$ is given by (40) with $\epsilon_S = 1$ and any $K_{S,0} \geq 0$, then $\hat{\mathbf{h}}_k - \mathbf{h}$ is asymptotically Gaussian and*

$$\lim_{k \rightarrow +\infty} \frac{k}{MN} \mathbb{E} \left[\left\| \hat{\mathbf{h}}_k - \mathbf{h} \right\|_2^2 \mid \hat{\boldsymbol{\psi}}_k \rightarrow \boldsymbol{\psi} \right] = C_S^{\min}(\boldsymbol{\psi}). \quad (42)$$

Proof. See Appendix F. ■

Theorem 3 tells us ϵ_S should not be too large or too small. By Theorem 3, if $\epsilon_S = 1$, then we achieve the minimum CRLB asymptotically with high probability.

VI. RECURSIVE BEAM TRACKING FOR DYNAMIC CASE I : PERFORMANCE BOUND, CONVERGENCE AND OPTIMALITY

In Dynamic Case I, the channel gain changes fast while the beam direction changes slowly. We assume that the beam direction keeps static, i.e., $\mathbf{x}_k = \mathbf{x} = [x_1, x_2]^T$. When the channel gain β_k changes fast, establishing theorems of tracking channel gain and beam direction simultaneously, as in Section V, is very difficult. Fortunately, acquiring the beam direction information is sufficient for alignment in mmWave mobile communication with analog beamforming. Hence, we only focus on beam direction tracking in Dynamic Case I.

In this section, we choose one special case to study for Dynamic Case I, i.e., β_k satisfies the Rayleigh distribution with $\mathbb{E}[|\beta_k|^2] = \sigma_\beta^2$. The conditional probability density function of the observation vector $\mathbf{y}_k \triangleq [y_{k,1}, y_{k,2}, y_{k,3}]^T$ is given by

$$p_{DI}(\mathbf{y}_k | \mathbf{x}, \mathbf{W}_k) = \frac{1}{\pi^3 |\Sigma_{\mathbf{y},k}|} e^{-\mathbf{y}_k^H \Sigma_{\mathbf{y},k}^{-1} \mathbf{y}_k}, \quad (43)$$

where $\Sigma_{\mathbf{y},k}$ is the covariance matrix of \mathbf{y}_k defined as follows:

$$\Sigma_{\mathbf{y},k} \triangleq \mathbb{E}[\mathbf{y}_k^H \mathbf{y}_k] = |\mathbf{s}|^2 \sigma_\beta^2 \mathbf{W}_k^H \mathbf{a}(\mathbf{x}) (\mathbf{W}_k^H \mathbf{a}(\mathbf{x}))^H + \sigma_z^2 \mathbf{J}_3 \quad (44)$$

with \mathbf{J}_3 denoting the 3-order identity matrix. Immediately, we can obtain that

$$|\Sigma_{\mathbf{y},k}| = \sigma_z^4 (\sigma_z^2 + |\mathbf{W}_k^H \mathbf{a}(\mathbf{x})|^2). \quad (45)$$

The following structure of this section is similar to Section V: we first formulate the beam tracking problem and provide the lower bound of it. Then we develop a tracking algorithm and prove this algorithm can converge to the minimum CRLB.

A. Problem Formulation

Since we only need to track the beam direction in Dynamic Case I, the estimation function in (8) is reformulated as follows:

$$\hat{\mathbf{x}}_k = \mathbf{F}_{DI,k}^e(\mathbf{W}_1, \dots, \mathbf{W}_k, \mathbf{y}_1, \dots, \mathbf{y}_k) \quad (46)$$

Let $\Xi_{DI,k} = (\mathbf{F}_k^c, \mathbf{F}_{DI,k}^e)$ denote a *causal* beam tracking scheme in k -th ECC: based on previously used EBMs $\mathbf{W}_1, \dots, \mathbf{W}_{k-1}$ and historical observations $\mathbf{y}_1, \dots, \mathbf{y}_{k-1}$, choose an appropriate EBM

\mathbf{W}_k , apply it to obtain \mathbf{y}_k and make an estimation of the DPV \mathbf{x} in k -th ECC by using all EBMs and observations available. Hence, in k -th ECC, the beam tracking problem is formulated as:

$$\min_{\Xi_{DI,k}} \mathbb{E} [\|\hat{\mathbf{x}}_k - \mathbf{x}\|_2^2] \quad (47)$$

$$\text{s.t. } \mathbb{E} [\hat{\mathbf{x}}_k] = \mathbf{x}, \quad (48)$$

$$(1), (2), (5), (7), (13), (46),$$

where the constraint (48) ensures that $\hat{\mathbf{x}}_k$ is an unbiased estimate of the DPV \mathbf{x} .

Before providing a specific tracking algorithm, we will first explore the performance bound of problem (47).

B. Cramér-Rao Lower Bound of Tracking Error

We now perform some theoretical analysis on beam tracking problem. Based on the CRLB theory in [26], we introduce the following lemma to obtain the lower bound of tracking error:

Lemma 4. *In Dynamic Case I, given $\mathbf{W}_1, \dots, \mathbf{W}_k$, the MSE of the DPV in (47) is lower bounded as follows:*

$$\mathbb{E} [\|\hat{\mathbf{x}}_k - \mathbf{x}\|_2^2] \geq \text{Tr} \left\{ \left(\sum_{l=1}^k \mathbf{I}_{DI}(\mathbf{x}, \mathbf{W}_l) \right)^{-1} \right\}. \quad (49)$$

The Fisher information matrix $\mathbf{I}_{DI}(\mathbf{x}, \mathbf{W}_l)$ is given by

$$\mathbf{I}_{DI}(\mathbf{x}, \mathbf{W}_l) \triangleq \mathbb{E} \left[\frac{\partial \log p_{DI}(\mathbf{y}_k | \mathbf{x}, \mathbf{W}_l)}{\partial \mathbf{x}} \cdot \frac{\partial \log p_{DI}(\mathbf{y}_k | \mathbf{x}, \mathbf{W}_l)}{\partial \mathbf{x}^T} \right], \quad (50)$$

where the p -th row, j -th column ($p = 1, 2; j = 1, 2$) of $\mathbf{I}_{DI}(\mathbf{x}, \mathbf{W}_l)$ is given in (51):

$$[\mathbf{I}_{DI}(\mathbf{x}, \mathbf{W}_l)]_{p,j} = \frac{\sigma_z^6 |\mathbf{s}|^6 \sigma_\beta^6}{|\Sigma_{\mathbf{y},k}|^2} \left\{ -2|\mathbf{g}_l|^2 \tilde{g}_{l,p} \tilde{g}_{l,j} + \frac{\sigma_z^2}{|\mathbf{s}|^2 \sigma_\beta^2} \text{Tr} \{ \mathbf{G}_{l,p} \mathbf{G}_{l,j} \} + \mathbf{g}_l^H (\mathbf{G}_{l,p} \mathbf{G}_{l,j} + \mathbf{G}_{l,j} \mathbf{G}_{l,p}) \mathbf{g}_l \right\} \quad (51)$$

with \mathbf{g}_l , $\tilde{g}_{l,p}$ and $\mathbf{G}_{l,p}$ defined below:

$$\begin{cases} \mathbf{g}_l \triangleq \mathbf{W}_l^H \mathbf{a}(\mathbf{x}) \\ \tilde{g}_{l,p} \triangleq \frac{\partial |\mathbf{g}_l|^2}{\partial x_p}, p = 1, 2 \\ \mathbf{G}_{l,p} \triangleq \frac{\partial \mathbf{g}_l \mathbf{g}_l^H}{\partial x_p}, p = 1, 2 \end{cases}. \quad (52)$$

Proof. We use Theorem 3.2 in [26] to prove Lemma 4. For the detailed proof, see Appendix G in [27]. ■

The CRLB in (49) is a function of the EBMs $\mathbf{W}_1, \dots, \mathbf{W}_k$. Similar to that in Quasi-static Case, we consider the normalized CRLB:

$$C_{DI}(\mathbf{x}, \mathbf{W}) \triangleq \text{Tr} \{ \mathbf{I}_{DI}(\mathbf{x}, \mathbf{W})^{-1} \}. \quad (53)$$

By optimizing only one EBM \mathbf{W} , we can further get the *minimum CRLB*, given by

$$C_{DI}^{\min}(\mathbf{x}) = \min_{\mathbf{W}} C_{DI}(\mathbf{x}, \mathbf{W}) = C_{DI}(\mathbf{x}, \mathbf{W}_{DI}^*). \quad (54)$$

Solving problem (54) yields the optimal EBM $\mathbf{W}_{DI}^* = [\mathbf{w}_{DI,1}^*, \mathbf{w}_{DI,2}^*, \mathbf{w}_{DI,3}^*]$:

$$\mathbf{w}_{DI,i}^* = \frac{1}{\sqrt{MN}} \mathbf{a}(\mathbf{x} + \Delta_{DI,i}^*), i = 1, 2, 3, \quad (55)$$

where $\Delta_{DI,1}^*, \Delta_{DI,2}^*, \Delta_{DI,3}^*$ denote the optimal exploring offsets in Dynamic Case I.

C. Asymptotically Optimal EBM

Consider the optimal EBM \mathbf{W}_{DI}^* now. In (54), three EBVs need to be optimized, i.e., three 2D exploring offsets need to be determined. Numerical search is a feasible way to obtain the three optimal exploring offsets. However, it may result in high complexity since these optimal offsets may change with some system parameters, e.g., channel gain parameter σ_β^2 , the DPV \mathbf{x} and antenna array size M, N . This leads to the question that how these parameters affect the optimal offsets. Then the following lemma is proposed to answer the question.

Lemma 5. *In Dynamic Case I, the optimal exploring offsets $\Delta_{DI,1}^*, \Delta_{DI,2}^*, \Delta_{DI,3}^*$ have the following three properties:*

- 1) $\Delta_{DI,1}^*, \Delta_{DI,2}^*, \Delta_{DI,3}^*$ are invariant to the DPV \mathbf{x} ;
- 2) $\Delta_{DI,1}^*, \Delta_{DI,2}^*, \Delta_{DI,3}^*$ are variant to $\frac{|s|^2 \sigma_\beta^2}{\sigma_z^2}$ and converge to constant values as $\frac{|s|^2 \sigma_\beta^2}{\sigma_z^2} \rightarrow +\infty$;
- 3) $\Delta_{DI,1}^*, \Delta_{DI,2}^*, \Delta_{DI,3}^*$ converge to constant values as $M, N \rightarrow +\infty$:

$$\tilde{\Delta}_{DI,i}^* \triangleq \lim_{M, N \rightarrow +\infty} \Delta_{DI,i}^*, i = 1, 2, 3 \quad (56)$$

and $\tilde{\Delta}_{DI,1}^*, \tilde{\Delta}_{DI,2}^*, \tilde{\Delta}_{DI,3}^*$ are unrelated to $\frac{|s|^2 \sigma_\beta^2}{\sigma_z^2}$.

Proof. Lemma 5 is obtained by exploring the property of the Fisher information matrix in (50). Due to the space limitation, the detailed proof is omitted here and provided in Appendix H of [27]. ■

Lemma 5 reveals that $\Delta_{DI,1}^*, \Delta_{DI,2}^*, \Delta_{DI,3}^*$ are only related to array size M, N and $\frac{|s|^2 \sigma_\beta^2}{\sigma_z^2}$. Hence, the numerical search times can be reduced to one for a particular array size M, N and a

TABLE II: Asymptotically optimal exploring offsets in Dynamic Case I.

$\tilde{\Delta}_{DI,1}^*$	$\tilde{\Delta}_{DI,2}^*$	$\tilde{\Delta}_{DI,3}^*$
$[0.5486, 0.2451]^T$	$[-0.5462, 0.2482]^T$	$[-0.0012, -0.6837]^T$

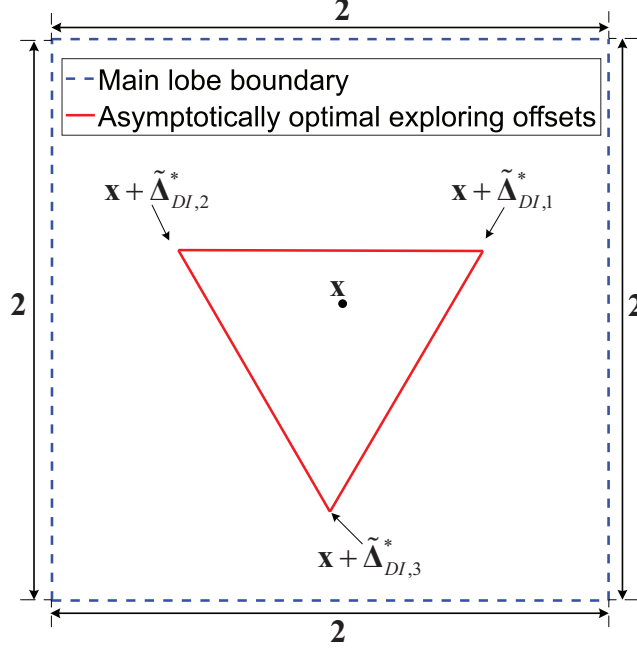


Fig. 5: Asymptotically optimal exploring offsets in Dynamic Case I.

particular $\frac{|s|^2 \sigma_\beta^2}{\sigma_z^2}$. Numerically, we find later that even if $\Delta_{DI,1}^*$, $\Delta_{DI,2}^*$, $\Delta_{DI,3}^*$ may change for different array sizes and $\frac{|s|^2 \sigma_\beta^2}{\sigma_z^2}$, $\tilde{\Delta}_{DI,1}^*$, $\tilde{\Delta}_{DI,2}^*$, $\tilde{\Delta}_{DI,3}^*$ can be used to take the place of $\Delta_{DI,1}^*$, $\Delta_{DI,2}^*$, $\Delta_{DI,3}^*$ as long as M and N are sufficiently large and $\frac{|s|^2 \sigma_\beta^2}{\sigma_z^2}$ is not quite small. Therefore, the numerical search times is reduced to one in the end.

By numerical search in the main lobe of the DPV in (6), we can obtain the asymptotically optimal exploring offsets $\tilde{\Delta}_{DI,1}^*$, $\tilde{\Delta}_{DI,2}^*$, $\tilde{\Delta}_{DI,3}^*$ in TABLE II and Fig. 5. With these offsets, a general way to generate the asymptotically optimal EBM $\tilde{\mathbf{W}}_{DI}^* = [\tilde{\mathbf{w}}_{DI,1}^*, \tilde{\mathbf{w}}_{DI,2}^*, \tilde{\mathbf{w}}_{DI,3}^*]$ is obtained to achieve the minimum CRLB as below:

$$\tilde{\mathbf{w}}_{DI,i}^* = \frac{1}{\sqrt{MN}} \mathbf{a}(\mathbf{x} + \tilde{\Delta}_{DI,i}^*), i = 1, 2, 3. \quad (57)$$

By adopting $\tilde{\Delta}_{DI,1}^*$, $\tilde{\Delta}_{DI,2}^*$, $\tilde{\Delta}_{DI,3}^*$ to smaller size antenna arrays when $\frac{|s|^2 \sigma_\beta^2}{\sigma_z^2} = 0\text{dB}$, we compare the minimum CRLB and the CRLB achieved by $\tilde{\Delta}_{DI,1}^*$, $\tilde{\Delta}_{DI,2}^*$, $\tilde{\Delta}_{DI,3}^*$ in TABLE II.

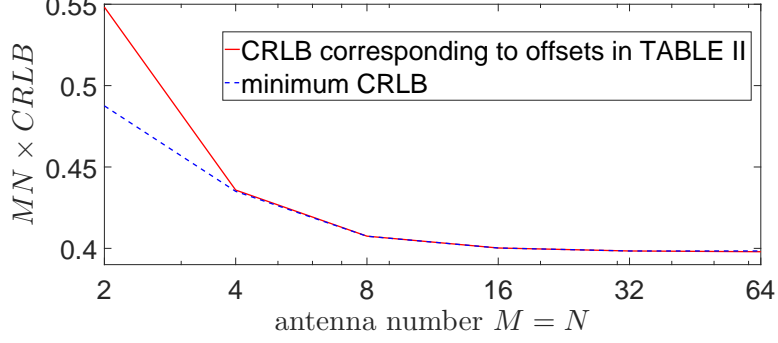


Fig. 6: Performance of offsets in TABLE II when $\frac{|s|^2 \sigma_\beta^2}{\sigma_z^2} = 0\text{dB}$.

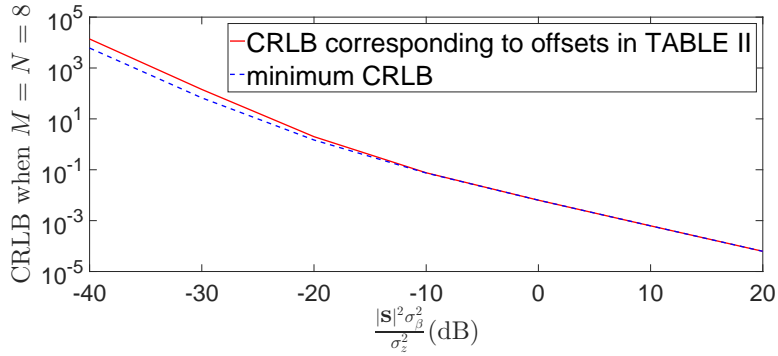


Fig. 7: Performance of offsets in TABLE II when $M = N = 8$.

As illustrated in Fig. 6, when antenna number $M = N \geq 8$, we can approach the minimum CRLB with a relative error less than 0.1% by using $\tilde{\Delta}_{DI,1}^*$, $\tilde{\Delta}_{DI,2}^*$, $\tilde{\Delta}_{DI,3}^*$.

By applying $\tilde{\Delta}_{DI,1}^*$, $\tilde{\Delta}_{DI,2}^*$, $\tilde{\Delta}_{DI,3}^*$ to different $\frac{|s|^2 \sigma_\beta^2}{\sigma_z^2}$ when $M = N = 8$, we compare the minimum CRLB and the CRLB achieved by $\tilde{\Delta}_{DI,1}^*$, $\tilde{\Delta}_{DI,2}^*$, $\tilde{\Delta}_{DI,3}^*$ in TABLE II. As illustrated in Fig. 7, when $\frac{|s|^2 \sigma_\beta^2}{\sigma_z^2} \geq 0\text{dB}$, we can approach the minimum CRLB with a relative error less than 0.1% by using $\tilde{\Delta}_{DI,1}^*$, $\tilde{\Delta}_{DI,2}^*$, $\tilde{\Delta}_{DI,3}^*$.

Therefore, with $\tilde{\Delta}_{DI,1}^*$, $\tilde{\Delta}_{DI,2}^*$, $\tilde{\Delta}_{DI,3}^*$, the minimum CRLB is obtained for different beam directions, different $\frac{|s|^2 \sigma_\beta^2}{\sigma_z^2}$ and different antenna numbers when $\frac{|s|^2 \sigma_\beta^2}{\sigma_z^2} \geq 0\text{dB}$ and $M = N > 8$.

Algorithm 2 Recursive Beam Tracking for Dynamic Case I

1) **Exploration and Receive:** Transmit 3 pilot sequences in each ECC. The corresponding EPV for receiving the i -th pilot sequence in k -th ECC is given below:

$$\mathbf{w}_{k,i} = \frac{1}{\sqrt{MN}} \mathbf{a} \left(\hat{\mathbf{x}}_{k-1} + \tilde{\mathbf{\Delta}}_{DI,i}^* \right), i = 1, 2, 3, \quad (59)$$

where $\hat{\mathbf{x}}_k = [\hat{x}_{k,1}, \hat{x}_{k,2}]^T$ and $\tilde{\mathbf{\Delta}}_{DI,i}^*$ ($i = 1, 2, 3$) are given by TABLE II. After match filtering, the observation vector \mathbf{y}_k is obtained in (3).

2) **Estimate Update:** The estimate $\hat{\mathbf{x}}_k = [\hat{x}_{k,1}, \hat{x}_{k,2}]^T$ is updated by

$$\hat{\mathbf{x}}_k = \hat{\mathbf{x}}_{k-1} + b_{DI,k} \mathbf{I}_{DI}(\hat{\mathbf{x}}_{k-1}, \mathbf{W}_k)^{-1} \left. \frac{\partial \log p_{DI}(\mathbf{y}_k | \mathbf{x}, \mathbf{W}_k)}{\partial \mathbf{x}} \right|_{\mathbf{x}=\hat{\mathbf{x}}_{k-1}}, \quad (60)$$

where $\mathbf{I}_{DI}(\hat{\mathbf{x}}_{k-1}, \mathbf{W}_k)$ is defined in (50) and $b_{DI,k}$ is the step size that will be specified later.

D. Recursive Beam Tracking with Asymptotic Optimality Analysis

We now provide a specific beam tracking algorithm to approach the minimum CRLB in (54). The proposed tracker is motivated by the following maximization likelihood problem:

$$\max_{\mathbf{W}_k} \left\{ \max_{\hat{\mathbf{x}}} \mathbb{E} \left[\sum_{l=1}^k \left(\log p_S(\mathbf{y}_l | \hat{\mathbf{x}}, \mathbf{W}_l) \middle| \begin{array}{c} \mathbf{W}_1, \dots, \mathbf{W}_{l-1} \\ \mathbf{y}_1, \dots, \mathbf{y}_{l-1} \end{array} \right) \right] \right\}. \quad (58)$$

Similar to that in Section V, we propose a two-layer nested optimization algorithm to find the solution of (58). Finally, the proposed tracking algorithm is given in Algorithm 2.

We now perform the asymptotic optimality analysis. Diminishing step-size is adopted in (61), according to [30]–[32]

$$b_{DI,k} = \frac{\epsilon_{DI}}{k + K_{DI,0}}, k = 1, 2, \dots \quad (61)$$

where $K_{DI,0} \geq 0$ and $\epsilon_{DI} > 0$. Then we can prove that if the initial estimate $\hat{\mathbf{x}}_0$ is within the main lobe and $\epsilon_{DI} = 1$, the proposed algorithm can converge to \mathbf{x} with the minimum CRLB asymptotically, i.e.,

$$\lim_{k \rightarrow +\infty} k \mathbb{E} [\|\hat{\mathbf{x}}_k - \mathbf{x}\|_2^2] = C_{DI}^{\min}(\mathbf{x}). \quad (62)$$

The proof is similar to that in Section V and the details are omitted here since nothing new is provided in the proof.

Algorithm 3 Joint Beam and Channel Tracking for Dynamic Case II

1) **Exploration and Receive:** Transmit 3 pilot sequences in each ECC. The corresponding EPV for receiving the i -th pilot sequence in k -th ECC is given below:

$$\mathbf{w}_{k,i} = \frac{1}{\sqrt{MN}} \mathbf{a}(\hat{\mathbf{x}}_{k-1} + \mathbf{\Delta}_{DII,i}), i = 1, 2, 3, \quad (64)$$

where $\hat{\mathbf{x}}_k = [\hat{x}_{k,1}, \hat{x}_{k,2}]^T$ and $\mathbf{\Delta}_{DII,i} = \tilde{\mathbf{\Delta}}_{S,i}^*$ ($i = 1, 2, 3$) are given by TABLE I. After match filtering, the observation vector \mathbf{y}_k is obtained in (3).

2) **Estimate Update:** The estimate $\hat{\boldsymbol{\psi}}_k = [\hat{\beta}_k^{\text{re}}, \hat{\beta}_k^{\text{im}}, \hat{x}_{k,1}, \hat{x}_{k,2}]^T$ is updated by

$$\hat{\boldsymbol{\psi}}_k = \hat{\boldsymbol{\psi}}_{k-1} + b_{DII,k} \mathbf{I}_S(\hat{\boldsymbol{\psi}}_{k-1}, \mathbf{W}_k)^{-1} \left. \frac{\partial \log p_{DII}(\mathbf{y}_k | \boldsymbol{\psi}_k, \mathbf{W}_k)}{\partial \boldsymbol{\psi}_k} \right|_{\boldsymbol{\psi}_k = \hat{\boldsymbol{\psi}}_{k-1}},$$

where $\mathbf{I}_S(\hat{\boldsymbol{\psi}}_{k-1}, \mathbf{W}_k)$ is the Fisher information matrix defined in (18) and $b_{DII,k}$ is the step size for Dynamic Case II.

VII. JOINT BEAM AND CHANNEL TRACKING FOR DYNAMIC CASE II

In Dynamic Case II where both the channel gain β_k and the DPV \mathbf{x}_k change fast, the conditional probability density function of the observation vector \mathbf{y}_k is given by

$$p_{DII}(\mathbf{y}_k | \boldsymbol{\psi}_k, \mathbf{W}_k) = \frac{1}{\pi^3 \sigma_z^6} e^{-\frac{\|\mathbf{y}_k - |s| \beta_k \mathbf{W}_k^H \mathbf{a}(\mathbf{x}_k)\|_2^2}{\sigma_z^2}}. \quad (63)$$

Establishing theorems of tracking, as in Section V and Section VI, is very difficult in Dynamic Case II. Even if theoretical analysis is not conducted in this section, we still provide a tracking algorithm.

Inspired by the asymptotically optimal tracking algorithm in Section V and Section VI, we design a similar joint beam and channel tracking algorithm in Algorithm 3.

Different from the step-size in Quasi-static Case and Dynamic Case I, we adopt constant step-size in Dynamic Case II because diminishing step-size cannot track the fast-changing β_k and \mathbf{x}_k . The constant step-size $b_{DII,k}$ will be specified later.

VIII. NUMERICAL RESULTS

We obtain some numerical results to verify the performance of our proposed tracking algorithms for Quasi-static Case, Dynamic Case I and Dynamic Case II. Reference algorithms include the compressed sensing algorithm in [9], the IEEE 802.11ad algorithm in [15], the

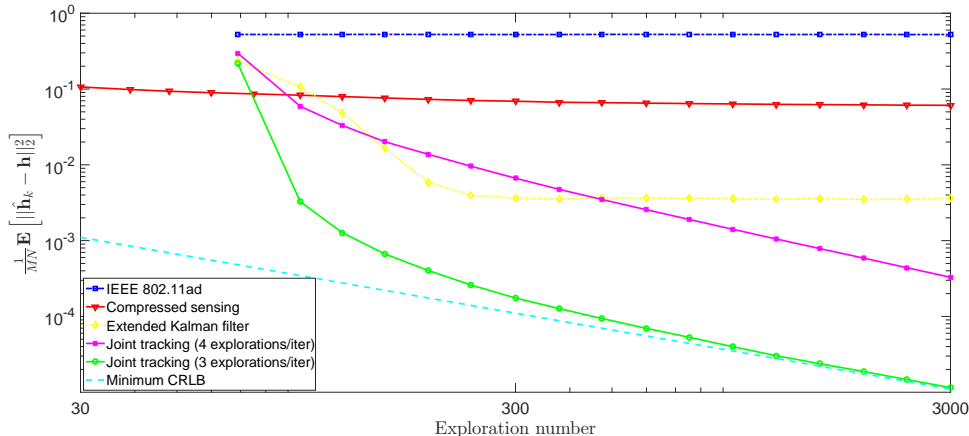


Fig. 8: $\frac{1}{MN}\text{MSE}_{\mathbf{h}}$ in Quasi-static Case.

extended Kalman filter (EKF) method in [16] and the joint beam and channel tracking algorithm in [18] (using two explorations to track each dimension of the 2D beam direction).

Based on the model in Section II, the parameters are set as: $M=N=8$, the antenna spacing $d_1=d_2=\frac{\lambda}{2}$, the codebook size $M_0=2M$, $N_0=2N$, and the transmit SNR $=\frac{|\mathbf{s}|^2}{\sigma_z^2}=5\text{dB}$.

For initial estimate before tracking in Fig. 2, an exhaustive beam sweeping is conducted for our proposed algorithms and the EKF method in [16]. Then an initial estimate is obtained by using the orthogonal matching pursuit method in [33]. This ensures that the initial estimated DPV $\hat{\mathbf{x}}_0$ is within the main lobe in (6). As for the compressed sensing and IEEE 802.11ad tracking algorithm, the initial estimate can be obtained by the algorithm itself.

As for tracking, three explorations are conducted in each ECC for all the algorithms to ensure fairness. When adopting the joint beam and channel tracking algorithm by using four explorations, we use a buffer to store the received observations and update the estimate when receiving four new observations. Next we will show the performance of these tracking algorithms separately.

A. Quasi-static Case

In Quasi-static Case, the AoA (θ, ϕ) as defined in Section II is chosen evenly and randomly in $\theta \in [0, \frac{\pi}{2}]$, $\phi \in [-\pi, \pi)$. The channel gain β is modeled as Rician fading with a K-factor $\kappa=15\text{dB}$, according to the channel model in [34]. The step-size is set as $b_{S,k}=\frac{1}{k}$. Simulation results are averaged over 1000 random system realizations. Fig. 8 indicates that the channel

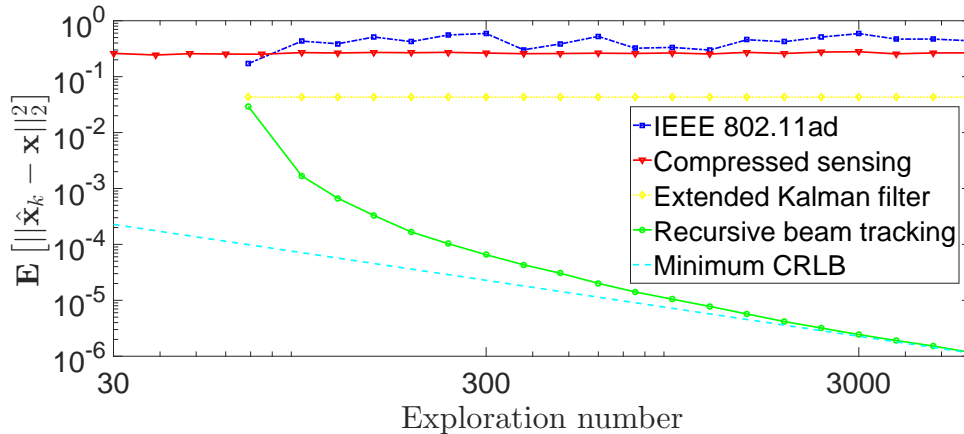


Fig. 9: MSE_x in Dynamic Case I.

vector MSE of our proposed algorithm approaches the minimum CRLB quickly and achieves much lower tracking error than other algorithms.

B. Dynamic Case I

In Dynamic Case I, the AoA (θ, ϕ) as defined in Section II is chosen evenly and randomly in $\theta \in [0, \frac{\pi}{2}]$, $\phi \in [-\pi, \pi)$. The channel gain β_k is modeled as Rayleigh fading with $\frac{|s|^2 \sigma_\beta^2}{\sigma_z^2} = 5\text{dB}$. The tracking step-size is set as $b_{DI,k} = \frac{1}{k}$. Simulation results are averaged over 1000 random system realizations. Fig. 9 indicates that the DPV MSE of our proposed algorithm can converge to the minimum CRLB and achieves much lower tracking error than other algorithms.

C. Dynamic Case II

In Dynamic Case II, the AoA (θ_k, ϕ_k) as defined in Section II is modeled as a random walk process, i.e., $\theta_{k+1} = \theta_k + \Delta\theta$, $\phi_{k+1} = \phi_k + \Delta\phi$; $\Delta\theta, \Delta\phi \sim \mathcal{CN}(0, \delta_A^2)$. The initial AoA values are chosen evenly and randomly in $\theta_0 \in [0, \frac{\pi}{2}]$, $\phi_0 \in [-\pi, \pi)$. The channel gain is modeled as a first-order Gaussian-Markov process, i.e., $\beta_{k+1} = \rho\beta_k + \gamma_k$, where $\gamma_k \sim \mathcal{CN}(0, 1 - \rho^2)$. We adopt $\rho = 0.995$ in simulation. The initial channel gain β_0 is modeled as Rician fading with a K-factor $\kappa=15\text{dB}$, according to the channel model in [34]. As for the step-size, numerical results show that when $b_{DII,k} = 0.7$, the joint beam and channel tracking algorithm can track beams with higher velocity. Hence the step-size is set as a constant $b_{DII,k} = 0.7$. Simulation results are averaged over 1000 random system realizations. Fig. 10 indicates the proposed algorithm can

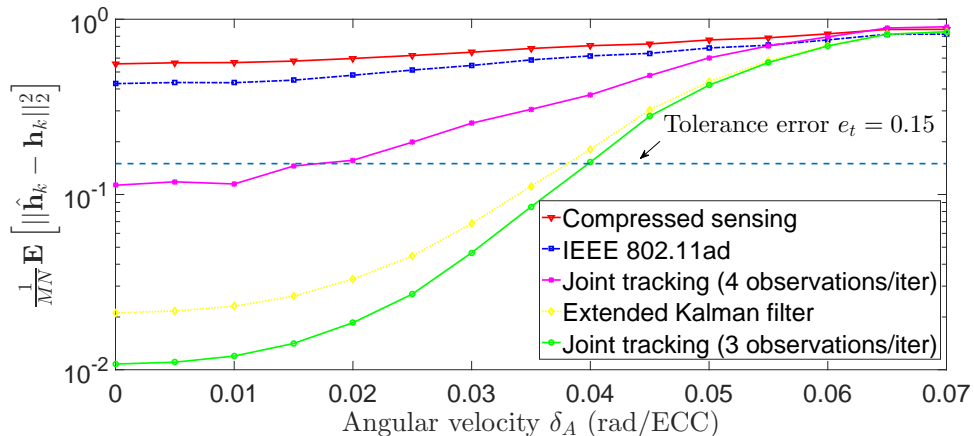


Fig. 10: $\frac{1}{MN} \text{MSE}_{\mathbf{h}_k}$ in Dynamic Case II.

achieve higher tracking accuracy than the other four algorithms. In addition, if we set a tolerance error e_t , e.g., $e_t = 0.15$, then our algorithm can support higher angular velocities.

IX. CONCLUSION

This paper focuses on fast accurate beam and channel tracking for 2D phased antenna arrays. We have developed corresponding tracking algorithms according to different practical channel change models. In Quasi-static Case and Dynamic Case I, the proposed algorithms are proved to converge to the minimum CRLB. In Dynamic Case II, our algorithm can achieve faster and more accurate tracking than several existing algorithms.

This work is the first step to beam and channel tracking with 2D phased antenna arrays. In future work, we will further study the following problems: i) establishing the corresponding theorems in Dynamic Case II; ii) jointly tracking multiple paths; iii) tracking at both the transmitter and receiver.

REFERENCES

- [1] Z. Pi and F. Khan, "An introduction to millimeter-wave mobile broadband systems," *IEEE Commun. Mag.*, vol. 49, no. 6, Jun. 2011.
- [2] E. G. Larsson, O. Edfors, F. Tufvesson, and T. L. Marzetta, "Massive MIMO for next generation wireless systems," *IEEE Commun. Mag.*, vol. 52, no. 2, Feb. 2014.
- [3] S. Han, C. L. I, Z. Xu, and C. Rowell, "Large-scale antenna systems with hybrid analog and digital beamforming for millimeter wave 5G," *IEEE Commun. Mag.*, vol. 53, no. 1, Jan. 2015.
- [4] R. W. Heath, N. González-Prelcic, S. Rangan, W. Roh, and A. M. Sayeed, "An overview of signal processing techniques for millimeter wave MIMO systems," *IEEE J. Sel. Top. Signal Process.*, Apr. 2016.

- [5] A. F. Molisch and V. V. R. and, "Hybrid beamforming for massive MIMO-a survey," *IEEE Commun. Mag.*, vol. 55, no. 9, Sep. 2017.
- [6] S. Hur, T. Kim, D. J. Love, J. V. Krogmeier, T. A. Thomas, and A. Ghosh, "Millimeter wave beamforming for wireless backhaul and access in small cell networks," *IEEE Trans. Commun.*, Oct. 2013.
- [7] A. Alkhateeb, O. E. Ayach, G. Leus, and R. W. Heath, "Channel estimation and hybrid precoding for millimeter wave cellular systems," *IEEE J. Sel. Top. Signal Process.*, vol. 8, no. 5, Oct. 2014.
- [8] D. Zhu, J. Choi, and R. W. Heath Jr, "Auxiliary beam pair enabled AoD and AoA estimation in closed-loop large-scale mmWave MIMO system," *arXiv preprint arXiv:1610.05587*, 2016.
- [9] A. Alkhateeb, G. Leusz, and R. W. Heath, "Compressed sensing based multi-user millimeter wave systems: How many measurements are needed?" in *IEEE ICASSP*, Apr. 2015.
- [10] A. Alkhateeb, G. Leus, and R. W. Heath, "Limited feedback hybrid precoding for multi-user millimeter wave systems," *IEEE Trans. Wireless Commun.*, vol. 14, no. 11, Nov. 2015.
- [11] C. Zhang, D. Guo, and P. Fan, "Mobile millimeter wave channel acquisition, tracking, and abrupt change detection," *arXiv preprint arXiv:1610.09626*, 2016.
- [12] S. Sun, T. S. Rappaport, R. W. Heath, A. Nix, and S. Rangan, "MIMO for millimeter-wave wireless communications: Beamforming, spatial multiplexing, or both?" *IEEE Commun. Mag.*, vol. 52, no. 12, Dec. 2014.
- [13] A. Puglielli, A. Townley, G. LaCaille, V. Milovanovi, P. Lu, K. Trotskovsky, A. Whitcombe, N. Narevsky, G. Wright, T. Courtade, E. Alon, B. Nikoli, and A. M. Niknejad, "Design of energy- and cost-efficient massive MIMO arrays," *Proc. IEEE*, vol. 104, no. 3, Mar. 2016.
- [14] X. Gao, L. Dai, Y. Zhang, T. Xie, X. Dai, and Z. Wang, "Fast channel tracking for Terahertz beamspace massive MIMO systems," *IEEE Trans. Veh. Technol.*, vol. 66, no. 7, Jul. 2017.
- [15] IEEE standard, "IEEE 802.11ad WLAN enhancements for very high throughput in the 60 GHz band," Dec. 2012.
- [16] V. Va, H. Vikalo, and R. W. Heath, "Beam tracking for mobile millimeter wave communication systems," in *IEEE GlobalSIP*, Dec. 2016.
- [17] J. Li, Y. Sun, L. Xiao, S. Zhou, and C. E. Koksall, "Analog beam tracking in linear antenna arrays: Convergence, optimality, and performance," in *51st Asilomar Conference*, 2017.
- [18] J. Li, Y. Sun, L. Xiao, S. Zhou, and A. Sabharwal, "How to mobilize mmWave: A joint beam and channel tracking approach," *arXiv preprint arXiv:1802.02125*, 2018.
- [19] T. S. Rappaport, F. Gutierrez, E. Ben-Dor, J. N. Murdock, Y. Qiao, and J. I. Tamir, "Broadband millimeter-wave propagation measurements and models using adaptive-beam antennas for outdoor urban cellular communications," *IEEE Trans. Antennas and Propag.*, vol. 61, no. 4, Apr. 2013.
- [20] G. Brown, O. Koymen, and M. Branda, "The promise of 5G mmWave - How do we make it mobile?" *Qualcomm Technologies*, Jun. 2016.
- [21] W. Roh, J. Y. Seol, and et al, "Millimeter-wave beamforming as an enabling technology for 5G cellular communications: Theoretical feasibility and prototype results," *IEEE Commun. Mag.*, vol. 52, no. 2, Feb. 2014.
- [22] R. Bhattacharya, T. K. Bhattacharyya, and R. Garg, "Position mutated hierarchical particle swarm optimization and its application in synthesis of unequally spaced antenna arrays," *IEEE Trans. Antennas Propag.*, vol. 60, no. 7, Jul. 2012.
- [23] Z. Xiao, P. Xia, and X. gen Xia, "Enabling UAV cellular with millimeter-wave communication: potentials and approaches," *IEEE Commun. Mag.*, vol. 54, no. 5, May. 2016.
- [24] Hauskrecht.M, "Value-function approximations for partially observable markov decisionprocesses," *Journal of Artificial Intelligence Research*, vol. 13, no. 1, pp. 33–94, 2000.

- [25] W. S. Lovejoy, "Computationally feasible bounds for partially observed markov decision processes," *Operations Research*, vol. 39, no. 1, pp. 162–175, 1991.
- [26] S. Sengijpta, "Fundamentals of statistical signal processing: Estimation theory," *Technometrics*, vol. 37, Nov. 1995.
- [27] Y. Liu, J. Li, X. Zhang, and S. Zhou, "Fast accurate beam and channel tracking for two-dimensional phased antenna arrays," *arXiv preprint arXiv:1907.00173*, 2019.
- [28] J. C. Spall, *Introduction to Stochastic Search and Optimization*, 2003.
- [29] J. Chung, M. Chung, J. T. Slagel, and L. Tenorio, "Stochastic newton and quasi-newton methods for large linear least-squares problems," *arXiv preprint arXiv:1702.07367*, 2017.
- [30] M. B. Nevel'son and R. Z. Has'minskii, *Stochastic approximation and recursive estimation*, 1973.
- [31] H. Kushner and G. G. Yin, *Stochastic approximation and recursive algorithms and applications*, 2003, vol. 35.
- [32] V. S. Borkar, *Stochastic approximation: a dynamical systems viewpoint*, 2008.
- [33] L. W. T Tony Cai, "Orthogonal matching pursuit for sparse signal recovery with noise," *IEEE Transactions on Information Theory*, vol. 57, no. 7, pp. 4680–4688, 2011.
- [34] S. S. M. K. Samimi, G. R. MacCartney and T. S. Rappaport, "28 GHz millimeter-wave ultrawideband small-scale fading models in wireless channels," in *2016 IEEE VTC Spring*, May. 2016.
- [35] J. Li, Y. Sun, L. Xiao, S. Zhou, and C. E. Koksal, "Fast analog beam tracking in phased antenna arrays: Theory and performance," *arXiv preprint arXiv:1710.07873*, 2017.

APPENDIX A

PROOF OF LEMMA 1

If the EBVs are of steering vector forms, i.e., $\mathbf{w}_{k,i} = \frac{1}{\sqrt{MN}} \mathbf{a}(\omega_{k,i})$, where $\omega_{k,i} = [\omega_{k,i1}, \omega_{k,i2}]^T$ denotes the i -th exploring DPV in k -th ECC, then the noiseless complex observation equation for the i -th observation is given below:

$$\begin{aligned}
 y_{k,i} &= \frac{|\mathbf{s}| \beta_k}{\sqrt{MN}} \mathbf{a}(\omega_{k,i})^H \mathbf{a}(\mathbf{x}_k) \\
 &= \frac{|\mathbf{s}| \beta_k}{\sqrt{MN}} \sum_{m=1}^M \sum_{n=1}^N e^{-j2\pi \left[\frac{(m-1)(\omega_{k,i1} - x_{k,1})}{M} + \frac{(n-1)(\omega_{k,i2} - x_{k,2})}{N} \right]} \\
 &= \frac{|\mathbf{s}| \beta_k}{\sqrt{MN}} \frac{\sin \left[\pi(\omega_{k,i1} - x_{k,1}) \right]}{\sin \left[\frac{\pi(\omega_{k,i1} - x_{k,1})}{M} \right]} \frac{\sin \left[\pi(\omega_{k,i2} - x_{k,2}) \right]}{\sin \left[\frac{\pi(\omega_{k,i2} - x_{k,2})}{N} \right]} e^{-j\pi \left[\frac{M-1}{M}(\omega_{k,i1} - x_{k,1}) + \frac{N-1}{N}(\omega_{k,i2} - x_{k,2}) \right]} \\
 &\stackrel{(a)}{=} \frac{|\mathbf{s}| \beta_k}{\sqrt{MN}} y_a(\omega_{k,i} - \mathbf{x}_k) e^{-j\pi \left[\frac{M-1}{M}(\omega_{k,i1} - x_{k,1}) + \frac{N-1}{N}(\omega_{k,i2} - x_{k,2}) \right]},
 \end{aligned} \tag{65}$$

where Step (a) follows the definition of $y_a(\Delta)$:

$$y_a(\Delta) \triangleq \frac{\sin(\pi \delta_1) \sin(\pi \delta_2)}{\sin\left(\frac{\pi \delta_1}{M}\right) \sin\left(\frac{\pi \delta_2}{N}\right)} \tag{66}$$

with $\Delta = [\delta_1, \delta_2]^T$.

The complex observation equation in (65) contains two real equations, i.e., an amplitude equation and a phase angle equation. From (65), we can obtain the phase angle equation:

$$\begin{cases} \angle(y_{k,i}) = \angle(|\mathbf{s}|\beta_k) - \pi \left[\frac{M-1}{M}(\omega_{k,i1} - x_{k,1}) + \frac{N-1}{N}(\omega_{k,i2} - x_{k,2}) \right], y_a(\boldsymbol{\omega}_{k,i} - \mathbf{x}_k) \geq 0 \\ \angle(y_{k,i}) = \angle(|\mathbf{s}|\beta_k) - \pi \left[\frac{M-1}{M}(\omega_{k,i1} - x_{k,1}) + \frac{N-1}{N}(\omega_{k,i2} - x_{k,2}) \right] + \pi, y_a(\boldsymbol{\omega}_{k,i} - \mathbf{x}_k) < 0 \end{cases} \quad (67)$$

Then the relationship between the phase angles of two different observations $y_{k,i}$ and $y_{k,j}$ ($i \neq j$) is given in (68),

$$\begin{cases} \angle(y_{k,i}) - \angle(y_{k,j}) = \pi \left[\frac{M-1}{M}(\omega_{k,j1} - \omega_{k,i1}) + \frac{N-1}{N}(\omega_{k,j2} - \omega_{k,i2}) \right], y_a(\boldsymbol{\omega}_{k,j} - \mathbf{x}_k) y_a(\boldsymbol{\omega}_{k,i} - \mathbf{x}_k) > 0 \\ \angle(y_{k,i}) - \angle(y_{k,j}) = \pi \left[\frac{M-1}{M}(\omega_{k,j1} - \omega_{k,i1}) + \frac{N-1}{N}(\omega_{k,j2} - \omega_{k,i2}) \right] + \pi, \text{else} \end{cases} \quad (68)$$

where $\omega_{k,j1} - \omega_{k,i1}$ and $\omega_{k,j2} - \omega_{k,i2}$ are determined by the exploring DPV and unrelated to the channel parameter vector $\boldsymbol{\psi}_k$. From (68), we can know that once the exploring directions are determined, the relative phase angle between two observations belongs to one of the two constant values that are unrelated to $\boldsymbol{\psi}_k$. In other words, the relative phase angles can help nothing in unique estimation.

Then we explore the minimum observation overhead of the following two cases:

1) If we want to obtain unique estimate of $\boldsymbol{\psi}_k$ within one ECC, at least 4 independent real equations with respect to $\boldsymbol{\psi}_k$ are needed since $\boldsymbol{\psi}_k$ contains four real variables (i.e., the real part β_k^{re} , the imaginary part β_k^{im} of channel gain β_k and the two direction parameters $x_{k,1}, x_{k,2}$). After q explorations in each ECC, we can obtain q independent amplitude equations and only 1 independent phase angle equation, which are $q + 1$ independent real equations with respect to $\boldsymbol{\psi}_k$ in total. Hence, at least 3 explorations are needed to obtain 4 independent real equations and estimate 4 real variables of $\boldsymbol{\psi}_k$.

2) If we only want to obtain unique estimate of \mathbf{x}_k within one ECC, at least 2 independent real equations with respect to \mathbf{x}_k are needed since \mathbf{x}_k contains two real variables (i.e., two direction parameters $x_{k,1}, x_{k,2}$). It seems that fewer explorations are sufficient. However, we cannot obtain any absolute amplitude and phase information with respect to \mathbf{x}_k from one observation in (65) since β_k is unknown. In addition, the relative phase angles are one of two determined values that are unrelated to \mathbf{x}_k . Thus, the phase angle equations are useless for estimating \mathbf{x}_k . After q explorations in each ECC, we can obtain $q - 1$ independent relative amplitude equations with respect to \mathbf{x}_k in total. Hence, at least 3 explorations are needed to obtain 2 independent real equations and estimate 2 real variables of \mathbf{x}_k .

Therefore, the proof is completed.

APPENDIX B

PROOF OF LEMMA 2

In problem (14), the constraint (10) ensures that $\hat{\mathbf{h}}_k$ is an unbiased estimate of \mathbf{h} . Consider each element of the channel vector \mathbf{h} , i.e., $h_{mn}(\boldsymbol{\psi}) = \beta e^{j2\pi(\frac{m-1}{M}x_1 + \frac{n-1}{N}x_2)}$. Immediately we have $\mathbb{E}[h_{mn}(\hat{\boldsymbol{\psi}}_k)] = h_{mn}(\boldsymbol{\psi})$ since $\mathbb{E}[\hat{\mathbf{h}}_k] = \mathbf{h}$. According to section 3.8 of [26], if a function $f(\hat{\boldsymbol{\psi}})$ is an unbiased estimate of $f(\boldsymbol{\psi})$, i.e., $\mathbb{E}[f(\hat{\boldsymbol{\psi}})] = f(\boldsymbol{\psi})$, then we can obtain that

$$\text{Var}[f(\hat{\boldsymbol{\psi}})] \geq \frac{\partial f(\boldsymbol{\psi})}{\partial \boldsymbol{\psi}^T} \mathbf{I}(\boldsymbol{\psi})^{-1} \left(\frac{\partial f(\boldsymbol{\psi})}{\partial \boldsymbol{\psi}^T} \right)^H, \quad (69)$$

where $\text{Var}[f(\hat{\boldsymbol{\psi}})]$ denotes the variance of $f(\hat{\boldsymbol{\psi}})$ and $\mathbf{I}(\boldsymbol{\psi})$ is the corresponding Fisher information matrix.

Combining (14) and (69), we have

$$\begin{aligned} \frac{1}{MN} \mathbb{E} \left[\left\| \hat{\mathbf{h}}_k - \mathbf{h} \right\|_2^2 \right] &= \frac{1}{MN} \sum_{m=1}^M \sum_{n=1}^N \mathbb{E} \left[|h_{mn}(\hat{\boldsymbol{\psi}}) - h_{mn}(\boldsymbol{\psi})|^2 \right] \\ &\stackrel{(a)}{\geq} \frac{1}{MN} \sum_{m=1}^M \sum_{n=1}^N \left(\frac{\partial h_{mn}(\boldsymbol{\psi})}{\partial \boldsymbol{\psi}^T} \left(\sum_{l=1}^k \mathbf{I}_S(\boldsymbol{\psi}, \mathbf{W}_l) \right)^{-1} \left(\frac{\partial h_{mn}(\boldsymbol{\psi})}{\partial \boldsymbol{\psi}^T} \right)^H \right) \\ &= \frac{1}{MN} \text{Tr} \left\{ \left(\sum_{l=1}^k \mathbf{I}_S(\boldsymbol{\psi}, \mathbf{W}_l) \right)^{-1} \sum_{m=1}^M \sum_{n=1}^N \left(\left(\frac{\partial h_{mn}(\boldsymbol{\psi})}{\partial \boldsymbol{\psi}^T} \right)^H \frac{\partial h_{mn}(\boldsymbol{\psi})}{\partial \boldsymbol{\psi}^T} \right) \right\} \\ &= \frac{1}{MN} \text{Tr} \left\{ \left(\sum_{l=1}^k \mathbf{I}_S(\boldsymbol{\psi}, \mathbf{W}_l) \right)^{-1} \left(\frac{\partial \mathbf{h}}{\partial \boldsymbol{\psi}^T} \right)^H \frac{\partial \mathbf{h}}{\partial \boldsymbol{\psi}^T} \right\}, \\ &\stackrel{(b)}{=} \frac{1}{MN} \text{Tr} \left\{ \left(\sum_{l=1}^k \mathbf{I}_S(\boldsymbol{\psi}, \mathbf{W}_l) \right)^{-1} \mathbf{V}^H \mathbf{V} \right\}, \end{aligned} \quad (70)$$

where Step (a) is obtained by substituting (69) into (70) and Step (b) is due to the definition of \mathbf{V} in (17).

As for the Fisher information matrix in (18), we can obtain $\frac{\partial \log p_S(\mathbf{y}_l | \boldsymbol{\psi}, \mathbf{W}_l)}{\partial \beta^{\text{re}}}$ as follows:

$$\begin{aligned} \frac{\partial \log p_S(\mathbf{y}_l | \boldsymbol{\psi}, \mathbf{W}_l)}{\partial \beta^{\text{re}}} &= -\frac{1}{\sigma_z^2} (\mathbf{y}_l - |\mathbf{s}| \mathbf{W}_l^H \mathbf{h})^H \left(-|\mathbf{s}| \mathbf{W}_l^H \frac{\partial \mathbf{h}}{\partial \beta^{\text{re}}} \right) + \frac{1}{\sigma_z^2} \left(|\mathbf{s}| \mathbf{W}_l^H \frac{\partial \mathbf{h}}{\partial \beta^{\text{re}}} \right)^H (\mathbf{y}_l - |\mathbf{s}| \mathbf{W}_l^H \mathbf{h}) \\ &= \frac{2|\mathbf{s}|}{\sigma_z^2} \text{Re} \left\{ (\mathbf{y}_l - |\mathbf{s}| \mathbf{W}_l^H \mathbf{h})^H \left(\mathbf{W}_l^H \frac{\partial \mathbf{h}}{\partial \beta^{\text{re}}} \right) \right\} \\ &= \frac{2|\mathbf{s}|}{\sigma_z^2} \text{Re} \left\{ \mathbf{z}_l^H \mathbf{W}_l^H \frac{\partial \mathbf{h}}{\partial \beta^{\text{re}}} \right\}. \end{aligned} \quad (71)$$

Similarly, $\frac{\partial \log p_S(\mathbf{y}_l|\boldsymbol{\psi}, \mathbf{W}_l)}{\partial \beta^{\text{im}}}$, $\frac{\partial \log p_S(\mathbf{y}_l|\boldsymbol{\psi}, \mathbf{W}_l)}{\partial x_1}$, and $\frac{\partial \log p_S(\mathbf{y}_l|\boldsymbol{\psi}, \mathbf{W}_l)}{\partial x_2}$ are given as

$$\begin{cases} \frac{\partial \log p_S(\mathbf{y}_l|\boldsymbol{\psi}, \mathbf{W}_l)}{\partial \beta^{\text{im}}} = \frac{2|\mathbf{s}|}{\sigma_z^2} \text{Re} \left\{ \mathbf{z}_l^H \mathbf{W}_l^H \frac{\partial \mathbf{h}}{\partial \beta^{\text{im}}} \right\} \\ \frac{\partial \log p_S(\mathbf{y}_l|\boldsymbol{\psi}, \mathbf{W}_l)}{\partial x_1} = \frac{2|\mathbf{s}|}{\sigma_z^2} \text{Re} \left\{ \mathbf{z}_l^H \mathbf{W}_l^H \frac{\partial \mathbf{h}}{\partial x_1} \right\} \\ \frac{\partial \log p_S(\mathbf{y}_l|\boldsymbol{\psi}, \mathbf{W}_l)}{\partial x_2} = \frac{2|\mathbf{s}|}{\sigma_z^2} \text{Re} \left\{ \mathbf{z}_l^H \mathbf{W}_l^H \frac{\partial \mathbf{h}}{\partial x_2} \right\} \end{cases} . \quad (72)$$

Hence, the gradient of $\log p_S(\mathbf{y}_l|\boldsymbol{\psi}, \mathbf{W}_l)$ is obtained as follows:

$$\frac{\partial \log p_S(\mathbf{y}_l|\boldsymbol{\psi}, \mathbf{W}_l)}{\partial \boldsymbol{\psi}} = \frac{2|\mathbf{s}|}{\sigma_z^2} \text{Re} \left\{ \begin{bmatrix} \mathbf{z}_l^H \mathbf{W}_l^H \frac{\partial \mathbf{h}}{\partial \beta^{\text{re}}} \\ \mathbf{z}_l^H \mathbf{W}_l^H \frac{\partial \mathbf{h}}{\partial \beta^{\text{im}}} \\ \mathbf{z}_l^H \mathbf{W}_l^H \frac{\partial \mathbf{h}}{\partial x_1} \\ \mathbf{z}_l^H \mathbf{W}_l^H \frac{\partial \mathbf{h}}{\partial x_2} \end{bmatrix} \right\} = \frac{2|\mathbf{s}|}{\sigma_z^2} \text{Re} \left\{ (\mathbf{z}_l^H \mathbf{W}_l^H \mathbf{V})^T \right\} . \quad (73)$$

With the help of (73), we can obtain that

$$\frac{\partial \log p_S(\mathbf{y}_l|\boldsymbol{\psi}, \mathbf{W}_l)}{\partial \boldsymbol{\psi}^T} = \left(\frac{\partial \log p_S(\mathbf{y}_l|\boldsymbol{\psi}, \mathbf{W}_l)}{\partial \boldsymbol{\psi}} \right)^T = \frac{2|\mathbf{s}|}{\sigma_z^2} \text{Re} \left\{ \mathbf{z}_l^H \mathbf{W}_l^H \mathbf{V} \right\} . \quad (74)$$

Substituting (73) and (74) into (18), the Fisher information matrix is given as follows:

$$\begin{aligned} \mathbf{I}_S(\boldsymbol{\psi}, \mathbf{W}_l) &\triangleq \mathbb{E} \left[\frac{\partial \log p_S(\mathbf{y}_l|\boldsymbol{\psi}, \mathbf{W}_l)}{\partial \boldsymbol{\psi}} \cdot \frac{\partial \log p_S(\mathbf{y}_l|\boldsymbol{\psi}, \mathbf{W}_l)}{\partial \boldsymbol{\psi}^T} \right] \\ &= \frac{4|\mathbf{s}|^2}{\sigma_z^4} \mathbb{E} \left[\text{Re} \left\{ (\mathbf{z}_l^H \mathbf{W}_l^H \mathbf{V})^T \right\} \text{Re} \left\{ \mathbf{z}_l^H \mathbf{W}_l^H \mathbf{V} \right\} \right] \\ &\stackrel{(c)}{=} \frac{2|\mathbf{s}|^2}{\sigma_z^4} \mathbb{E} \left[\text{Re} \left\{ (\mathbf{z}_l^H \mathbf{W}_l^H \mathbf{V})^T \mathbf{z}_l^H \mathbf{W}_l^H \mathbf{V} \right\} \right] + \frac{2|\mathbf{s}|^2}{\sigma_z^4} \mathbb{E} \left[\text{Re} \left\{ (\mathbf{z}_l^H \mathbf{W}_l^H \mathbf{V})^H \mathbf{z}_l^H \mathbf{W}_l^H \mathbf{V} \right\} \right] \\ &\stackrel{(d)}{=} \frac{2|\mathbf{s}|^2}{\sigma_z^4} \mathbb{E} \left[\text{Re} \left\{ (\mathbf{z}_l^H \mathbf{W}_l^H \mathbf{V})^H \mathbf{z}_l^H \mathbf{W}_l^H \mathbf{V} \right\} \right] \\ &\stackrel{(e)}{=} \frac{2|\mathbf{s}|^2}{\sigma_z^2} \text{Re} \left\{ \mathbf{V}^H \mathbf{W}_l \mathbf{W}_l^H \mathbf{V} \right\} , \end{aligned} \quad (75)$$

where in Step (c) we have used the following property of $\text{Re} \{ \cdot \}$:

$$\text{Re} \{ \mathbf{u} \} \text{Re} \{ \mathbf{v}^T \} = \frac{1}{2} \text{Re} \{ \mathbf{u} \mathbf{v}^T \} + \frac{1}{2} \text{Re} \{ \bar{\mathbf{u}} \mathbf{v}^T \} \quad (76)$$

with \mathbf{u}, \mathbf{v} denoting column vectors and $\bar{\mathbf{u}}$ denoting the conjugate of \mathbf{u} . Step (d) is due to the exchangeability of $\mathbb{E} [\cdot]$ and $\text{Re} \{ \cdot \}$:

$$\begin{aligned} \mathbb{E} \left[\text{Re} \left\{ (\mathbf{z}_l^H \mathbf{W}_l^H \mathbf{V})^T \mathbf{z}_l^H \mathbf{W}_l^H \mathbf{V} \right\} \right] &= \text{Re} \left\{ \mathbb{E} \left[(\mathbf{z}_l^H \mathbf{W}_l^H \mathbf{V})^T \mathbf{z}_l^H \mathbf{W}_l^H \mathbf{V} \right] \right\} \\ &= \text{Re} \left\{ (\mathbf{W}_l^H \mathbf{V})^T \mathbb{E} \left[(\mathbf{z}_l^H)^T \mathbf{z}_l^H \right] \mathbf{W}_l^H \mathbf{V} \right\} \\ &\stackrel{(f)}{=} \mathbf{0} . \end{aligned} \quad (77)$$

Step (e) is due to the *i.i.d.* circularly symmetric complex Gaussian property of each element of \mathbf{z}_l , which means that $\mathbb{E} [\mathbf{z}_l \mathbf{z}_l^H] = \sigma_z^2 \mathbf{J}_3$, where \mathbf{J}_3 is a 3-order identity matrix. Step (f) in (77) results from the property of complex Gaussian noise:

$$\mathbb{E} \left[(\mathbf{z}_l^H)^T \mathbf{z}_l^H \right] = \mathbf{0}. \quad (78)$$

Proof. For $\mathbf{z}_k = [z_{k,1}, z_{k,2}, \dots, z_{k,q}]^T$ and $z_{k,i} \sim \mathcal{CN}(0, \sigma_z^2)$, $i = 1, 2, \dots, q$ as an *i.i.d.* circularly symmetric complex Gaussian random variable, assume that $z_{k,i} = z_{k,i}^x + j z_{k,i}^y$. Then we have

$$\begin{cases} \mathbb{E} \left[(z_{k,i}^x)^2 \right] = \frac{\sigma_z^2}{2} \\ \mathbb{E} \left[(z_{k,i}^y)^2 \right] = \frac{\sigma_z^2}{2} \\ \mathbb{E} \left[z_{k,i}^x z_{k,i}^y \right] = 0 \end{cases}. \quad (79)$$

Hence, we can obtain that

$$\mathbb{E} [z_{k,i}^2] = \mathbb{E} \left[(z_{k,i}^x + j z_{k,i}^y)^2 \right] = \mathbb{E} \left[(z_{k,i}^x)^2 \right] - \mathbb{E} \left[(z_{k,i}^y)^2 \right] + 2j \mathbb{E} [z_{k,i}^x z_{k,i}^y] = 0 \quad (80)$$

and $\mathbb{E} [z_{k,i} z_{k,j}] = 0$, for $i \neq j$ because $z_{k,i}$ and $z_{k,j}$ are independent.

Correspondingly, $\mathbb{E} [\mathbf{z}_l \mathbf{z}_l^T] = \mathbf{0}$ and

$$\mathbb{E} \left[(\mathbf{z}_l^H)^T \mathbf{z}_l^H \right] = \left(\mathbb{E} \left[\left((\mathbf{z}_l^H)^T \mathbf{z}_l^H \right)^H \right] \right)^H = \left(\mathbb{E} [\mathbf{z}_l \mathbf{z}_l^T] \right)^H = \mathbf{0}, \quad (81)$$

which yields the result of Step (f). ■

Therefore, the Fisher information matrix is derived in (75) and Lemma 2 is proved in the end.

APPENDIX C

PROOF OF LEMMA 3

Lemma 3 is proved in three steps:

Step 1: We prove that $\Delta_{S,1}^*$, $\Delta_{S,2}^*$, $\Delta_{S,3}^*$ are unrelated to the channel gain β .

The basic method is block matrix inversion. We first rewrite the Jacobian matrix \mathbf{V} in (17) as follows:

$$\mathbf{V} = [\mathbf{V}_1, \beta \mathbf{V}_2], \quad (82)$$

where \mathbf{V}_1 and \mathbf{V}_2 are given by

$$\begin{cases} \mathbf{V}_1 \triangleq [\mathbf{a}(\mathbf{x}), j\mathbf{a}(\mathbf{x})] \\ \mathbf{V}_2 \triangleq \left[\frac{\partial \mathbf{a}(\mathbf{x})}{\partial x_1}, \frac{\partial \mathbf{a}(\mathbf{x})}{\partial x_2} \right] \end{cases}. \quad (83)$$

It is clear that both \mathbf{V}_1 and \mathbf{V}_2 are unrelated to β . Besides, we can obtain the following property of \mathbf{V}_1 :

$$\begin{cases} \mathbf{V}_1 \mathbf{X} \mathbf{V}_1^T = \mathbf{0} \\ \bar{\mathbf{V}}_1 \mathbf{X} \mathbf{V}_1^H = \mathbf{0} \end{cases}, \quad (84)$$

where \mathbf{X} is an arbitrary 2×2 matrix and $\bar{\mathbf{V}}_1$ denote the conjugate of \mathbf{V}_1 . With the help of Jacobian matrix \mathbf{V} in (82), the Fisher information matrix in (18) can be divided into four 2×2 matrices as follows:

$$\begin{aligned} \mathbf{I}_S(\boldsymbol{\psi}, \mathbf{W}) &= \frac{2|\mathbf{s}|^2}{\sigma_z^2} \text{Re} \{ \mathbf{V}^H \mathbf{W} \mathbf{W}^H \mathbf{V} \} = \frac{2|\mathbf{s}|^2}{\sigma_z^2} \begin{bmatrix} \text{Re} \{ \mathbf{V}_1^H \mathbf{W} \mathbf{W}^H \mathbf{V}_1 \} & \text{Re} \{ \beta \mathbf{V}_1^H \mathbf{W} \mathbf{W}^H \mathbf{V}_2 \} \\ \text{Re} \{ \bar{\beta} \mathbf{V}_2^H \mathbf{W} \mathbf{W}^H \mathbf{V}_1 \} & |\beta|^2 \text{Re} \{ \mathbf{V}_2^H \mathbf{W} \mathbf{W}^H \mathbf{V}_2 \} \end{bmatrix} \\ &= \frac{2|\mathbf{s}|^2}{\sigma_z^2} \begin{bmatrix} \mathbf{A} & \text{Re} \{ \beta \mathbf{B} \} \\ \text{Re} \{ \bar{\beta} \mathbf{B}^H \} & |\beta|^2 \mathbf{D} \end{bmatrix}, \end{aligned} \quad (85)$$

where $\bar{\beta}$ denotes the conjugate of β and \mathbf{A} , \mathbf{B} , \mathbf{D} are defined as:

$$\begin{cases} \mathbf{A} \triangleq \text{Re} \{ \mathbf{V}_1^H \mathbf{W} \mathbf{W}^H \mathbf{V}_1 \} \\ \mathbf{B} \triangleq \mathbf{V}_1^H \mathbf{W} \mathbf{W}^H \mathbf{V}_2. \\ \mathbf{D} \triangleq \text{Re} \{ \mathbf{V}_2^H \mathbf{W} \mathbf{W}^H \mathbf{V}_2 \} \end{cases} \quad (86)$$

By combining (84) and (86), we can obtain the property of \mathbf{B} :

$$\begin{cases} \mathbf{B}^H \mathbf{X} \bar{\mathbf{B}} = \mathbf{0} \\ \mathbf{B}^T \mathbf{X} \mathbf{B} = \mathbf{0} \\ \mathbf{B}^H \mathbf{X} \mathbf{V}_1^T = \mathbf{V}_1 \mathbf{X} \bar{\mathbf{B}} = \mathbf{0} \\ \mathbf{B}^T \mathbf{X} \mathbf{V}_1^H = \bar{\mathbf{V}}_1 \mathbf{X} \mathbf{B} = \mathbf{0} \end{cases}, \quad (87)$$

where \mathbf{X} is an arbitrary 2×2 matrix.

By using the block matrix inversion method, the inverse of the Fisher information matrix in (85) is given by

$$\mathbf{I}_S(\boldsymbol{\psi}, \mathbf{W})^{-1} = \frac{\sigma_z^2}{2|\mathbf{s}|^2} \{ \mathbf{I}_{ip_1} + \mathbf{I}_{ip_2}(\beta) \}, \quad (88)$$

where \mathbf{I}_{ip_1} and $\mathbf{I}_{ip_2}(\beta)$ are defined in (89) and (90):

$$\mathbf{I}_{ip_1} \triangleq \begin{bmatrix} \mathbf{A}^{-1} & \mathbf{0} \\ \mathbf{0} & \mathbf{0} \end{bmatrix} \quad (89)$$

$$\mathbf{I}_{ip_2}(\beta) \triangleq \begin{bmatrix} \mathbf{A}^{-1} \text{Re}\{\beta \mathbf{B}\} \\ -\mathbf{J}_2 \end{bmatrix} (|\beta|^2 \mathbf{D} - \text{Re}\{\bar{\beta} \mathbf{B}^H\} \mathbf{A}^{-1} \text{Re}\{\beta \mathbf{B}\})^{-1} \begin{bmatrix} \text{Re}\{\bar{\beta} \mathbf{B}^H\} \mathbf{A}^{-1} & -\mathbf{J}_2 \end{bmatrix} \quad (90)$$

with \mathbf{J}_2 denoting a 2-order identity matrix. The middle part of \mathbf{I}_{ip_2} , i.e., $(|\beta|^2 \mathbf{D} - \text{Re}\{\bar{\beta} \mathbf{B}^H\} \mathbf{A}^{-1} \text{Re}\{\beta \mathbf{B}\})$, can be rewritten as follows:

$$\begin{aligned} |\beta|^2 \mathbf{D} - \text{Re}\{\bar{\beta} \mathbf{B}^H\} \mathbf{A}^{-1} \text{Re}\{\beta \mathbf{B}\} &= |\beta|^2 \mathbf{D} - \frac{\bar{\beta} \mathbf{B}^H + \beta \mathbf{B}^T}{2} \mathbf{A}^{-1} \frac{\beta \mathbf{B} + \bar{\beta} \bar{\mathbf{B}}}{2} \\ &\stackrel{(a)}{=} |\beta|^2 \mathbf{D} - \frac{\bar{\beta} \mathbf{B}^H \mathbf{A}^{-1} \beta \mathbf{B} + \beta \mathbf{B}^T \mathbf{A}^{-1} \bar{\beta} \bar{\mathbf{B}}}{4} \\ &\stackrel{(b)}{=} |\beta|^2 \mathbf{D} - \frac{\text{Re}\{\bar{\beta} \mathbf{B}^H \mathbf{A}^{-1} \beta \mathbf{B}\}}{2} \\ &= |\beta|^2 \left(\mathbf{D} - \frac{\text{Re}\{\mathbf{B}^H \mathbf{A}^{-1} \mathbf{B}\}}{2} \right) \\ &\stackrel{(c)}{=} |\beta|^2 \mathbf{I}_s, \end{aligned} \quad (91)$$

where Step (a) results from the property of \mathbf{B} in (87), Step (b) is due to that \mathbf{A} defined in (86) is a real matrix and Step (c) is due to the definition of \mathbf{I}_s :

$$\mathbf{I}_s \triangleq \mathbf{D} - \frac{\text{Re}\{\mathbf{B}^H \mathbf{A}^{-1} \mathbf{B}\}}{2}. \quad (92)$$

Therefore, we can rewrite \mathbf{I}_{ip_2} in (90) as follows:

$$\mathbf{I}_{ip_2}(\beta) = \begin{bmatrix} \mathbf{A}^{-1} \text{Re}\{\beta \mathbf{B}\} \\ -\mathbf{J}_2 \end{bmatrix} (|\beta|^2 \mathbf{I}_s)^{-1} \begin{bmatrix} \text{Re}\{\bar{\beta} \mathbf{B}^H\} \mathbf{A}^{-1} & -\mathbf{J}_2 \end{bmatrix}. \quad (93)$$

By combining (20) and (88), we can obtain that

$$\begin{aligned} C_S(\boldsymbol{\psi}, \mathbf{W}) &= \frac{1}{MN} \text{Tr}\{(\mathbf{I}_S(\boldsymbol{\psi}, \mathbf{W}))^{-1} \mathbf{V}^H \mathbf{V}\} \\ &= \frac{1}{MN} \frac{\sigma_z^2}{2|\mathbf{s}|^2} (\text{Tr}\{\mathbf{I}_{ip_1} \mathbf{V}^H \mathbf{V}\} + \text{Tr}\{\mathbf{I}_{ip_2}(\beta) \mathbf{V}^H \mathbf{V}\}) \\ &\stackrel{(d)}{=} \frac{1}{MN} \frac{\sigma_z^2}{2|\mathbf{s}|^2} (\text{Tr}\{\mathbf{A}^{-1} \mathbf{V}_1^H \mathbf{V}_1\} + \text{Tr}\{\mathbf{I}_{ip_2}(\beta) \mathbf{V}^H \mathbf{V}\}), \end{aligned} \quad (94)$$

where Step (d) is by substituting (82) and (89) into (94). Since both \mathbf{V}_1 in (83) and \mathbf{A} in (86) are unrelated to the channel gain β , the first part of (94), i.e., $\text{Tr} \{ \mathbf{A}^{-1} \mathbf{V}_1^H \mathbf{V}_1 \}$ are unrelated to β . By substituting (82) and (93), we can obtain the second part of (94), i.e., $\text{Tr} \{ \mathbf{I}_{ip_2}(\beta) \mathbf{V}^H \mathbf{V} \}$ in (95),

$$\begin{aligned}
\text{Tr} \{ \mathbf{I}_{ip_2}(\beta) \mathbf{V}^H \mathbf{V} \} &= \text{Tr} \left\{ \begin{bmatrix} \mathbf{A}^{-1} \text{Re} \{ \beta \mathbf{B} \} \\ -\mathbf{J}_2 \end{bmatrix} (|\beta|^2 \mathbf{I}_s)^{-1} \begin{bmatrix} \text{Re} \{ \bar{\beta} \mathbf{B}^H \} \mathbf{A}^{-1} & -\mathbf{J}_2 \end{bmatrix} \begin{bmatrix} \mathbf{V}_1^H \mathbf{V}_1 & \beta \mathbf{V}_1^H \mathbf{V}_2 \\ \bar{\beta} \mathbf{V}_2^H \mathbf{V}_1 & |\beta|^2 \mathbf{V}_2^H \mathbf{V}_2 \end{bmatrix} \right\} \\
&= \text{Tr} \left\{ \mathbf{A}^{-1} \text{Re} \{ \beta \mathbf{B} \} (|\beta|^2 \mathbf{I}_s)^{-1} (\text{Re} \{ \bar{\beta} \mathbf{B}^H \} \mathbf{A}^{-1} \mathbf{V}_1^H \mathbf{V}_1 - \bar{\beta} \mathbf{V}_2^H \mathbf{V}_1) \right\} \\
&\quad + \text{Tr} \left\{ (|\beta|^2 \mathbf{I}_s)^{-1} (|\beta|^2 \mathbf{V}_2^H \mathbf{V}_2 - \text{Re} \{ \bar{\beta} \mathbf{B}^H \} \mathbf{A}^{-1} \beta \mathbf{V}_1^H \mathbf{V}_2) \right\} \\
&= \text{Tr} \left\{ \mathbf{A}^{-1} \frac{\beta \mathbf{B} + \bar{\beta} \bar{\mathbf{B}}}{2} (|\beta|^2 \mathbf{I}_s)^{-1} \left(\frac{\bar{\beta} \mathbf{B}^H + \beta \mathbf{B}^T}{2} \mathbf{A}^{-1} \mathbf{V}_1^H \mathbf{V}_1 - \bar{\beta} \mathbf{V}_2^H \mathbf{V}_1 \right) \right\} \\
&\quad + \text{Tr} \left\{ (|\beta|^2 \mathbf{I}_s)^{-1} \left(|\beta|^2 \mathbf{V}_2^H \mathbf{V}_2 - \frac{\bar{\beta} \mathbf{B}^H + \beta \mathbf{B}^T}{2} \mathbf{A}^{-1} \beta \mathbf{V}_1^H \mathbf{V}_2 \right) \right\} \\
&\stackrel{(e)}{=} \text{Tr} \left\{ \mathbf{A}^{-1} \frac{\beta \mathbf{B} + \bar{\beta} \bar{\mathbf{B}}}{2} (|\beta|^2 \mathbf{I}_s)^{-1} \left(\frac{\bar{\beta} \mathbf{B}^H}{2} \mathbf{A}^{-1} \mathbf{V}_1^H \mathbf{V}_1 - \bar{\beta} \mathbf{V}_2^H \mathbf{V}_1 \right) \right\} \\
&\quad + \text{Tr} \left\{ (|\beta|^2 \mathbf{I}_s)^{-1} \left(|\beta|^2 \mathbf{V}_2^H \mathbf{V}_2 - \frac{\bar{\beta} \mathbf{B}^H}{2} \mathbf{A}^{-1} \beta \mathbf{V}_1^H \mathbf{V}_2 \right) \right\} \\
&= \text{Tr} \left\{ \left(\frac{\bar{\beta} \mathbf{B}^H}{2} \mathbf{A}^{-1} \mathbf{V}_1^H \mathbf{V}_1 - \bar{\beta} \mathbf{V}_2^H \mathbf{V}_1 \right) \mathbf{A}^{-1} \frac{\beta \mathbf{B} + \bar{\beta} \bar{\mathbf{B}}}{2} (|\beta|^2 \mathbf{I}_s)^{-1} \right\} \\
&\quad + \text{Tr} \left\{ \mathbf{I}_s^{-1} \left(\mathbf{V}_2^H \mathbf{V}_2 - \frac{\mathbf{B}^H \mathbf{A}^{-1} \mathbf{V}_1^H \mathbf{V}_2}{2} \right) \right\} \\
&\stackrel{(f)}{=} \text{Tr} \left\{ \left(\frac{\bar{\beta} \mathbf{B}^H}{2} \mathbf{A}^{-1} \mathbf{V}_1^H \mathbf{V}_1 - \bar{\beta} \mathbf{V}_2^H \mathbf{V}_1 \right) \mathbf{A}^{-1} \frac{\beta \mathbf{B}}{2} (|\beta|^2 \mathbf{I}_s)^{-1} \right\} \\
&\quad + \text{Tr} \left\{ \mathbf{I}_s^{-1} \left(\mathbf{V}_2^H \mathbf{V}_2 - \frac{\mathbf{B}^H \mathbf{A}^{-1} \mathbf{V}_1^H \mathbf{V}_2}{2} \right) \right\} \\
&= \text{Tr} \left\{ \left(\frac{\mathbf{B}^H}{2} \mathbf{A}^{-1} \mathbf{V}_1^H \mathbf{V}_1 - \mathbf{V}_2^H \mathbf{V}_1 \right) \mathbf{A}^{-1} \frac{\mathbf{B}}{2} \mathbf{I}_s^{-1} \right\} \\
&\quad + \text{Tr} \left\{ \mathbf{I}_s^{-1} \left(\mathbf{V}_2^H \mathbf{V}_2 - \frac{\mathbf{B}^H \mathbf{A}^{-1} \mathbf{V}_1^H \mathbf{V}_2}{2} \right) \right\} \\
&= \text{Tr} \left\{ \mathbf{I}_s^{-1} \left(\frac{\mathbf{B}^H \mathbf{A}^{-1} \mathbf{V}_1^H \mathbf{V}_1 \mathbf{A}^{-1} \mathbf{B}}{4} + \mathbf{V}_2^H \mathbf{V}_2 - \frac{\mathbf{B}^H \mathbf{A}^{-1} \mathbf{V}_1^H \mathbf{V}_2 + \mathbf{V}_2^H \mathbf{V}_1 \mathbf{A}^{-1} \mathbf{B}}{2} \right) \right\}, \tag{95}
\end{aligned}$$

where Step (e) and Step (f) follow the property of the \mathbf{B} in (87). It is clear that $\text{Tr} \{ \mathbf{I}_{ip_2}(\beta) \mathbf{V}^H \mathbf{V} \}$ is also unrelated to β because none of the matrix \mathbf{A} , \mathbf{B} , \mathbf{V}_1 , \mathbf{V}_2 is related to β . Hence, $C_S(\boldsymbol{\psi}, \mathbf{W})$ is unrelated to β .

Since $C_S(\boldsymbol{\psi}, \mathbf{W})$ is unrelated to β , the minimum CRLB in (21) and the optimal EBM \mathbf{W}_S^* are also unrelated to β , i.e., the optimal exploring offsets $\Delta_{S,1}^*$, $\Delta_{S,2}^*$, $\Delta_{S,3}^*$ are unrelated to the channel gain β .

Step 2: We prove that $\Delta_{S,1}^$, $\Delta_{S,2}^*$, $\Delta_{S,3}^*$ are unrelated to the DPV \mathbf{x} .*

Consider the CRLB in (20). we will first prove that the Fisher information matrix $\mathbf{I}_S(\boldsymbol{\psi}, \mathbf{W})$ is unrelated to the DPV \mathbf{x} . Next we will prove that $\mathbf{V}^H \mathbf{V}$ is also unrelated to \mathbf{x} . Then it is clear that the minimum CRLB and the optimal exploring offsets $\Delta_{S,1}^*$, $\Delta_{S,2}^*$, $\Delta_{S,3}^*$ are unrelated to \mathbf{x} .

The Fisher information matrix in (85) tells us that only $\mathbf{W}^H \mathbf{V}$ may be related to \mathbf{x} , which is given by

$$\mathbf{W}^H \mathbf{V} = \left[\mathbf{W}^H \mathbf{a}(\mathbf{x}), j \mathbf{W}^H \mathbf{a}(\mathbf{x}), \beta \mathbf{W}^H \frac{\partial \mathbf{a}(\mathbf{x})}{\partial x_1}, \beta \mathbf{W}^H \frac{\partial \mathbf{a}(\mathbf{x})}{\partial x_2} \right] \quad (96)$$

with $\mathbf{W}^H \mathbf{a}(\mathbf{x})$, $\mathbf{W}^H \frac{\partial \mathbf{a}(\mathbf{x})}{\partial x_1}$ and $\mathbf{W}^H \frac{\partial \mathbf{a}(\mathbf{x})}{\partial x_2}$ expanded as follows:

$$\begin{cases} \mathbf{W}^H \mathbf{a}(\mathbf{x}) = [\mathbf{w}_1^H \mathbf{a}(\mathbf{x}), \mathbf{w}_2^H \mathbf{a}(\mathbf{x}), \mathbf{w}_3^H \mathbf{a}(\mathbf{x})]^T \\ \mathbf{W}^H \frac{\partial \mathbf{a}(\mathbf{x})}{\partial x_1} = \left[\mathbf{w}_1^H \frac{\partial \mathbf{a}(\mathbf{x})}{\partial x_1}, \mathbf{w}_2^H \frac{\partial \mathbf{a}(\mathbf{x})}{\partial x_1}, \mathbf{w}_3^H \frac{\partial \mathbf{a}(\mathbf{x})}{\partial x_1} \right]^T \\ \mathbf{W}^H \frac{\partial \mathbf{a}(\mathbf{x})}{\partial x_2} = \left[\mathbf{w}_1^H \frac{\partial \mathbf{a}(\mathbf{x})}{\partial x_2}, \mathbf{w}_2^H \frac{\partial \mathbf{a}(\mathbf{x})}{\partial x_2}, \mathbf{w}_3^H \frac{\partial \mathbf{a}(\mathbf{x})}{\partial x_2} \right]^T \end{cases} \quad (97)$$

Since the EBVs are of steering vector forms, i.e., $\mathbf{w}_i = \frac{1}{\sqrt{MN}} \mathbf{a}(\mathbf{x} + \boldsymbol{\Delta}_i)$, where $\boldsymbol{\Delta}_i = [\delta_{i1}, \delta_{i2}]^T$ denotes the i -th exploring offset, the elements of $\mathbf{W}^H \mathbf{a}(\mathbf{x})$ and $\mathbf{W}^H \frac{\partial \mathbf{a}(\mathbf{x})}{\partial x_1}$ can be written as:

$$\begin{aligned} \mathbf{w}_i^H \mathbf{a}(\mathbf{x}) &= \frac{1}{\sqrt{MN}} \mathbf{a}(\mathbf{x} + \boldsymbol{\Delta}_i)^H \mathbf{a}(\mathbf{x}) = \frac{1}{\sqrt{MN}} \sum_{m=1}^M \sum_{n=1}^N e^{-j2\pi \left[\frac{(m-1)\delta_{i1}}{M} + \frac{(n-1)\delta_{i2}}{N} \right]} \\ &= \frac{1}{\sqrt{MN}} \frac{\sin(\pi \delta_{i1})}{\sin\left(\frac{\pi \delta_{i1}}{M}\right)} \frac{\sin(\pi \delta_{i2})}{\sin\left(\frac{\pi \delta_{i2}}{N}\right)} e^{-j\pi \left(\frac{M-1}{M} \delta_{i1} + \frac{N-1}{N} \delta_{i2} \right)}. \end{aligned} \quad (98)$$

$$\begin{aligned} \mathbf{w}_i^H \frac{\partial \mathbf{a}(\mathbf{x})}{\partial x_1} &= \frac{1}{\sqrt{MN}} \mathbf{a}(\mathbf{x} + \boldsymbol{\Delta}_i)^H \frac{\partial \mathbf{a}(\mathbf{x})}{\partial x_1} \\ &= \frac{1}{\sqrt{MN}} \left(\sum_{m=1}^M \sum_{n=1}^N j2\pi \frac{m-1}{M} e^{-j2\pi \left[\frac{(m-1)\delta_{i1}}{M} + \frac{(n-1)\delta_{i2}}{N} \right]} \right) \\ &= \frac{j2\pi}{M\sqrt{MN}} \left(\frac{\sin(\pi \delta_{i2})}{\sin\left(\frac{\pi \delta_{i2}}{N}\right)} e^{-j\pi \frac{N-1}{N} \delta_{i2}} \frac{(M-1)e^{-j2\pi \delta_{i1}} - M e^{-j2\pi \frac{M-1}{M} \delta_{i1}} + 1}{\left[1 - e^{-j2\pi \frac{\delta_{i1}}{M}}\right]^2} e^{-j2\pi \frac{\delta_{i1}}{M}} \right). \end{aligned} \quad (99)$$

As shown in (98) and (99), both $\mathbf{w}_i^H \mathbf{a}(\mathbf{x})$ and $\mathbf{w}_i^H \frac{\partial \mathbf{a}(\mathbf{x})}{\partial x_1}$ have nothing to do with the DPV \mathbf{x} . Similarly, $\mathbf{w}_i^H \frac{\partial \mathbf{a}(\mathbf{x})}{\partial x_2}$ also has nothing to do with \mathbf{x} . Therefore, $\mathbf{W}^H \mathbf{V}$ in (96) is unrelated to \mathbf{x} . Hence, the whole Fisher information matrix in (85) is invariant to \mathbf{x} .

As for $\mathbf{V}^H\mathbf{V}$, we write it as below:

$$\begin{aligned} \mathbf{V}^H\mathbf{V} &= \begin{bmatrix} \mathbf{a}(\mathbf{x})^H \\ -j\mathbf{a}(\mathbf{x})^H \\ \bar{\beta}\frac{\partial\mathbf{a}(\mathbf{x})^H}{\partial x_1} \\ \bar{\beta}\frac{\partial\mathbf{a}(\mathbf{x})^H}{\partial x_2} \end{bmatrix} \begin{bmatrix} \mathbf{a}(\mathbf{x}), j\mathbf{a}(\mathbf{x}), \beta\frac{\partial\mathbf{a}(\mathbf{x})}{\partial x_1}, \beta\frac{\partial\mathbf{a}(\mathbf{x})}{\partial x_2} \end{bmatrix} \\ &= MN \begin{bmatrix} 1 & j & j\pi\beta\frac{M-1}{M} & j\pi\beta\frac{N-1}{N} \\ -j & 1 & \pi\beta\frac{M-1}{M} & \pi\beta\frac{N-1}{N} \\ -j\pi\bar{\beta}\frac{M-1}{M} & \pi\bar{\beta}\frac{M-1}{M} & \frac{2}{3}\pi^2|\beta|^2\frac{(M-1)(2M-1)}{M^2} & \pi^2|\beta|^2\frac{(M-1)(N-1)}{MN} \\ -j\pi\bar{\beta}\frac{N-1}{N} & \pi\bar{\beta}\frac{N-1}{N} & \pi^2|\beta|^2\frac{(M-1)(N-1)}{MN} & \frac{2}{3}\pi^2|\beta|^2M\frac{(N-1)(2N-1)}{N^2} \end{bmatrix}, \quad (100) \end{aligned}$$

which shows that $\mathbf{V}^H\mathbf{V}$ has nothing to do with \mathbf{x} .

Now it is clear that the CRLB in (20), i.e., $C_S(\boldsymbol{\psi}, \mathbf{W})$, is unrelated to \mathbf{x} because both the Fisher information matrix $\mathbf{I}_S(\boldsymbol{\psi}, \mathbf{W})$ and $\mathbf{V}^H\mathbf{V}$ have nothing to do with \mathbf{x} . Therefore, the minimum CRLB in (21) and the optimal exploring offsets $\Delta_{S,1}^*$, $\Delta_{S,2}^*$, $\Delta_{S,3}^*$ are invariant to the DPV \mathbf{x} .

Step 3: We prove that $\Delta_{S,1}^*$, $\Delta_{S,2}^*$, $\Delta_{S,3}^*$ converge to constant values as $M, N \rightarrow +\infty$.

Let us go into the asymptotic features of (20). According to (98) and (99), when antenna number $M, N \rightarrow +\infty$, the limit of i -th ($i = 1, 2, 3$) element of $\mathbf{W}^H\mathbf{a}(\mathbf{x})$, $\mathbf{W}^H\frac{\partial\mathbf{a}(\mathbf{x})}{\partial x_1}$ and $\mathbf{W}^H\frac{\partial\mathbf{a}(\mathbf{x})}{\partial x_2}$ in (97) are given as follows:

$$\left\{ \begin{array}{l} \lim_{M, N \rightarrow +\infty} \frac{\mathbf{w}_i^H\mathbf{a}(\mathbf{x})}{\sqrt{MN}} = \text{Sa}[\pi\delta_{i1}] \text{Sa}[\pi\delta_{i2}] e^{-j\pi(\delta_{i1}+\delta_{i2})} \\ \lim_{M, N \rightarrow +\infty} \frac{\mathbf{w}_i^H\frac{\partial\mathbf{a}(\mathbf{x})}{\partial x_1}}{\sqrt{MN}} = j2\pi \text{Sa}[\pi\delta_{i2}] e^{-j\pi\delta_{i2}} \frac{e^{-j2\pi\delta_{i1}}(1+j2\pi\delta_{i1})-1}{(2\pi\delta_{i1})^2} \\ \lim_{M, N \rightarrow +\infty} \frac{\mathbf{w}_i^H\frac{\partial\mathbf{a}(\mathbf{x})}{\partial x_2}}{\sqrt{MN}} = j2\pi \text{Sa}[\pi\delta_{i1}] e^{-j\pi\delta_{i1}} \frac{e^{-j2\pi\delta_{i2}}(1+j2\pi\delta_{i2})-1}{(2\pi\delta_{i2})^2} \end{array} \right. \quad (101)$$

Hence, each element of $\mathbf{W}^H\mathbf{V}/\sqrt{MN}$ in (96) converges when $M, N \rightarrow +\infty$, which results in that $\mathbf{I}_S(\boldsymbol{\psi}, \mathbf{W})/MN$ in (85) also converges. The limit is defined as follows:

$$\mathbf{I}_l(\boldsymbol{\psi}, \mathbf{W}) \triangleq \lim_{M, N \rightarrow +\infty} \frac{1}{MN} \mathbf{I}_S(\boldsymbol{\psi}, \mathbf{W}). \quad (102)$$

The limit of $\mathbf{V}^H\mathbf{V}$ in (100) is given by

$$\lim_{M,N \rightarrow +\infty} \frac{1}{MN} \mathbf{V}^H \mathbf{V} = \begin{bmatrix} 1 & j & j\pi\beta & j\pi\beta \\ -j & 1 & \pi\beta & \pi\beta \\ -j\pi\bar{\beta} & \pi\bar{\beta} & \frac{4}{3}\pi^2|\beta|^2 & \pi^2|\beta|^2 \\ -j\pi\bar{\beta} & \pi\bar{\beta} & \pi^2|\beta|^2 & \frac{4}{3}\pi^2|\beta|^2 \end{bmatrix} \triangleq \mathbf{H}_l. \quad (103)$$

By combining (102) and (103), we obtain the limit of $C_S(\boldsymbol{\psi}, \mathbf{W})$ in (20) as $M, N \rightarrow +\infty$:

$$\begin{aligned} \lim_{M,N \rightarrow +\infty} (MN \times C_S(\boldsymbol{\psi}, \mathbf{W})) &= \lim_{M,N \rightarrow +\infty} \text{Tr} \{ (\mathbf{I}_S(\boldsymbol{\psi}, \mathbf{W}))^{-1} \mathbf{V}^H \mathbf{V} \} \\ &= \lim_{M,N \rightarrow +\infty} \text{Tr} \{ (MN \mathbf{I}_l(\boldsymbol{\psi}, \mathbf{W}))^{-1} \mathbf{V}^H \mathbf{V} \} \\ &= \lim_{M,N \rightarrow +\infty} \text{Tr} \left\{ (\mathbf{I}_l(\boldsymbol{\psi}, \mathbf{W}))^{-1} \frac{1}{MN} \mathbf{V}^H \mathbf{V} \right\} \\ &= \text{Tr} \{ (\mathbf{I}_l(\boldsymbol{\psi}, \mathbf{W}))^{-1} \mathbf{H}_l \}, \end{aligned} \quad (104)$$

which reveals that the minimum CRLB in (21), i.e., $C_S^{\min}(\boldsymbol{\psi})$, converges and the optimal exploring offsets $\Delta_{S,1}^*$, $\Delta_{S,2}^*$, $\Delta_{S,3}^*$ also converge to constant values determined by (104).

Therefore, Lemma 3 gets proved.

APPENDIX D

PROOF OF THEOREM 1

Recall the beam and channel tracking procedure in (38). Since $\mathbf{z}_k \triangleq [z_{k,1}, z_{k,2}, z_{k,3}]$ in (37) is composed of three *i.i.d.* circularly symmetric complex Gaussian random variables, the expectation

of $\hat{\mathbf{z}}_k$ is $\mathbb{E}[\hat{\mathbf{z}}_k] = \mathbf{0}$ and the covariance matrix is given as follows:

$$\begin{aligned}
& \mathbb{E} \left[(\hat{\mathbf{z}}_k - \mathbb{E}[\hat{\mathbf{z}}_k]) (\hat{\mathbf{z}}_k - \mathbb{E}[\hat{\mathbf{z}}_k])^T \right] \\
&= \frac{4|\mathbf{s}|^2}{\sigma_z^4} \mathbf{I}_S \left(\hat{\boldsymbol{\psi}}_{k-1}, \mathbf{W}_k \right)^{-1} \mathbb{E} \left\{ \begin{array}{c} \left[\begin{array}{cc} \text{Re}\{\mathbf{e}_k^H \mathbf{z}_k\} & \text{Re}\{\mathbf{e}_k^H \mathbf{z}_k\} \\ \text{Im}\{\mathbf{e}_k^H \mathbf{z}_k\} & \text{Im}\{\mathbf{e}_k^H \mathbf{z}_k\} \\ \text{Re}\{\tilde{\mathbf{e}}_{k1}^H \mathbf{z}_k\} & \text{Re}\{\tilde{\mathbf{e}}_{k1}^H \mathbf{z}_k\} \\ \text{Re}\{\tilde{\mathbf{e}}_{k2}^H \mathbf{z}_k\} & \text{Re}\{\tilde{\mathbf{e}}_{k2}^H \mathbf{z}_k\} \end{array} \right] \end{array} \right\} \mathbf{I}_S \left(\hat{\boldsymbol{\psi}}_{k-1}, \mathbf{W}_k \right)^{-1} \\
&= \frac{4|\mathbf{s}|^2}{\sigma_z^4} \mathbf{I}_S \left(\hat{\boldsymbol{\psi}}_{k-1}, \mathbf{W}_k \right)^{-1} \mathbb{E} \left\{ \begin{array}{c} \left[\begin{array}{c} \text{Re} \left\{ \begin{array}{c} \mathbf{z}_k^H \mathbf{W}_k^H \frac{\partial \hat{\mathbf{h}}_{k-1}}{\partial \hat{\beta}_{k-1}^{\text{re}}} \\ \mathbf{z}_k^H \mathbf{W}_k^H \frac{\partial \hat{\mathbf{h}}_{k-1}}{\partial \hat{\beta}_{k-1}^{\text{im}}} \\ \mathbf{z}_k^H \mathbf{W}_k^H \frac{\partial \hat{\mathbf{h}}_{k-1}}{\partial \hat{x}_{k-1,1}} \\ \mathbf{z}_k^H \mathbf{W}_k^H \frac{\partial \hat{\mathbf{h}}_{k-1}}{\partial \hat{x}_{k-1,2}} \end{array} \right\} \\ \text{Re} \left\{ \begin{array}{c} \mathbf{z}_k^H \mathbf{W}_k^H \frac{\partial \hat{\mathbf{h}}_{k-1}}{\partial \hat{\beta}_{k-1}^{\text{re}}} \\ \mathbf{z}_k^H \mathbf{W}_k^H \frac{\partial \hat{\mathbf{h}}_{k-1}}{\partial \hat{\beta}_{k-1}^{\text{im}}} \\ \mathbf{z}_k^H \mathbf{W}_k^H \frac{\partial \hat{\mathbf{h}}_{k-1}}{\partial \hat{x}_{k-1,1}} \\ \mathbf{z}_k^H \mathbf{W}_k^H \frac{\partial \hat{\mathbf{h}}_{k-1}}{\partial \hat{x}_{k-1,2}} \end{array} \right\} \end{array} \right\} \mathbf{I}_S \left(\hat{\boldsymbol{\psi}}_{k-1}, \mathbf{W}_k \right)^{-1} \\
&\stackrel{(a)}{=} \frac{4|\mathbf{s}|^2}{\sigma_z^4} \mathbf{I}_S \left(\hat{\boldsymbol{\psi}}_{k-1}, \mathbf{W}_k \right)^{-1} \mathbb{E} \left\{ \frac{\sigma_z^2}{2|\mathbf{s}|} \frac{\partial \log p_S(\mathbf{y}_k | \hat{\boldsymbol{\psi}}_{k-1}, \mathbf{W}_k)}{\partial \hat{\boldsymbol{\psi}}_{k-1}} \frac{\sigma_z^2}{2|\mathbf{s}|} \frac{\partial \log p_S(\mathbf{y}_k | \hat{\boldsymbol{\psi}}_{k-1}, \mathbf{W}_k)}{\partial \hat{\boldsymbol{\psi}}_{k-1}^T} \right\} \mathbf{I}_S \left(\hat{\boldsymbol{\psi}}_{k-1}, \mathbf{W}_k \right)^{-1} \\
&\stackrel{(b)}{=} \mathbf{I}_S \left(\hat{\boldsymbol{\psi}}_{k-1}, \mathbf{W}_k \right)^{-1} \mathbf{I}_S \left(\hat{\boldsymbol{\psi}}_{k-1}, \mathbf{W}_k \right) \mathbf{I}_S \left(\hat{\boldsymbol{\psi}}_{k-1}, \mathbf{W}_k \right)^{-1} \\
&= \mathbf{I}_S \left(\hat{\boldsymbol{\psi}}_{k-1}, \mathbf{W}_k \right)^{-1}, \tag{105}
\end{aligned}$$

where Step (a) is the result of (73) and Step (b) follows the definition of the Fisher information matrix in (18).

Assume $\{\mathcal{G}_k : k \geq 0\}$ is an increasing sequence of σ -fields of $\{\hat{\boldsymbol{\psi}}_0, \hat{\boldsymbol{\psi}}_1, \hat{\boldsymbol{\psi}}_2, \dots\}$, i.e., $\mathcal{G}_{k-1} \subset \mathcal{G}_k$, where $\mathcal{G}_0 \triangleq \sigma(\hat{\boldsymbol{\psi}}_0)$ and $\mathcal{G}_k \triangleq \sigma(\hat{\boldsymbol{\psi}}_0, \hat{\mathbf{z}}_1, \dots, \hat{\mathbf{z}}_k)$ for $k \geq 1$. Because the $\hat{\mathbf{z}}_k$'s are composed of *i.i.d.* circularly symmetric complex Gaussian random variables with zero mean, $\hat{\mathbf{z}}_k$ is independent of \mathcal{G}_{k-1} , and $\hat{\boldsymbol{\psi}}_{k-1} \in \mathcal{G}_{k-1}$. Hence, we have

$$\mathbb{E} \left[\mathbf{f} \left(\hat{\boldsymbol{\psi}}_{k-1}, \boldsymbol{\psi} \right) + \hat{\mathbf{z}}_k \middle| \mathcal{G}_{k-1} \right] = \mathbb{E} \left[\mathbf{f} \left(\hat{\boldsymbol{\psi}}_{k-1}, \boldsymbol{\psi} \right) \middle| \mathcal{G}_{k-1} \right] + \mathbb{E}[\hat{\mathbf{z}}_k | \mathcal{G}_{k-1}] = \mathbf{f} \left(\hat{\boldsymbol{\psi}}_{k-1}, \boldsymbol{\psi} \right), \tag{106}$$

for $k \geq 1$ and $\boldsymbol{\varsigma}_k = \mathbf{f} \left(\hat{\boldsymbol{\psi}}_{k-1}, \boldsymbol{\psi} \right) + \hat{\mathbf{z}}_k$ is also independent of \mathcal{G}_{k-1} .

Theorem 5.2.1 in [31, Section 5.2.1] gives the conditions that ensure $\hat{\boldsymbol{\psi}}_k$ converges to a unique point with probability one when there are several stable points. Next, we will prove that if the step-size $b_{S,k}$ is given by (40) with any $\varepsilon_S > 0$ and $K_{S,0} \geq 0$, the joint beam and channel tracking algorithm in (32) satisfies the corresponding conditions below:

1) Step-size requirements:

$$\left\{ \begin{array}{l} b_{S,k} = \frac{\varepsilon_S}{k + K_{S,0}} \rightarrow 0, \\ \sum_{k=1}^{+\infty} b_{S,k} = \sum_{k=1}^{+\infty} \frac{\varepsilon_S}{k + K_{S,0}} = +\infty, \\ \sum_{k=1}^{+\infty} b_{S,k}^2 = \sum_{k=1}^{+\infty} \frac{\varepsilon_S^2}{(k + K_{S,0})^2} \leq \sum_{l=1}^{+\infty} \frac{\varepsilon_S^2}{l^2} < +\infty. \end{array} \right. \quad (107)$$

2) It is necessary to prove that $\sup_k \mathbb{E} \left[\left\| \mathbf{f}(\hat{\boldsymbol{\psi}}_{k-1}, \boldsymbol{\psi}) + \hat{\mathbf{z}}_k \right\|_2^2 \right] < +\infty$.

From (38) and (105), we have

$$\begin{aligned} \mathbb{E} \left[\left\| \mathbf{f}(\hat{\boldsymbol{\psi}}_{k-1}, \boldsymbol{\psi}) + \hat{\mathbf{z}}_k \right\|_2^2 \right] &= \mathbb{E} \left[\left\| \mathbf{f}(\hat{\boldsymbol{\psi}}_{k-1}, \boldsymbol{\psi}) \right\|_2^2 + 2\mathbf{f}(\hat{\boldsymbol{\psi}}_{k-1}, \boldsymbol{\psi})^H \hat{\mathbf{z}}_k + \|\hat{\mathbf{z}}_k\|_2^2 \right] \\ &\stackrel{(c)}{=} \mathbb{E} \left[\left\| \mathbf{f}(\hat{\boldsymbol{\psi}}_{k-1}, \boldsymbol{\psi}) \right\|_2^2 \right] + \text{Tr} \left\{ \mathbf{I}_S(\hat{\boldsymbol{\psi}}_{k-1}, \mathbf{W}_k)^{-1} \right\}, \end{aligned} \quad (108)$$

where Step (c) is due to (105) and that $\hat{\mathbf{z}}_k$ is independent of $\mathbf{f}(\hat{\boldsymbol{\psi}}_{k-1}, \boldsymbol{\psi})$.

From (36), we have

$$\left\| \mathbf{f}(\hat{\boldsymbol{\psi}}_{k-1}, \boldsymbol{\psi}) \right\|_2^2 \leq \left\| \mathbf{I}_S(\hat{\boldsymbol{\psi}}_{k-1}, \mathbf{W}_k)^{-1} \right\|_F^2 \cdot \left\| \frac{2\|\mathbf{s}\|^2}{\sigma_z^2} \begin{bmatrix} \text{Re} \left\{ \mathbf{e}_k^H (\beta_k \mathbf{W}_k^H \mathbf{a}(\mathbf{x}_k) - \hat{\beta}_{k-1} \mathbf{e}_k) \right\} \\ \text{Im} \left\{ \mathbf{e}_k^H (\beta_k \mathbf{W}_k^H \mathbf{a}(\mathbf{x}_k) - \hat{\beta}_{k-1} \mathbf{e}_k) \right\} \\ \text{Re} \left\{ \tilde{\mathbf{e}}_{k1}^H (\beta_k \mathbf{W}_k^H \mathbf{a}(\mathbf{x}_k) - \hat{\beta}_{k-1} \mathbf{e}_k) \right\} \\ \text{Re} \left\{ \tilde{\mathbf{e}}_{k2}^H (\beta_k \mathbf{W}_k^H \mathbf{a}(\mathbf{x}_k) - \hat{\beta}_{k-1} \mathbf{e}_k) \right\} \end{bmatrix} \right\|_2^2. \quad (109)$$

As the Fisher information matrix is invertible, we get

$$\left\| \mathbf{I}_S(\hat{\boldsymbol{\psi}}_{k-1}, \mathbf{W}_k)^{-1} \right\|_F^2 < +\infty. \quad (110)$$

Besides, $\mathbf{W}_k = [\mathbf{w}_{k,1}, \mathbf{w}_{k,2}, \mathbf{w}_{k,3}]$, $\mathbf{e}_k = \mathbf{W}_k^H \mathbf{a}(\hat{\mathbf{x}}_{k-1})$, $\tilde{\mathbf{e}}_{k1} = \hat{\beta}_{k-1} \mathbf{W}_k^H \frac{\partial \mathbf{a}(\hat{\mathbf{x}}_{k-1})}{\partial x_1}$, $\tilde{\mathbf{e}}_{k2} = \hat{\beta}_{k-1} \mathbf{W}_k^H \frac{\partial \mathbf{a}(\hat{\mathbf{x}}_{k-1})}{\partial x_2}$, hence we have

$$\begin{aligned} \left| \mathbf{w}_{k,i}^H \mathbf{a}(\mathbf{x}) \right| &= \left| \frac{1}{\sqrt{MN}} \sum_{m=1}^M \sum_{n=1}^N e^{-j2\pi \left(\frac{(m-1)\delta_{k,i1}}{M} + \frac{(n-1)\delta_{k,i2}}{N} \right)} \right| \\ &\leq \frac{1}{\sqrt{MN}} \sum_{m=1}^M \sum_{n=1}^N \left| e^{-j2\pi \left(\frac{(m-1)\delta_{k,i1}}{M} + \frac{(n-1)\delta_{k,i2}}{N} \right)} \right| \\ &= \sqrt{MN} < +\infty, \end{aligned} \quad (111)$$

$$\begin{aligned}
\left| \mathbf{w}_{k,i}^H \frac{\partial \mathbf{a}(\mathbf{x})}{\partial x_1} \right| &= \left| \frac{1}{\sqrt{MN}} \sum_{m=1}^M \sum_{n=1}^N j 2\pi \frac{m-1}{M} e^{-j 2\pi \left(\frac{(m-1)\delta_{k,i1}}{M} + \frac{(n-1)\delta_{k,i2}}{N} \right)} \right| \\
&\leq \frac{2\pi}{M\sqrt{MN}} \sum_{m=1}^M \sum_{n=1}^N (m-1) \left| e^{-j 2\pi \left(\frac{(m-1)\delta_{k,i1}}{M} + \frac{(n-1)\delta_{k,i2}}{N} \right)} \right| \\
&= \sqrt{MN} (M-1) < +\infty,
\end{aligned} \tag{112}$$

and

$$\begin{aligned}
\left| \mathbf{w}_{k,i}^H \frac{\partial \mathbf{a}(\mathbf{x})}{\partial x_2} \right| &= \left| \frac{1}{\sqrt{MN}} \sum_{m=1}^M \sum_{n=1}^N j 2\pi \frac{n-1}{N} e^{-j 2\pi \left(\frac{(m-1)\delta_{k,i1}}{M} + \frac{(n-1)\delta_{k,i2}}{N} \right)} \right| \\
&\leq \frac{2\pi}{N\sqrt{MN}} \sum_{m=1}^M \sum_{n=1}^N (n-1) \left| e^{-j 2\pi \left(\frac{(m-1)\delta_{k,i1}}{M} + \frac{(n-1)\delta_{k,i2}}{N} \right)} \right| \\
&= \sqrt{MN} (N-1) < +\infty,
\end{aligned} \tag{113}$$

for $i = 1, 2, 3$ and all possible $\mathbf{w}_{k,i}$ and \mathbf{x} , where $[\delta_{k,i1}, \delta_{k,i2}]^T = \boldsymbol{\omega}_{k,i} - \mathbf{x}$. Thus we can get

$$\left\| \frac{2\|\mathbf{s}\|^2}{\sigma_z^2} \begin{bmatrix} \text{Re} \left\{ \mathbf{e}_k^H \left(\beta_k \mathbf{W}_k^H \mathbf{a}(\mathbf{x}_k) - \hat{\beta}_{k-1} \mathbf{e}_k \right) \right\} \\ \text{Im} \left\{ \mathbf{e}_k^H \left(\beta_k \mathbf{W}_k^H \mathbf{a}(\mathbf{x}_k) - \hat{\beta}_{k-1} \mathbf{e}_k \right) \right\} \\ \text{Re} \left\{ \tilde{\mathbf{e}}_{k1}^H \left(\beta_k \mathbf{W}_k^H \mathbf{a}(\mathbf{x}_k) - \hat{\beta}_{k-1} \mathbf{e}_k \right) \right\} \\ \text{Re} \left\{ \tilde{\mathbf{e}}_{k2}^H \left(\beta_k \mathbf{W}_k^H \mathbf{a}(\mathbf{x}_k) - \hat{\beta}_{k-1} \mathbf{e}_k \right) \right\} \end{bmatrix} \right\|_2 < +\infty. \tag{114}$$

Combining (110) and (114), we have

$$\mathbb{E} \left[\left\| \mathbf{f} \left(\hat{\boldsymbol{\psi}}_{k-1}, \boldsymbol{\psi} \right) \right\|_2^2 \right] < +\infty. \tag{115}$$

According to (110), it is clear that $\text{Tr} \left\{ \mathbf{I} \left(\hat{\boldsymbol{\psi}}_{k-1}, \mathbf{W}_k \right)^{-1} \right\} < +\infty$. Then, we can get that

$$\sup_k \mathbb{E} \left[\left\| \mathbf{f} \left(\hat{\boldsymbol{\psi}}_{k-1}, \boldsymbol{\psi} \right) + \hat{\mathbf{z}}_k \right\|_2^2 \right] < +\infty. \tag{116}$$

3) The function $\mathbf{f} \left(\hat{\boldsymbol{\psi}}_{k-1}, \boldsymbol{\psi} \right)$ should be continuous with respect to $\hat{\boldsymbol{\psi}}_{k-1}$.

By using (36), we know that each element of $\mathbf{f} \left(\hat{\boldsymbol{\psi}}_{k-1}, \boldsymbol{\psi} \right)$ is continuous with respect to $\hat{\boldsymbol{\psi}}_{k-1} = \left[\hat{\beta}_{k-1}^{re}, \hat{\beta}_{k-1}^{im}, \hat{x}_{k-1,1}, \hat{x}_{k-1,2} \right]^T$. Therefore, $\mathbf{f} \left(\hat{\boldsymbol{\psi}}_{k-1}, \boldsymbol{\psi} \right)$ is continuous with respect to $\hat{\boldsymbol{\psi}}_{k-1}$.

4) Let $\boldsymbol{\mu}_k = \mathbb{E} \left[\mathbf{f} \left(\hat{\boldsymbol{\psi}}_{k-1}, \boldsymbol{\psi} \right) + \hat{\mathbf{z}}_k \middle| \mathcal{G}_{k-1} \right] - \mathbf{f} \left(\hat{\boldsymbol{\psi}}_{k-1}, \boldsymbol{\psi} \right)$. We need to prove that $\sum_{k=1}^{+\infty} \|b_{S,k} \boldsymbol{\mu}_k\|_2 < +\infty$ with probability one.

From (106), we get $\boldsymbol{\mu}_k = \mathbf{0}$ for all $k \geq 1$. So we have $\sum_{k=1}^{+\infty} \|b_{S,k} \boldsymbol{\mu}_k\|_2 = 0 < +\infty$ with probability one.

By Theorem 5.2.1 in [31], $\hat{\boldsymbol{\psi}}_k$ converges to a unique stable point within the stable points set with probability one.

APPENDIX E

PROOF OF THEOREM 2

Theorem E is proven in three steps:

Step 1: Two continuous processes based on the discrete process $\hat{\boldsymbol{\psi}}_k = [\hat{\beta}_k^{re}, \hat{\beta}_k^{im}, \hat{x}_{k,1}, \hat{x}_{k,2}]^T$ are established, i.e., $\bar{\boldsymbol{\psi}}(t) \triangleq [\bar{\beta}^{re}(t), \bar{\beta}^{im}(t), \bar{x}_1(t), \bar{x}_2(t)]^T$ and $\tilde{\boldsymbol{\psi}}^k(t) \triangleq [\tilde{\beta}^{re,k}(t), \tilde{\beta}^{im,k}(t), \tilde{x}_1^k(t), \tilde{x}_2^k(t)]^T$.

The discrete time parameters are defined as: $t_0 \triangleq 0$, $t_k \triangleq \sum_{l=1}^k b_{S,l}$, $k \geq 1$. The first continuous process $\bar{\boldsymbol{\psi}}(t)$, $t \geq 0$ is constructed as the linear interpolation of the sequence $\hat{\boldsymbol{\psi}}_k$, $k \geq 0$, where $\bar{\boldsymbol{\psi}}(t_k) = \hat{\boldsymbol{\psi}}_k$, $k \geq 0$. Therefore, $\bar{\boldsymbol{\psi}}(t)$ is given by

$$\bar{\boldsymbol{\psi}}(t) = \bar{\boldsymbol{\psi}}(t_k) + \frac{(t-t_k)}{b_{S,k+1}} [\bar{\boldsymbol{\psi}}(t_{k+1}) - \bar{\boldsymbol{\psi}}(t_k)], t \in [t_k, t_{k+1}]. \quad (117)$$

The second continuous process $\tilde{\boldsymbol{\psi}}^k(t)$ is the solution of the following ordinary differential equation (ODE):

$$\frac{d\tilde{\boldsymbol{\psi}}^k(t)}{dt} = \mathbf{f}(\tilde{\boldsymbol{\psi}}^k(t), \boldsymbol{\psi}), \quad (118)$$

for $t \in [t_k, \infty)$, where $\tilde{\boldsymbol{\psi}}^k(t_k) = \bar{\boldsymbol{\psi}}(t_k) = \hat{\boldsymbol{\psi}}_k$, $k \geq 0$. Thus, $\tilde{\boldsymbol{\psi}}^k(t)$ can be given as

$$\tilde{\boldsymbol{\psi}}^k(t) = \bar{\boldsymbol{\psi}}(t_k) + \int_{t_k}^t \mathbf{f}(\tilde{\boldsymbol{\psi}}^k(v), \boldsymbol{\psi}) dv, t \geq t_k. \quad (119)$$

Step 2: By using the two continuous processes $\bar{\boldsymbol{\psi}}(t)$ and $\tilde{\boldsymbol{\psi}}^k(t)$ constructed in Step 1, a sufficient condition for the convergence of the discrete process $\hat{\boldsymbol{x}}_k$ is provided here.

We first construct a time-invariant set \mathcal{I} that includes the DPV \mathbf{x} within the main lobe, i.e., $\mathbf{x} \in \mathcal{I} \subset \mathcal{B}(\mathbf{x})$. Define $\tilde{\mathbf{x}}^0(t) \triangleq [\tilde{x}_1^0(t), \tilde{x}_2^0(t)]^T$ and denote $\hat{\mathbf{x}}_b = \tilde{\mathbf{x}}^0(t_b)$ as the beam direction of the process $\tilde{\boldsymbol{\psi}}^0(t)$ that is closest to the boundary of the main lobe, which is given by³

$$\inf_{\mathbf{v} \in \partial \mathcal{B}(\mathbf{x}), t \geq 0} \|\mathbf{v} - \tilde{\mathbf{x}}^0(t)\|_2 = \inf_{\mathbf{v} \in \partial \mathcal{B}(\mathbf{x})} \|\mathbf{v} - \hat{\mathbf{x}}_b\|_2 > 0. \quad (120)$$

³The boundary of the set $\mathcal{B}(\mathbf{x})$ is denoted by $\partial \mathcal{B}(\mathbf{x})$.

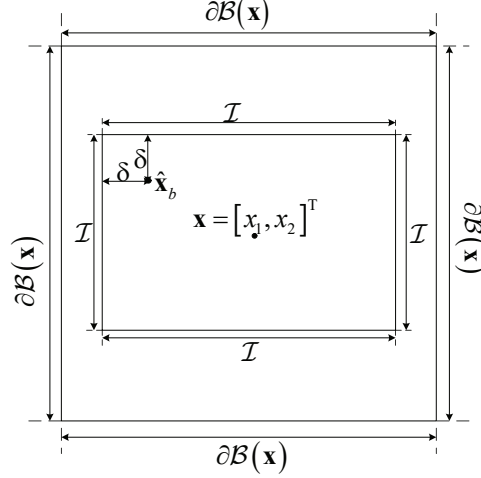


Fig. 11: An illustration of the invariant set \mathcal{I} .

Then we pick δ such that

$$\min \left\{ \inf_{\mathbf{v} \in \partial \mathcal{B}(x)} \|\mathbf{v} - \hat{\mathbf{x}}_b\|_{-\infty}, \|\hat{\mathbf{x}}_b - \mathbf{x}\|_{-\infty} \right\} > \delta > 0, \quad (121)$$

where $\|\mathbf{u}\|_{-\infty} = \min_{l=1,2}[\mathbf{u}]_l$ denotes the minimum element of \mathbf{u} . Note that when $t \geq t_b$, the solution $\tilde{\psi}^0(t)$ of the ODE (118) will approach the real channel gain β and DPV \mathbf{x} monotonically as time t increases. Hence, we construct the invariant set \mathcal{I} below:

$$\mathcal{I} = \left(x_1 - |x_1 - \hat{x}_{1,b}| - \delta, x_1 + |x_1 - \hat{x}_{1,b}| + \delta \right) \times \left(x_2 - |x_2 - \hat{x}_{2,b}| - \delta, x_2 + |x_2 - \hat{x}_{2,b}| + \delta \right) \subset \mathcal{B}(\mathbf{x}). \quad (122)$$

An example of the invariant set \mathcal{I} is shown in Fig. 11.

Then, a sufficient condition will be established in Lemma 6 that ensures $\hat{\mathbf{x}}_k \in \mathcal{I}$ for $k \geq 0$, and hence from Corollary 2.5 in [32], we can obtain that $\hat{\mathbf{x}}_k$ converges to \mathbf{x} . Before giving Lemma 6, let us provide some definitions first:

- Pick $T > 0$ such that the solution $\tilde{\psi}^0(t)$, $t \geq 0$ of the ODE (118) with $\tilde{\psi}^0(0) = [\hat{\beta}_0^{\text{re}}, \hat{\beta}_0^{\text{im}}, \hat{x}_{0,1}, \hat{x}_{0,2}]^T$ satisfies $\inf_{\mathbf{v} \in \partial \mathcal{B}} |\mathbf{v} - \tilde{\mathbf{x}}^0(t)| \geq 2\delta$ for $t \geq T$. Since when $t \geq t_b$, $\tilde{\mathbf{x}}^0(t)$ will approach the DPV \mathbf{x} monotonically as time t increases. One possible T is given by

$$T = \arg \min_{t \in [t_b, +\infty)} \left| \left| \int_{t_b}^t \mathbf{f} \left(\tilde{\psi}^0(v), \boldsymbol{\psi} \right) dv \right|_3 - \delta \right|, \quad (123)$$

where $[\cdot]_i$ denotes the i -th element of the vector.

- Let $T_0 \triangleq 0$ and $T_{l+1} \triangleq \min \{t_i : t_i \geq T_l + T, i \geq 0\}$ for $l \geq 0$. Then $T_{l+1} - T_l \in [T, T + b_{S,1}]$ and $T_l = t_{\tilde{k}(l)}$ for some $\tilde{k}(l) \uparrow +\infty$, where $\tilde{k}(0) = 0$. Let $\tilde{\psi}^{\tilde{k}(l)}(t)$ denotes the solution of ODE (118) for $t \in I_l \triangleq [T_l, T_{l+1}]$ with $\tilde{\psi}^{\tilde{k}(l)}(T_l) = \bar{\boldsymbol{\psi}}(T_l)$, $l \geq 0$.

Hence, we can obtain the following lemma:

Lemma 6. If $\sup_{t \in I_l} \left\| \bar{\mathbf{x}}(t) - \tilde{\mathbf{x}}^{\tilde{k}(l)}(t) \right\|_2 \leq \delta$ for all $l \geq 0$, then $\hat{\mathbf{x}}_k \in \mathcal{I}$ for all $k \geq 0$.

Proof. If $\sup_{t \in I_l} \left\| \bar{\mathbf{x}}(t) - \tilde{\mathbf{x}}^{\tilde{k}(l)}(t) \right\|_2 \leq \delta$ for all $l \geq 0$, then $\sup_{t \in I_l} \left| \bar{x}_1(t) - \tilde{x}_1^{\tilde{k}(l)}(t) \right| \leq \delta$ and $\sup_{t \in I_l} \left| \bar{x}_2(t) - \tilde{x}_2^{\tilde{k}(l)}(t) \right| \leq \delta$.

According to Lemma 1 in [18], $\hat{x}_{k,1} \in \mathcal{I}$ for all $k \geq 0$ and $\hat{x}_{k,2} \in \mathcal{I}$ for all $k \geq 0$. Hence, $\hat{\mathbf{x}}_k \in \mathcal{I}$ for all $k \geq 0$. ■

Step 3: We will derive the probability lower bound for the condition in Lemma 6, which is also a lower bound for $P(\hat{\mathbf{x}}_k \rightarrow \mathbf{x} | \hat{\mathbf{x}}_0 \in \mathcal{B}(\mathbf{x}))$.

We will derive the probability lower bound for the condition in Lemma 6, which results in the following lemma:

Lemma 7. If (i) the initial point satisfies $\hat{\mathbf{x}}_0 \in \mathcal{B}(\mathbf{x})$, (ii) $b_{S,k}$ is given by (40) with any $\epsilon_S > 0$, then there exist $K_{S,0} \geq 0$ and $R > 0$ such that

$$P(\hat{\mathbf{x}}_k \in \mathcal{I}, \forall k \geq 0) \geq 1 - 8e^{-\frac{R|s|^2}{\epsilon_S^2 \sigma_z^2}}. \quad (124)$$

Proof. See Appendix I. ■

Finally, applying Lemma 7 and Corollary 2.5 in [32], we can obtain

$$P(\hat{\mathbf{x}}_k \rightarrow \mathbf{x} | \hat{\mathbf{x}}_0 \in \mathcal{B}) \geq P(\hat{\mathbf{x}}_k \in \mathcal{I}, \forall k \geq 0) \geq 1 - 8e^{-\frac{R|s|^2}{\epsilon_S^2 \sigma_z^2}},$$

which completes the proof of Theorem 2.

APPENDIX F

PROOF OF THEOREM 3

If the step-size $b_{S,k}$ is given by (40) with any $\epsilon_S > 0$ and $K_{S,0} \geq 0$, the sufficient conditions are provided by Theorem 6.6.1 [30, Section 6.6] to prove the asymptotic normality of $\sqrt{k}(\hat{\mathbf{x}}_k - \mathbf{x})$, i.e., $\sqrt{k}(\hat{\mathbf{x}}_k - \mathbf{x}) \xrightarrow{d} \mathcal{N}(0, \Sigma_{\mathbf{x}})$. With the condition that $\hat{\boldsymbol{\psi}}_k \rightarrow \boldsymbol{\psi}$, we can prove that the beam and channel tracking algorithm satisfies the conditions above and obtain the variance $\Sigma_{\mathbf{x}}$ as follows:

- 1) Equation (38) is supposed to satisfy: (i) there exists an increasing sequence of σ -fields $\{\mathcal{F}_k : k \geq 0\}$ such that $\mathcal{F}_l \subset \mathcal{F}_k$ for $l < k$, and (ii) the random noise $\hat{\mathbf{z}}_k$ is \mathcal{F}_k -measurable and independent of \mathcal{F}_{k-1} .

As is shown in Appendix D, there exists an increasing sequence of σ -fields $\{\mathcal{G}_k : k \geq 0\}$, where ς_k is measurable with respect to \mathcal{G}_{k-1} and independent of \mathcal{G}_{k-1} .

2) $\hat{\mathbf{x}}_k$ should converge to \mathbf{x} almost surely as $k \rightarrow +\infty$.

We assume that $\hat{\boldsymbol{\psi}}_k \rightarrow \boldsymbol{\psi}$, hence $\hat{\mathbf{x}}_k$ converges to \mathbf{x} almost surely when $k \rightarrow +\infty$.

3) The stable condition:

In (36), we rewrite $\mathbf{f}(\hat{\boldsymbol{\psi}}_{k-1}, \boldsymbol{\psi})$ as follows:

$$\mathbf{f}(\hat{\boldsymbol{\psi}}_{k-1}, \boldsymbol{\psi}) = \mathbf{D}_1(\hat{\boldsymbol{\psi}}_{k-1} - \boldsymbol{\psi}) + \begin{bmatrix} o(\|\hat{\boldsymbol{\psi}}_{k-1} - \boldsymbol{\psi}\|_2) \\ o(\|\hat{\boldsymbol{\psi}}_{k-1} - \boldsymbol{\psi}\|_2) \\ o(\|\hat{\boldsymbol{\psi}}_{k-1} - \boldsymbol{\psi}\|_2) \\ o(\|\hat{\boldsymbol{\psi}}_{k-1} - \boldsymbol{\psi}\|_2) \end{bmatrix}, \quad (125)$$

where \mathbf{D}_1 is given by

$$\mathbf{D}_1 = \left. \frac{\partial \mathbf{f}(\hat{\boldsymbol{\psi}}_{k-1}, \boldsymbol{\psi})}{\partial \hat{\boldsymbol{\psi}}_{k-1}^T} \right|_{\hat{\boldsymbol{\psi}}_{k-1} = \boldsymbol{\psi}} = - \begin{bmatrix} 1 & 0 & 0 & 0 \\ 0 & 1 & 0 & 0 \\ 0 & 0 & 1 & 0 \\ 0 & 0 & 0 & 1 \end{bmatrix}. \quad (126)$$

Then the stable condition is obtained that:

$$\mathbf{E} = \mathbf{D}_1 \cdot \varepsilon_S + \frac{1}{2} = \begin{bmatrix} \frac{1}{2} - \varepsilon_S & 0 & 0 & 0 \\ 0 & \frac{1}{2} - \varepsilon_S & 0 & 0 \\ 0 & 0 & \frac{1}{2} - \varepsilon_S & 0 \\ 0 & 0 & 0 & \frac{1}{2} - \varepsilon_S \end{bmatrix} \prec 0, \quad (127)$$

which leads to $\varepsilon_S > \frac{1}{2}$.

4) The noise vector $\hat{\mathbf{z}}_k$ satisfies:

$$\mathbb{E} [\|\hat{\mathbf{z}}_k\|_2^2] = \text{tr} \left\{ \mathbf{I}_S(\hat{\boldsymbol{\psi}}_{k-1}, \mathbf{W}_k)^{-1} \right\} < +\infty, \quad (128)$$

and

$$\lim_{v \rightarrow +\infty} \sup_{k \geq 1} \int_{\|\hat{\mathbf{z}}_k\|_2 > v} \|\hat{\mathbf{z}}_k\|_2^2 p(\hat{\mathbf{z}}_k) d\hat{\mathbf{z}}_k = 0. \quad (129)$$

Let

$$\begin{aligned} \mathbf{F} &= \lim_{k \rightarrow +\infty} \mathbb{E} [\hat{\mathbf{z}}_k \hat{\mathbf{z}}_k^T] \stackrel{(a)}{=} \lim_{k \rightarrow +\infty} \mathbf{I}_S(\hat{\boldsymbol{\psi}}_{k-1}, \mathbf{W}_k)^{-1} = \mathbf{I}_S(\boldsymbol{\psi}, \tilde{\mathbf{W}}_S^*)^{-1}, \\ \hat{\boldsymbol{\psi}}_k &\rightarrow \boldsymbol{\psi} \qquad \qquad \hat{\boldsymbol{\psi}}_k \rightarrow \boldsymbol{\psi} \end{aligned}$$

where step (a) is obtained from (105).

By Theorem 6.6.1 [30, Section 6.6], we have

$$\sqrt{k + K_{S,0}} \left(\hat{\boldsymbol{\psi}}_k - \boldsymbol{\psi} \right) \xrightarrow{d} \mathcal{N}(0, \boldsymbol{\Sigma}_x),$$

where

$$\boldsymbol{\Sigma}_x = \varepsilon_S^2 \cdot \int_0^\infty e^{\mathbf{E}v} \mathbf{F} e^{\mathbf{E}^H v} dv = \frac{\varepsilon_S^2}{2\varepsilon_S - 1} \mathbf{I}_S(\boldsymbol{\psi}, \tilde{\mathbf{W}}^*)^{-1}. \quad (130)$$

Due to that $\lim_{k \rightarrow +\infty} \sqrt{(k + K_{S,0})/k} = 1$, we have

$$\sqrt{k} \left(\hat{\boldsymbol{\psi}}_k - \boldsymbol{\psi} \right) \rightarrow \sqrt{k} \cdot \sqrt{\frac{k + K_{S,0}}{k}} \left(\hat{\boldsymbol{\psi}}_k - \boldsymbol{\psi} \right) \xrightarrow{d} \mathcal{N}(0, \boldsymbol{\Sigma}_x),$$

if $k \rightarrow +\infty$. Thus, we can get

$$\sqrt{k} \left(\hat{\boldsymbol{\psi}}_k - \boldsymbol{\psi} \right) \xrightarrow{d} \mathcal{N}(0, \boldsymbol{\Sigma}_x). \quad (131)$$

By adopting $\varepsilon_S = 1$ in (130), we can obtain

$$\sqrt{k} \left(\hat{\boldsymbol{\psi}}_k - \boldsymbol{\psi} \right) \xrightarrow{d} \mathcal{N}\left(0, \mathbf{I}_S(\boldsymbol{\psi}, \tilde{\mathbf{W}}^*)^{-1}\right). \quad (132)$$

Since $\hat{\boldsymbol{\psi}}_k \rightarrow \boldsymbol{\psi}$ as $k \rightarrow +\infty$, $\hat{\mathbf{h}}_k - \mathbf{h}$ is linear to $\hat{\boldsymbol{\psi}}_k - \boldsymbol{\psi}$. Hence, $\hat{\mathbf{h}}_k - \mathbf{h}$ is also asymptotically Gaussian.

Combining (69), (132) and (21), we can conclude that

$$\lim_{k \rightarrow +\infty} \frac{k}{MN} \mathbb{E} \left[\left\| \hat{\mathbf{h}}_k - \mathbf{h} \right\|_2^2 \middle| \hat{\boldsymbol{\psi}}_k \rightarrow \boldsymbol{\psi} \right] = C_S^{\min}(\boldsymbol{\psi}). \quad (133)$$

APPENDIX G

PROOF OF LEMMA 4

In problem (47), the constraint (48) ensures that $\hat{\mathbf{x}}_k$ is an unbiased estimate of \mathbf{x} . According to section 3.7 of [26], if $\hat{\mathbf{x}}$ is an unbiased estimate of \mathbf{x} , then we can obtain that

$$\text{Cov}(\hat{\mathbf{x}}) - \mathbf{I}^{-1}(\mathbf{x}) \succeq \mathbf{0}, \quad (134)$$

where $\text{Cov}(\hat{\mathbf{x}})$ denotes the covariance matrix of $\hat{\mathbf{x}}$, $\mathbf{I}(\mathbf{x})$ is the corresponding Fisher information matrix and $\mathbf{A} \succeq \mathbf{0}$ means that the matrix \mathbf{A} is nonnegative definite. From (134), we can get that

$$\text{Cov}(\hat{\mathbf{x}}_k) - \left(\sum_{l=1}^k \mathbf{I}_{DI}(\mathbf{x}, \mathbf{W}_l) \right) \succeq \mathbf{0}, \quad (135)$$

which implies that the diagonal elements of the matrix on the left side of ' \succeq ' are nonnegative because all matrices are 2×2 in (135). Therefore, we obtain that

$$\text{Tr} \{ \text{Cov}(\hat{\mathbf{x}}_k) \} - \text{Tr} \left\{ \left(\sum_{l=1}^k \mathbf{I}(\mathbf{x}, \mathbf{W}_l) \right) \right\} \geq 0, \quad (136)$$

i.e.,

$$\mathbb{E} [\|\hat{\mathbf{x}}_k - \mathbf{x}\|_2^2] - \text{Tr} \left\{ \left(\sum_{l=1}^k \mathbf{I}_{DI}(\mathbf{x}, \mathbf{W}_l) \right) \right\} \geq 0, \quad (137)$$

which yields the result of (49).

Now we try to obtain the Fisher information matrix in (50). According to (44), the determinant and inverse of covariance matrix can be written as follows:

$$\begin{cases} |\Sigma_{\mathbf{y},k}| = \sigma_z^4 \left(|\mathbf{s}|^2 \sigma_\beta^2 (\mathbf{W}_k^H \mathbf{a}(\mathbf{x}))^H \mathbf{W}_k^H \mathbf{a}(\mathbf{x}) + \sigma_z^2 \right) \\ \Sigma_{\mathbf{y},k}^{-1} = \frac{\mathbf{J}_3}{\sigma_z^2} - \frac{\sigma_z^2 |\mathbf{s}|^2 \sigma_\beta^2 \mathbf{W}_k^H \mathbf{a}(\mathbf{x}) (\mathbf{W}_k^H \mathbf{a}(\mathbf{x}))^H}{|\Sigma_{\mathbf{y},k}|} \end{cases}. \quad (138)$$

Based on the definition in (52), the determinant and inverse of covariance matrix in (138) can be rewritten as

$$\begin{cases} |\Sigma_{\mathbf{y},k}| = \sigma_z^4 \left(|\mathbf{s}|^2 \sigma_\beta^2 \mathbf{g}_k^H \mathbf{g}_k + \sigma_z^2 \right) \\ \Sigma_{\mathbf{y},k}^{-1} = \frac{\mathbf{J}_3}{\sigma_z^2} - \frac{\sigma_z^2 |\mathbf{s}|^2 \sigma_\beta^2 \mathbf{g}_k \mathbf{g}_k^H}{|\Sigma_{\mathbf{y},k}|} \end{cases}. \quad (139)$$

In addition, with the help of (43), we can obtain that

$$\frac{\partial \log p_{DI}(\mathbf{y}_k | \mathbf{x}, \mathbf{W}_k)}{\partial x_p} = -\frac{1}{|\Sigma_{\mathbf{y},k}|} \frac{\partial |\Sigma_{\mathbf{y},k}|}{\partial x_p} - \mathbf{y}_k^H \frac{\partial \Sigma_{\mathbf{y},k}^{-1}}{\partial x_p} \mathbf{y}_k, \quad (140)$$

where $\frac{\partial |\Sigma_{\mathbf{y},k}|}{\partial x_p}$ and $\frac{\partial \Sigma_{\mathbf{y},k}^{-1}}{\partial x_p}$ are given by (141) according to (139):

$$\begin{cases} \frac{\partial |\Sigma_{\mathbf{y},k}|}{\partial x_p} = \sigma_z^4 |\mathbf{s}|^2 \sigma_\beta^2 \frac{\partial \mathbf{g}_k^H \mathbf{g}_k}{\partial x_p} \\ \frac{\partial \Sigma_{\mathbf{y},k}^{-1}}{\partial x_p} = -\sigma_z^2 |\mathbf{s}|^2 \sigma_\beta^2 \frac{\frac{\partial \mathbf{g}_k \mathbf{g}_k^H}{\partial x_p} |\Sigma_{\mathbf{y},k}| - \mathbf{g}_k \mathbf{g}_k^H \frac{\partial |\Sigma_{\mathbf{y},k}|}{\partial x_p}}{|\Sigma_{\mathbf{y},k}|^2} \end{cases}. \quad (141)$$

By combining (5), (44) and (140), we can obtain the p -th row, j -th column element of the Fisher information matrix in (50)

$$\begin{aligned}
[\mathbf{I}_{DI}(\mathbf{x}, \mathbf{W}_k)]_{p,j} &= \mathbb{E} \left[\frac{\partial \log p_{DI}(\mathbf{y}_k | \mathbf{x}, \mathbf{W}_k)}{\partial x_p} \frac{\partial \log p_{DI}(\mathbf{y}_k | \mathbf{x}, \mathbf{W}_k)}{\partial x_j} \right] \\
&= -\frac{1}{|\Sigma_{\mathbf{y},k}|} \frac{\partial |\Sigma_{\mathbf{y},k}|}{\partial x_p} \frac{\partial |\Sigma_{\mathbf{y},k}|}{\partial x_j} + 2|\mathbf{s}|^4 \sigma_\beta^4 \mathbf{g}_k^H \frac{\partial \Sigma_{\mathbf{y},k}^{-1}}{\partial x_p} \mathbf{g}_k \mathbf{g}_k^H \frac{\partial \Sigma_{\mathbf{y},k}^{-1}}{\partial x_j} \mathbf{g}_k \\
&\quad + \sigma_z^2 |\mathbf{s}|^2 \sigma_\beta^2 \mathbf{g}_k^H \frac{\partial \Sigma_{\mathbf{y},k}^{-1}}{\partial x_p} \mathbf{g}_k \text{Tr} \left\{ \frac{\partial \Sigma_{\mathbf{y},k}^{-1}}{\partial x_j} \right\} + \sigma_z^2 |\mathbf{s}|^2 \sigma_\beta^2 \mathbf{g}_k^H \frac{\partial \Sigma_{\mathbf{y},k}^{-1}}{\partial x_j} \mathbf{g}_k \text{Tr} \left\{ \frac{\partial \Sigma_{\mathbf{y},k}^{-1}}{\partial x_p} \right\} \\
&\quad + \sigma_z^4 \text{Tr} \left\{ \frac{\partial \Sigma_{\mathbf{y},k}^{-1}}{\partial x_p} \right\} \text{Tr} \left\{ \frac{\partial \Sigma_{\mathbf{y},k}^{-1}}{\partial x_j} \right\} + \sigma_z^4 \text{Tr} \left\{ \frac{\partial \Sigma_{\mathbf{y},k}^{-1}}{\partial x_p} \frac{\partial \Sigma_{\mathbf{y},k}^{-1}}{\partial x_j} \right\} \\
&\quad + \sigma_z^2 |\mathbf{s}|^2 \sigma_\beta^2 \mathbf{g}_k^H \left(\frac{\partial \Sigma_{\mathbf{y},k}^{-1}}{\partial x_p} \frac{\partial \Sigma_{\mathbf{y},k}^{-1}}{\partial x_j} + \frac{\partial \Sigma_{\mathbf{y},k}^{-1}}{\partial x_j} \frac{\partial \Sigma_{\mathbf{y},k}^{-1}}{\partial x_p} \right) \mathbf{g}_k.
\end{aligned} \tag{142}$$

Then we substitute (44), (45), (52), (139), (141) into (142), which yields the result of (51).

Finally, the proof Lemma 4 is completed.

APPENDIX H

PROOF OF LEMMA 5

The proof of property 1) in Lemma 5 is similar to the proof of those in Lemma 3. Hence, we focus on the proof of property 2) and property 3) in Lemma 5.

Consider the p -th row, j -th column element of the Fisher information matrix $\mathbf{I}_{DI}(\mathbf{x}, \mathbf{W}_k)$ in (51). We can rewrite it as follows:

$$\begin{aligned}
[\mathbf{I}_{DI}(\mathbf{x}, \mathbf{W}_k)]_{p,j} &= \frac{\sigma_z^6 |\mathbf{s}|^6 \sigma_\beta^6}{|\Sigma_{\mathbf{y},k}|^2} \left\{ -2|\mathbf{g}_k|^2 \tilde{g}_{k,p} \tilde{g}_{k,j} + \frac{\sigma_z^2}{|\mathbf{s}|^2 \sigma_\beta^2} \text{Tr} \{ \mathbf{G}_{k,p} \mathbf{G}_{k,j} \} + \mathbf{g}_k^H (\mathbf{G}_{k,p} \mathbf{G}_{k,j} + \mathbf{G}_{k,j} \mathbf{G}_{k,p}) \mathbf{g}_k \right\} \\
&\stackrel{(a)}{=} \frac{\sigma_z^6 |\mathbf{s}|^6 \sigma_\beta^6}{\sigma_z^8 \left(|\mathbf{s}|^2 \sigma_\beta^2 \mathbf{g}_k^H \mathbf{g}_k + \sigma_z^2 \right)^2} \left\{ -2|\mathbf{g}_k|^2 \tilde{g}_{k,p} \tilde{g}_{k,j} + \frac{\sigma_z^2}{|\mathbf{s}|^2 \sigma_\beta^2} \text{Tr} \{ \mathbf{G}_{k,p} \mathbf{G}_{k,j} \} + \mathbf{g}_k^H (\mathbf{G}_{k,p} \mathbf{G}_{k,j} + \mathbf{G}_{k,j} \mathbf{G}_{k,p}) \mathbf{g}_k \right\} \\
&= \frac{|\mathbf{s}|^2 \sigma_\beta^2}{\sigma_z^2 \left(\mathbf{g}_k^H \mathbf{g}_k + \frac{\sigma_z^2}{|\mathbf{s}|^2 \sigma_\beta^2} \right)^2} \left\{ -2|\mathbf{g}_k|^2 \tilde{g}_{k,p} \tilde{g}_{k,j} + \frac{\sigma_z^2}{|\mathbf{s}|^2 \sigma_\beta^2} \text{Tr} \{ \mathbf{G}_{k,p} \mathbf{G}_{k,j} \} + \mathbf{g}_k^H (\mathbf{G}_{k,p} \mathbf{G}_{k,j} + \mathbf{G}_{k,j} \mathbf{G}_{k,p}) \mathbf{g}_k \right\}, \tag{143}
\end{aligned}$$

where Step (a) is obtained by substituting (138) into (143). Immediately, we have that $\mathbf{I}_{DI}(\mathbf{x}, \mathbf{W}_k)$ is related to $\frac{|\mathbf{s}|^2 \sigma_\beta^2}{\sigma_z^2}$ and $\Delta_{DI,1}^*$, $\Delta_{DI,2}^*$, $\Delta_{DI,3}^*$ are variant to $\frac{|\mathbf{s}|^2 \sigma_\beta^2}{\sigma_z^2}$.

When $\frac{|\mathbf{s}|^2 \sigma_\beta^2}{\sigma_z^2} \rightarrow +\infty$, we can obtain the element of $\mathbf{I}_{DI}(\mathbf{x}, \mathbf{W}_k)$ as below:

$$\lim_{\frac{|\mathbf{s}|^2 \sigma_\beta^2}{\sigma_z^2} \rightarrow +\infty} \frac{\sigma_z^2}{|\mathbf{s}|^2 \sigma_\beta^2} [\mathbf{I}_{DI}(\mathbf{x}, \mathbf{W}_k)]_{p,j} = \frac{1}{(\mathbf{g}_k^H \mathbf{g}_k)^2} \left\{ -2|\mathbf{g}_k|^2 \tilde{g}_{k,p} \tilde{g}_{k,j} + \mathbf{g}_k^H (\mathbf{G}_{k,p} \mathbf{G}_{k,j} + \mathbf{G}_{k,j} \mathbf{G}_{k,p}) \mathbf{g}_k \right\}, \tag{144}$$

which reveals that $\frac{\sigma_z^2}{|\mathbf{s}|^2\sigma_\beta^2}\mathbf{I}_{DI}(\mathbf{x}, \mathbf{W}_k)$ converges as $\frac{|\mathbf{s}|^2\sigma_\beta^2}{\sigma_z^2} \rightarrow +\infty$ and $\Delta_{DI,1}^*, \Delta_{DI,2}^*, \Delta_{DI,3}^*$ also converge. Then the property 2) of Lemma 5 is completed.

Let us see the property 3) in Lemma 5. Similar to Step 3 in Appendix C, we can obtain that $\Delta_{DI,1}^*, \Delta_{DI,2}^*, \Delta_{DI,3}^*$ converge as $M, N \rightarrow +\infty$. According to (52) and (101), \mathbf{g}_k is $\Theta(\sqrt{MN})$ while $\tilde{g}_{k,p}$ and $\mathbf{G}_{k,p}$ are $\Theta(MN)$. Hence, $\sigma_z^2 \text{Tr}\{\mathbf{G}_{k,p}\mathbf{G}_{k,j}\}$ can be omitted since it is $\Theta((MN)^2)$ while other parts are $\Theta((MN)^{\frac{5}{2}})$. Then the p -th row, j -th column element of the Fisher information matrix in (145) can be rewritten as

$$\begin{aligned} \lim_{M,N \rightarrow +\infty} \frac{[\mathbf{I}_{DI}(\mathbf{x}, \mathbf{W}_k)]_{p,j}}{(MN)^{5/2}} &= \frac{\sigma_z^6 |\mathbf{s}|^4 \sigma_\beta^4}{|\Sigma_{\mathbf{y},k}|^2} \left\{ -2|\mathbf{s}|^2 \sigma_\beta^2 \frac{|\mathbf{g}_k|^2 \tilde{g}_{k,p} \tilde{g}_{k,j}}{(MN)^{5/2}} + |\mathbf{s}|^2 \sigma_\beta^2 \frac{\mathbf{g}_k^H (\mathbf{G}_{k,p} \mathbf{G}_{k,j} + \mathbf{G}_{k,j} \mathbf{G}_{k,p}) \mathbf{g}_k}{(MN)^{5/2}} \right\} \\ &= \frac{\sigma_z^6 |\mathbf{s}|^6 \sigma_\beta^6}{|\Sigma_{\mathbf{y},k}|^2} \left\{ -2 \frac{|\mathbf{g}_k|^2 \tilde{g}_{k,p} \tilde{g}_{k,j}}{(MN)^{5/2}} + \frac{\mathbf{g}_k^H (\mathbf{G}_{k,p} \mathbf{G}_{k,j} + \mathbf{G}_{k,j} \mathbf{G}_{k,p}) \mathbf{g}_k}{(MN)^{5/2}} \right\}, \end{aligned} \quad (145)$$

which reveals that $\tilde{\Delta}_{DI,1}^*, \tilde{\Delta}_{DI,2}^*, \tilde{\Delta}_{DI,3}^*$ are unrelated to $\frac{|\mathbf{s}|^2\sigma_\beta^2}{\sigma_z^2}$.

Finally, the proof is completed.

APPENDIX I

PROOF OF LEMMA 7

The following lemmas are introduced to prove Lemma 7.

Lemma 8 (Lemma 3 [18]). Given T by (123) and

$$k_T \triangleq \inf \{i \in \mathbb{Z} : t_{k+i} \geq t_k + T\}. \quad (146)$$

If there exists a constant $C > 0$, which satisfies

$$\left\| \bar{\boldsymbol{\psi}}(t_{k+l}) - \tilde{\boldsymbol{\psi}}^k(t_{k+l}) \right\|_2 \leq L \sum_{i=1}^l b_{S,k+i} \left\| \bar{\boldsymbol{\psi}}(t_{k+i-1}) - \tilde{\boldsymbol{\psi}}^k(t_{k+i-1}) \right\|_2 + C, \quad (147)$$

for all $k \geq 0$ and $1 \leq l \leq k_T$, then

$$\sup_{t \in [t_k, t_{k+k_T}]} \left\| \bar{\boldsymbol{\psi}}(t) - \tilde{\boldsymbol{\psi}}^k(t) \right\|_2 \leq \frac{C_f b_{S,k+1}}{2} + C e^{L(T+b_{S,1})}, \quad (148)$$

where L and C_f are defined in (153) and (154) separately.

Lemma 9 (Lemma 4 [35]). If $\{M_i : i = 1, 2, \dots\}$ satisfies that: (i) M_i is Gaussian distributed with zero mean, and (ii) M_i is a martingale in i , then

$$P \left(\sup_{0 \leq i \leq k} |M_i| > \eta \right) \leq 2 \exp \left\{ -\frac{\eta^2}{2 \text{Var}[M_k]} \right\}, \quad (149)$$

for any $\eta > 0$.

Lemma 10 (Lemma 5 [35]). If given a constant $C > 0$, then

$$G(v) = \frac{1}{v} \exp \left[-\frac{C}{v} \right], \quad (150)$$

is increasing for all $0 < v < C$.

Let $\xi_0 \triangleq \mathbf{0}$ and $\xi_k \triangleq \sum_{l=1}^k b_{S,l} \hat{\mathbf{z}}_l$, $k \geq 1$, where $\hat{\mathbf{z}}_l$ is given in (37). With (117) and (119), we have for t_{k+l} , $1 \leq l \leq k_T$,

$$\bar{\psi}(t_{k+l}) = \bar{\psi}(t_k) + \sum_{i=1}^l b_{S,k+i} \mathbf{f}(\bar{\psi}(t_{k+i-1}), \boldsymbol{\psi}) + (\xi_{k+l} - \xi_k), \quad (151)$$

and

$$\begin{aligned} \tilde{\psi}^n(t_{k+l}) &= \tilde{\psi}^k(t_k) + \int_{t_k}^{t_{k+l}} \mathbf{f}(\tilde{\psi}^k(v), \boldsymbol{\psi}) dv \\ &= \tilde{\psi}^k(t_k) + \sum_{i=1}^l b_{S,k+i} \mathbf{f}(\tilde{\psi}^k(t_{k+i-1}), \boldsymbol{\psi}) + \int_{t_k}^{t_{k+l}} \left[\mathbf{f}(\tilde{\psi}^k(v), \boldsymbol{\psi}) - \mathbf{f}(\tilde{\psi}^k(\underline{v}), \boldsymbol{\psi}) \right] dv, \end{aligned} \quad (152)$$

where $\underline{v} \triangleq \max \{t_k : t_k \leq v, k \geq 0\}$ for $v \geq 0$.

To bound $\int_{t_k}^{t_{k+l}} \left[\mathbf{f}(\tilde{\psi}^k(v), \boldsymbol{\psi}) - \mathbf{f}(\tilde{\psi}^k(\underline{v}), \boldsymbol{\psi}) \right] dv$ on the RHS of (152), we obtain the Lipschitz constant of function $\mathbf{f}(\mathbf{v}, \boldsymbol{\psi})$ considering the first variable \mathbf{v} , given by

$$L \triangleq \sup_{\mathbf{v}_1 \neq \mathbf{v}_2} \frac{\|\mathbf{f}(\mathbf{v}_1, \boldsymbol{\psi}) - \mathbf{f}(\mathbf{v}_2, \boldsymbol{\psi})\|_2}{\|\mathbf{v}_1 - \mathbf{v}_2\|_2}. \quad (153)$$

Similar to (109), for any $t \geq t_k$, we can obtain that there exists a constant $0 < C_f < +\infty$ such that

$$\left\| \mathbf{f}(\tilde{\psi}^k(t), \boldsymbol{\psi}) \right\|_2 \leq C_f. \quad (154)$$

Hence, we have

$$\begin{aligned}
& \left\| \int_{t_k}^{t_{k+m}} \left[\mathbf{f} \left(\tilde{\boldsymbol{\psi}}^k(v), \boldsymbol{\psi} \right) - \mathbf{f} \left(\tilde{\boldsymbol{\psi}}^k(\underline{v}), \boldsymbol{\psi} \right) \right] dv \right\|_2 & (155) \\
& \leq \int_{t_k}^{t_{k+l}} \left\| \mathbf{f} \left(\tilde{\boldsymbol{\psi}}^k(v), \boldsymbol{\psi} \right) - \mathbf{f} \left(\tilde{\boldsymbol{\psi}}^k(\underline{v}), \boldsymbol{\psi} \right) \right\|_2 dv \\
& \stackrel{(a)}{\leq} \int_{t_k}^{t_{k+l}} L \left\| \tilde{\boldsymbol{\psi}}^k(v) - \tilde{\boldsymbol{\psi}}^k(\underline{v}) \right\|_2 dv \\
& \stackrel{(b)}{\leq} \int_{t_k}^{t_{k+l}} L \left\| \int_{\underline{v}}^v \mathbf{f} \left(\tilde{\boldsymbol{\psi}}^k(s), \boldsymbol{\psi} \right) ds \right\|_2 dv \\
& \leq \int_{t_k}^{t_{k+l}} \int_{\underline{v}}^v L \left\| \mathbf{f} \left(\tilde{\boldsymbol{\psi}}^k(s), \boldsymbol{\psi} \right) \right\|_2 ds dv & (156) \\
& \stackrel{(c)}{\leq} \int_{t_k}^{t_{k+l}} \int_{\underline{v}}^v C_{\mathbf{f}} L ds dv = \int_{t_k}^{t_{k+l}} C_{\mathbf{f}} L (v - \underline{v}) dv \\
& = \sum_{i=1}^l \int_{t_{k+i-1}}^{t_{k+i}} C_{\mathbf{f}} L (v - t_{k+i-1}) dv \\
& = \sum_{i=1}^l \frac{C_{\mathbf{f}} L (t_{k+i} - t_{k+i-1})^2}{2} = \frac{C_{\mathbf{f}} L}{2} \sum_{i=1}^l b_{S,k+i}^2,
\end{aligned}$$

where Step (a) is due to (153), Step (b) is due to the definition in (119), and Step (c) is due to (154). Then, by subtracting $\tilde{\boldsymbol{\psi}}^k(t_{k+l})$ in (152) from $\bar{\boldsymbol{\psi}}(t_{k+l})$ in (151) and taking norms, the following inequality can be obtained from (153) and (155) for $k \geq 0, 1 \leq l \leq k_T$:

$$\begin{aligned}
\left\| \bar{\boldsymbol{\psi}}(t_{k+l}) - \tilde{\boldsymbol{\psi}}^k(t_{k+l}) \right\|_2 & \leq L \sum_{i=1}^l b_{S,k+i} \left\| \bar{\boldsymbol{\psi}}(t_{k+i-1}) - \tilde{\boldsymbol{\psi}}^k(t_{k+i-1}) \right\|_2 + \frac{C_{\mathbf{f}} L}{2} \sum_{i=1}^l b_{S,k+i}^2 + \left\| \boldsymbol{\xi}_{k+l} - \boldsymbol{\xi}_k \right\|_2 & (157) \\
& \leq L \sum_{i=1}^l b_{S,k+i} \left\| \bar{\boldsymbol{\psi}}(t_{k+i-1}) - \tilde{\boldsymbol{\psi}}^k(t_{k+i-1}) \right\|_2 + \frac{C_{\mathbf{f}} L}{2} \sum_{i=1}^{k_T} b_{S,k+i}^2 + \sup_{1 \leq l \leq k_T} \left\| \boldsymbol{\xi}_{k+l} - \boldsymbol{\xi}_k \right\|_2.
\end{aligned}$$

Applying Lemma 8 to (157) and letting

$$C = \frac{C_{\mathbf{f}} L}{2} \sum_{i=1}^{k_T} b_{S,k+i}^2 + \sup_{1 \leq l \leq k_T} \left\| \boldsymbol{\xi}_{k+l} - \boldsymbol{\xi}_k \right\|_2,$$

yields

$$\sup_{t \in [t_k, t_{k+k_T}]} \left\| \bar{\boldsymbol{\psi}}(t) - \tilde{\boldsymbol{\psi}}^k(t) \right\|_2 \leq C_e \left\{ \frac{C_{\mathbf{f}} L}{2} [c(k) - c(k+k_T)] + \sup_{1 \leq l \leq k_T} \left\| \boldsymbol{\xi}_{k+l} - \boldsymbol{\xi}_k \right\|_2 \right\} + \frac{C_{\mathbf{f}} c_{k+1}}{2}, \quad (158)$$

where $C_e \triangleq e^{L(T+bs_{s,1})}$, and $c(k) \triangleq \sum_{i>k} b_{S,i}^2$. Letting $k = \tilde{k}(l)$ in (158), we have $k+k_T = \tilde{k}(l+1)$ due to the definition of $T_{l+1} = t_{\tilde{k}(l+1)}$ in Step 2 of Appendix E and

$$\begin{aligned} & \sup_{t \in I_l} \left\| \bar{\boldsymbol{\psi}}(t) - \tilde{\boldsymbol{\psi}}^{\tilde{k}(l)}(t) \right\|_2 \\ & \leq C_e \left\{ \frac{C_f L}{2} [c(\tilde{k}(l)) - c(\tilde{k}(l+1))] + \sup_{\tilde{k}(l) \leq p \leq \tilde{k}(l+1)} \left\| \boldsymbol{\xi}_p - \boldsymbol{\xi}_{\tilde{k}(l)} \right\|_2 \right\} + \frac{C_f b_{S, \tilde{k}(l+1)}}{2}. \end{aligned} \quad (159)$$

Suppose that the step size $\{b_{S,k} : k > 0\}$ satisfies

$$C_e \frac{C_f L}{2} [c(\tilde{k}(l)) - c(\tilde{k}(l+1))] + \frac{C_f b_{S, \tilde{k}(l+1)}}{2} < \frac{\delta}{2}, \quad (160)$$

for $l \geq 0$.

Given $\sup_{t \in I_l} \left\| \bar{\mathbf{x}}(t) - \tilde{\mathbf{x}}^{\tilde{k}(l)}(t) \right\| > \delta$, we can obtain from (159) and (160) that

$$\begin{aligned} & \sup_{\tilde{k}(l) \leq p \leq \tilde{k}(l+1)} \left\| \boldsymbol{\xi}_p - \boldsymbol{\xi}_{\tilde{k}(l)} \right\|_2 \\ & \geq \frac{1}{C_e} \left(\sup_{t \in I_l} \left\| \bar{\boldsymbol{\psi}}(t) - \tilde{\boldsymbol{\psi}}^{\tilde{k}(l)}(t) \right\|_2 - \frac{C_f L}{2} [c(\tilde{k}(l)) - c(\tilde{k}(l+1))] - \frac{C_f b_{S, \tilde{k}(l+1)}}{2} \right) \\ & > \frac{1}{C_e} \left(\sup_{t \in I_l} \left| \bar{\mathbf{x}}(t) - \tilde{\mathbf{x}}^{\tilde{k}(l)}(t) \right| - \frac{\delta}{2} \right) \\ & > \frac{\delta}{2C_e}. \end{aligned}$$

Then, we get

$$\begin{aligned} & P \left(\sup_{t \in I_m} \left\| \bar{\mathbf{x}}(t) - \tilde{\mathbf{x}}^{\tilde{k}(l)}(t) \right\| > \delta \mid \sup_{t \in I_i} \left\| \bar{\mathbf{x}}(t) - \tilde{\mathbf{x}}^{\tilde{k}(i)}(t) \right\| \leq \delta, 0 \leq i < l \right) \\ & \leq P \left(\sup_{\tilde{k}(l) \leq p \leq \tilde{k}(l+1)} \left\| \boldsymbol{\xi}_p - \boldsymbol{\xi}_{\tilde{k}(l)} \right\|_2 > \frac{\delta}{2C_e} \mid \sup_{t \in I_i} \left\| \bar{\mathbf{x}}(t) - \tilde{\mathbf{x}}^{\tilde{k}(i)}(t) \right\| \leq \delta, 0 \leq i < l \right) \quad (161) \\ & \stackrel{(d)}{=} P \left(\sup_{\tilde{k}(l) \leq p \leq \tilde{k}(l+1)} \left\| \boldsymbol{\xi}_p - \boldsymbol{\xi}_{\tilde{k}(l)} \right\|_2 > \frac{\delta}{2C_e} \right), \end{aligned}$$

where Step (d) is due to the independence of noise, i.e., $\boldsymbol{\xi}_p - \boldsymbol{\xi}_{\tilde{k}(l)}$, $\tilde{k}(l) \leq p \leq \tilde{k}(l+1)$ are independent of $\hat{\mathbf{x}}_k$, $0 \leq k \leq \tilde{k}(l)$.

The lower bound of the probability that the sequence $\{\hat{\mathbf{x}}_k : k \geq 0\}$ remains in the invariant set \mathcal{I} is given by

$$\begin{aligned}
P(\hat{\mathbf{x}}_k \in \mathcal{I}, \forall k \geq 0) &\stackrel{(e)}{\geq} P\left(\sup_{t \in I_m} \|\bar{\mathbf{x}}(t) - \tilde{\mathbf{x}}^{\tilde{k}(l)}(t)\| \leq \delta, \forall l \geq 0\right) \\
&\stackrel{(f)}{\geq} 1 - \sum_{l \geq 0} P\left(\sup_{t \in I_m} \|\bar{\mathbf{x}}(t) - \tilde{\mathbf{x}}^{\tilde{k}(l)}(t)\| > \delta \mid \sup_{t \in I_i} \|\bar{\mathbf{x}}(t) - \tilde{\mathbf{x}}^{\tilde{k}(i)}(t)\| \leq \delta, 0 \leq i < l\right) \\
&\stackrel{(g)}{\geq} 1 - \sum_{l \geq 0} P\left(\sup_{\tilde{k}(l) \leq p \leq \tilde{k}(l+1)} \|\boldsymbol{\xi}_p - \boldsymbol{\xi}_{\tilde{k}(l)}\|_2 > \frac{\delta}{2C_e}\right), \tag{162}
\end{aligned}$$

where Step (e) is due to Lemma 6, Step (f) is due to Lemma 4.2 in [32], and Step (g) is due to (161). Let $\|\cdot\|_\infty$ denote the max-norm, i.e., $\|\mathbf{u}\|_\infty = \max_l |[\mathbf{u}]_l|$. Note that for $\mathbf{u} \in \mathbb{R}^D$, $\|\mathbf{u}\|_2 \leq \sqrt{D} \|\mathbf{u}\|_\infty$. Hence we have

$$\begin{aligned}
&P\left(\sup_{\tilde{k}(l) \leq p \leq \tilde{k}(l+1)} \|\boldsymbol{\xi}_p - \boldsymbol{\xi}_{\tilde{k}(l)}\|_2 > \frac{\delta}{2C_e}\right) \\
&\leq P\left(\sup_{\tilde{k}(l) \leq p \leq \tilde{k}(l+1)} \|\boldsymbol{\xi}_p - \boldsymbol{\xi}_{\tilde{k}(l)}\|_\infty > \frac{\delta}{4C_e}\right) \tag{163} \\
&= P\left(\sup_{\tilde{k}(l) \leq p \leq \tilde{k}(l+1)} \max_{1 \leq j \leq 4} |[\boldsymbol{\xi}_p]_j - [\boldsymbol{\xi}_{\tilde{k}(l)}]_j| > \frac{\delta}{4C_e}\right) \\
&= P\left(\max_{1 \leq j \leq 4} \sup_{\tilde{k}(l) \leq p \leq \tilde{k}(l+1)} |[\boldsymbol{\xi}_p]_j - [\boldsymbol{\xi}_{\tilde{k}(l)}]_j| > \frac{\delta}{4C_e}\right) \\
&\leq \sum_{j=1}^4 P\left(\sup_{\tilde{k}(l) \leq p \leq \tilde{k}(l+1)} |[\boldsymbol{\xi}_p]_j - [\boldsymbol{\xi}_{\tilde{k}(l)}]_j| > \frac{\delta}{4C_e}\right).
\end{aligned}$$

With the increasing σ -fields $\{\mathcal{G}_k : k \geq 0\}$ defined in Appendix D, we have for $k \geq 0$,

- 1) $\boldsymbol{\xi}_k = \sum_{l=1}^k b_{S,l} \hat{\mathbf{z}}_l \sim \mathcal{N}(0, \sum_{l=1}^k b_{S,k}^2 \mathbf{I}_S(\hat{\boldsymbol{\psi}}_{l-1}, \mathbf{W}_l)^{-1})$,
- 2) $\boldsymbol{\xi}_k$ is \mathcal{G}_k -measurable, i.e., $\mathbb{E}[\boldsymbol{\xi}_k | \mathcal{G}_k] = \boldsymbol{\xi}_k$,
- 3) $\mathbb{E}[\|\boldsymbol{\xi}_k\|_2^2] = \sum_{l=1}^k b_{S,k}^2 \text{tr}\left\{\mathbf{I}_S(\hat{\boldsymbol{\psi}}_{l-1}, \mathbf{W}_l)^{-1}\right\} < +\infty$,
- 4) $\mathbb{E}[\boldsymbol{\xi}_k | \mathcal{G}_l] = \boldsymbol{\xi}_l$ for all $0 \leq l < k$.

Therefore, $[\boldsymbol{\xi}_k]_j, j = 1, 2, 3, 4$ is a Gaussian martingale with respect to \mathcal{G}_k , and satisfies

$$\begin{aligned} \text{Var} \left[[\boldsymbol{\xi}_{k+l}]_j - [\boldsymbol{\xi}_k]_j \right] &= \sum_{i=k+1}^{k+l} b_{S,i}^2 \left[\mathbf{I}_S(\hat{\boldsymbol{\psi}}_{i-1}, \mathbf{W}_i)^{-1} \right]_{j,j} \\ &\leq \sum_{i=k+1}^{k+l} b_{S,i}^2 \frac{C_{\mathbf{I}} \sigma_z^2}{|\mathbf{s}|^2} \\ &= \frac{C_{\mathbf{I}} \sigma_z^2}{|\mathbf{s}|^2} [c(k) - c(k+l)], \end{aligned} \quad (164)$$

where $C_{\mathbf{I}} \triangleq \max_s \max_{i \geq 1} \frac{|\mathbf{s}|^2}{\sigma_z^2} \left[\mathbf{I}(\hat{\boldsymbol{\psi}}_{i-1}, \mathbf{W}_i)^{-1} \right]_{j,j}$. Let $\eta = \frac{\delta}{4C_e}$, $M_i = [\boldsymbol{\xi}_{\tilde{k}(l+i)}]_j - [\boldsymbol{\xi}_{\tilde{k}(l)}]_j, j = 1, 2, 3, 4$ and $p = \tilde{k}(l+1) - \tilde{k}(l)$ in Lemma 9, then from (163) and (164), we can obtain

$$\begin{aligned} &P \left(\sup_{\tilde{k}(l) \leq p \leq \tilde{k}(l+1)} \left| [\boldsymbol{\xi}_p]_j - [\boldsymbol{\xi}_{\tilde{k}(l)}]_j \right| > \frac{\delta}{4C_e} \right) \\ &\leq 2 \exp \left\{ - \frac{\delta^2}{32C_e^2 \text{Var} \left[[\boldsymbol{\xi}_{\tilde{k}(l+i)}]_j - [\boldsymbol{\xi}_{\tilde{k}(l)}]_j \right]} \right\} \\ &\leq 2 \exp \left\{ - \frac{\delta^2 |\mathbf{s}|^2}{32C_{\mathbf{I}} C_e^2 [c(\tilde{k}(l)) - c(\tilde{k}(l+1))] \sigma_z^2} \right\}. \end{aligned} \quad (165)$$

Combining (162), (163) and (165), we have

$$P(\hat{\mathbf{x}}_k \in \mathcal{I}, \forall k \geq 0) \geq 1 - 8 \sum_{l \geq 0} \exp \left\{ - \frac{\delta^2 |\mathbf{s}|^2}{32C_{\mathbf{I}} C_e^2 [c(\tilde{k}(l)) - c(\tilde{k}(l+1))] \sigma_z^2} \right\}. \quad (166)$$

To use Lemma 10, we assume that the step-size $b_{S,k}$ satisfies

$$c(0) = \sum_{i>0} b_{S,i}^2 \leq \frac{\delta^2 |\mathbf{s}|^2}{32C_{\mathbf{I}} C_e^2 \sigma_z^2}. \quad (167)$$

Then, from Lemma 10, we can obtain

$$\frac{\exp \left\{ - \frac{\delta^2 |\mathbf{s}|^2}{32C_{\mathbf{I}} C_e^2 [c(\tilde{k}(l)) - c(\tilde{k}(l+1))] \sigma_z^2} \right\}}{c(\tilde{k}(l)) - c(\tilde{k}(l+1))} \leq \frac{\exp \left\{ - \frac{\delta^2 |\mathbf{s}|^2}{32C_{\mathbf{I}} C_e^2 c(0) \sigma_z^2} \right\}}{c(0)}$$

for $c(\tilde{k}(l)) - c(\tilde{k}(l+1)) < c(\tilde{k}(l)) \leq c(0)$. Hence, we have

$$\begin{aligned} &\sum_{l \geq 0} \exp \left\{ - \frac{\delta^2 |\mathbf{s}|^2}{32C_{\mathbf{I}} C_e^2 [c(\tilde{k}(l)) - c(\tilde{k}(l+1))] \sigma_z^2} \right\} \\ &\leq \sum_{l \geq 0} [c(\tilde{k}(l)) - c(\tilde{k}(l+1))] \cdot \frac{\exp \left\{ - \frac{\delta^2 |\mathbf{s}|^2}{32C_{\mathbf{I}} C_e^2 c(0) \sigma_z^2} \right\}}{c(0)} \\ &= c(0) \cdot \frac{\exp \left\{ - \frac{\delta^2 |\mathbf{s}|^2}{32C_{\mathbf{I}} C_e^2 c(0) \sigma_z^2} \right\}}{c(0)} = \exp \left\{ - \frac{\delta^2 |\mathbf{s}|^2}{32C_{\mathbf{I}} C_e^2 c(0) \sigma_z^2} \right\}. \end{aligned} \quad (168)$$

As $C_e = e^{L(T+b_{S,1})}$, $c(0) = \sum_{i>0} b_{S,i}^2$, and $b_{S,k}, T, L$ are given by (40), (123), (153) separately, we can obtain

$$\frac{\delta^2 |\mathbf{s}|^2}{32C_{\mathbf{I}}C_e^2c(0)\sigma_z^2} = \frac{\delta^2 |\mathbf{s}|^2}{32C_{\mathbf{I}}e^{2L(T+\frac{\epsilon_S}{K_{S,0}+1})}\sigma_z^2 \sum_{i \geq 1} \frac{\epsilon_S^2}{(i+K_{S,0})^2}} = \frac{\delta^2}{\sum_{i \geq 1} \frac{32C_{\mathbf{I}}e^{2L(T+\frac{\epsilon_S}{K_{S,0}+1})}}{(i+K_{S,0})^2}} \cdot \frac{|\mathbf{s}|^2}{\epsilon_S^2\sigma_z^2}. \quad (169)$$

In (169), $0 < \delta < \inf_{\mathbf{v} \in \partial \mathcal{B}} \|\mathbf{v} - \hat{\mathbf{x}}_b\|$, (160) and (167) should be satisfied, where a sufficiently large $K_{S,0} \geq 0$ can make both (160) and (167) true.

To ensure that $\hat{\mathbf{x}}_0 + b_{S,1} \left[\mathbf{f}(\hat{\boldsymbol{\psi}}_0, \boldsymbol{\psi}) \right]_{3,4}$ does not exceed the main lobe $\mathcal{B}(\mathbf{x})$, i.e., the first step-size $b_{S,1}$ satisfies

$$\begin{aligned} \left| \hat{x}_{0,1} + b_{S,1} \left[\mathbf{f}(\hat{\boldsymbol{\psi}}_0, \boldsymbol{\psi}) \right]_3 - x_1 \right| &< 1 \\ \left| \hat{x}_{0,2} + b_{S,1} \left[\mathbf{f}(\hat{\boldsymbol{\psi}}_0, \boldsymbol{\psi}) \right]_4 - x_2 \right| &< 1, \end{aligned}$$

we can obtain the maximum ϵ_S as follows

$$\epsilon_{S,\max} = \min \frac{(K_{S,0} + 1)}{\left\| \left[\mathbf{f}(\hat{\boldsymbol{\psi}}_0, \boldsymbol{\psi}) \right]_3 \right\|} \{1 - |x_1 - \hat{x}_{0,1}|, 1 - |x_2 - \hat{x}_{0,2}|\} \leq \frac{(K_{S,0} + 1)}{\left\| \left[\mathbf{f}(\hat{\boldsymbol{\psi}}_0, \boldsymbol{\psi}) \right]_3 \right\|} \triangleq \epsilon_b. \quad (170)$$

Hence, from (169), we have

$$\frac{\delta^2 |\mathbf{s}|^2}{32C_{\mathbf{I}}C_e^2c(0)\sigma_z^2} \cdot \frac{\epsilon_S^2\sigma_z^2}{|\mathbf{s}|^2} \geq \frac{\delta^2}{\sum_{i \geq 1} \frac{32C_{\mathbf{I}}e^{2L(T+\frac{\epsilon_b}{K_{S,0}+1})}}{(i+K_{S,0})^2}} \triangleq R. \quad (171)$$

Combining (166), (168) and (171), yields

$$P(\hat{\mathbf{x}}_k \in \mathcal{I}, \forall k \geq 0) \geq 1 - 8e^{-\frac{R|\mathbf{s}|^2}{\epsilon_S^2\sigma_z^2}},$$

which completes the proof.